# A ROLE FOR PROTEIN PHOSPHATASE 2A IN THE PROLIFERATION-QUIESCENCE DECISION

**by**

**Dan Sun**

**A dissertation submitted in partial fulfillment**
**of the requirements for the degree of**
**Doctor of Philosophy**
**(Molecular, Cellular and Developmental Biology)**
**in The University of Michigan**
**2016**

**Doctoral Committee:**

**Assistant Professor Laura Buttitta, Chair**
**Professor Steven E. Clark**
**Associate Professor Cheng-Yu Lee**
**Assistant Professor Ann L. Miller**

**To my parents & grandparents**

# ACKNOWLEDGEMENTS

This thesis covers the majority of my research projects since the start of my Ph. D. program in fall, 2010. I am so grateful for the company of my family, friends and colleagues, and people who have provided me their generous help and support during my completion of this work.

First and foremost, I would like to express my sincere gratitude to my advisor Dr. Laura Buttitta for guiding me through the path with your inspiration, patience, encouragement, and great knowledge. I am extremely appreciate your support in every possible way that a graduate student needs. Through the 5.5 year-training under your supervision, I learned to think more critically and mastered new technical skills. With your great passion, dedication and insight for science. I feel extremely fortunate to be one of your first students and will never forget your encouragement and support. Thank you so much for providing a great environment for me to grow as a young scientist, both professionally and personally.

I would also like to thank my committee members, Dr. Steven Clark, Dr. Ann Miller and Dr. Cheng-Yu Lee for their valuable advice and suggestions throughout this

process. I always feel grateful for their helpful guidance and patience through my graduate study.

I would like to thank all my current and former colleagues in the lab for creating an amazing working atmosphere. In particular, I would like to thank my cohort colleague, Kerry Flegel, whose company in the last 6 years means a lot to my PhD study. We encouraged each other at our prelim examination, 1st committee meeting and all the way to the end, here dissertation writing and defense. Thanks, Kerry for your cheer-up Rosaline's tune, which I will not forget. Thanks to Yiqin Ma, Shyama Nandakumar, Ajai Pulianmackal, Dr. Kiriaki Kanakousaki and Dr. Olga Grushko for your support and inputs to my research projects in discussions. I also appreciate the joys and jokes we shared in our daily coffee tour. Thank Ellen Griggs, Lulia Kana, and Sapha Hassan for their help moving the science forward during their undergrad training in the Buttitta Lab.

Thank you to many labs inside or outside the MCDB department, especially Cadigan lab, Csankovszki lab, Wang lab, Nandakumar lab, O Shea lab and Taichman lab for generously sharing with us the reagents and equipment. I always feel grateful to the Lee lab in Life Sciences Institute for the useful comments and ideas exchanged during the joint lab meetings. I must express my great appreciation to all my collaborators Zhengda Li, Dr. Alexander Pearson, Dr. Greg Shelley, Dr. Kenji Yumoto and Dr. Janice E Berry for their great work, knowledge and support. Thanks to Dr. John Schiefelbein and Dr. Cathy Collins for providing me the great opportunities to rotate in

their labs, and thanks to Mary Carr and Diane Durfy for their invaluable administrative assistance during the past several years. I would also like to thank Gregg Sobocinski for his knowledge and help in the confocal microscopy. Particularly, I would like to express my gratitude to Chris A. Edwards in the Microscopy & Image-Analysis Lab for his advice and support in the live-cell image.

I would like to thank my friends for making my past six years full of memories. I would also like to thank my cohort classmates who are always supportive and nice to each other. The journey pursuing my Ph. D. would have been much harder without your support.

I would like to offer my special thanks to my family. I owe my deepest gratitude to my parents & grandparents, who always have faith in me and support me in my life. I cannot express with words my appreciation for their unconditional love and understanding for my 6-year absence at your sides. I feel extremely lucky being your daughter or granddaughter.

# TABLE OF CONTENTS

# LIST OF FIGURES

# LIST OF TABLES

# ABSTRACT

Metazoans precisely control the number of cell divisions during organ or tissue development or maintenance throughout their lifetime. In adult metazoans, most differentiated cells no longer proliferate and lie in a quiescent state, also termed cell cycle exit. The decision to proliferate or to lie in quiescence is essential for development and its dysregulation may lead to defects in organogenesis, wound healing and regeneration as well as tumor formation. However, at what stage of the cell cycle the proliferation-quiescence decision occurs and what molecular mechanisms control this decision remain controversial.

Here my thesis work revealed a novel role for PP2A in promoting the transition to quiescence upon terminal differentiation during tissue development. Using *Drosophila* eyes and wings as a model, I found that compromising PP2A activity during the final cell cycle prior to a developmentally controlled cell cycle exit leads to extra cell divisions and delayed normal exit. By systematically testing the regulatory subunits of *Drosophila* PP2A, I discovered that the B56 family member *widerborst* (*wdb*) is required for the role of PP2A in promoting the transition to quiescence. In particular, the PP2A/B56 complex targets cyclin-dependent kinase 2 several hours after mitosis to promote entry into quiescence, indicating when the decision occurs and how PP2A impacts the decision.

I also investigated the dynamic features of the proliferation-quiescence transition through the application of a novel fluorescent cell cycle reporter and time-lapse, live-cell imaging in mammalian cell culture. By monitoring the proliferation-quiescence transition without cell synchronization, I discovered that the quiescent state is heterogeneous. Mammalian cells can enter into either a transient or a prolonged quiescent state after mitosis, prior to the next round of cell cycle even under conditions of abundant nutrients. Notably, I showed that two sister cells born of the same mitosis can make different cell cycle decisions, with one cell entering long-term quiescence while the other re-entering the cell cycle. Consistent with my work in the *Drosophila* model, PP2A in mammals also plays a conserved role in promoting the entry into quiescence. The novel role of PP2A in modulation of the proliferation-quiescence decision may contribute to its tumor suppressor role and impact the emerging problem of tumor dormancy.

# Chapter 1. General Introduction

The cell cycle is a series of sequential molecular events that result in the production of two daughter cells. Cellular proliferation is fundamental to the development of all the eukaryotes. The cell cycle is artificially divided into specific phases during which cells grow and prepare for duplication (G1), replicate DNA (DNA synthesis), prepare for division (G2) and separate the two copies of DNA and cytoplasmic contents, forming two cells (Mitosis). Rapid cell proliferation is one major feature of early embryonic development. As tissues mature later in development, most cells differentiate into specialized cell types and slow or stop proliferation and contribute to organ function. Most adult animal cells have stopped dividing and enter a state termed G0 or cellular quiescence where most will remain for lifetime of the organism. The slowing or stopping of the proliferation at the right places and times, is critically important for proper tissue or organ development. Despite the importance of the proliferation-quiescence decision, most studies of cell cycle regulation have focused on rapidly dividing cells. It remains unknown why or how cells choose to enter quiescence during development, and how the developmental signals, tissue damage or nutrient abundance trigger specific cells to re-enter the cell cycle.

## 1.1 Key factors in the regulation of cell cycle progression

In order to understand how the proliferation-quiescence decision is regulated, it is worth reviewing the major regulatory components of the cell cycle.

Cell cycle progression is controlled by oscillations of the activity of different cyclin/Cyclin-dependent kinase complexes. In metazoans, multiple Cdks partner with specific cyclins to execute sequential functions in cell cycle progression. For example, Cdk4 or Cdk6 pairs with CycD and Cdk2 pairs with CycE to promote G1 phase progression, Cdk2 or Cdk1 pairs with CycA to promote S-G2 phase, and Cdk1 pairs with CycB as the maturation promoting factor to push mitotic entry (Morgan, 1997). Both cellular stress signals and environmental signals can impinge upon the regulation of different cyclin/Cyclin-dependent kinase activities at both transcriptional, post-transcriptional and post-translational levels.

**The major transcriptional machinery of the cell cycle—E2F and Rb**

E2F/DP transcriptional hetero-dimer complex is often considered to be a master regulator of the cell cycle, as it regulates transcription of hundreds of genes, most of which are essential for DNA replication and cell cycle progression, including the cyclins and Cdks. In mammals, “E2F” is a general term used for seven different transcription factor complexes (E2F1-E2F7), six of which need the hetero-dimerization with DP proteins to be functional. The E2F family can be divided into three groups based on

their transcriptional properties. E2Fs 1-3 are the activating E2Fs, required for the transactivation of target genes in the G1-S transition. In contrast, E2Fs 4 and 5 are considered transcriptional repressors, because they are mainly nuclear in G0/G1 and are primarily involved in the repression of E2F- responsive genes when bound to members of the retinoblastoma protein (pRB) family. E2F6 also acts as a transcriptional repressor but without interacting with the pRB family (Bracken et al., 2004; Müller and Helin, 2000).

Cyclin/Cdk complexes and E2F activator complexes promote the progression of the cell cycle. By contrast, the Cyclin-dependent Kinase Inhibitors (CKIs) and the retinoblastoma protein-family members (pRB,p107 and p130) are negative regulators of the cell cycle progression (Cobrinik, 2005; Vidal & Koff, 2000). Investigations into the function of the retinoblastoma proteins (pRB), the first identified tumor suppressor (Trimarchi and Lees, 2002; Huang et al., 1988), showed that pRB is quite important in inhibiting cell cycle entry by binding and suppressing E2F/DP complex activity, leading to the transcriptional repression of hundreds of cell-cycle regulators (Tamrakar et al., 2000; Burkhart and Sage, 2008; van den Heuvel and Dyson, 2008). This repression is counteracted by the G1 Cyclin/Cdk complexes Cyclin E/Cdk2 and Cyclin D/Cdk4 which catalyze the phosphorylation of RBs, resulting in the release of E2F/DP binding, (reviewed in Du and Pogoriler, 2006). Then activator E2F/DP complexes further promote Cyclin/Cdk expression, thus creating a positive feedback loop that promotes

G1 progression and robust commitment to cell cycle entry (Trimarchi and Lees, 2002; Blais and Dynlacht, 2004).

**The cyclin-dependent kinases (Cdks)**

The cyclin-dependent kinases are the catalytic subunits that coordinate the orderly events of the cell cycle and play roles in integrating growth-regulatory and intercellular signals with cell cycle progression. The expression level of the Cdks is relatively constant throughout the cell cycle. It is the different cyclins whose concentrations rise and fall with the cell cycle phases together with activating or inhibitory phosphorylations of Cdks that results in the oscillation of a series of active Cyclin-Cdk complexes.

The typical Cdk catalytic subunit contains a 300 amino acid catalytic core which is inactive when monomeric and phosphorylated (Morgan, 1995). Binding to a cyclin and phosphorylation of a conserved Thr residue in the activation loop (T-loop) are required to activate Cdk kinase activity. Phosphorylation of the Cdk T-loop is catalyzed by a Cdk-activating kinase (CAK) complex, composed of Cdk7, cyclin H, and MAT-1. The catalytic component Cdk7 is expressed uniformly during the cell cycle, as Cdk7 also plays an essential role as a component of the general transcription factor TFIIH, which phosphorylates the C- terminal domain (CTD) of the largest subunit of Pol II (Larochelle et al., 1998; Merrick et al., 2008; Fisher, 2005). *Drosophila* Cdk7 was first identified based on its requirement for proliferation, as it acts as a CAK to activate the Cdk1

complex *in vivo* (Larochelle et al., 1998). Indeed, the effects of Cdk7 loss on cell proliferation can be largely rescued by $Cdk2^{T160E}$ or $Cdk1^{T161E}$ phosphomimetic mutants in mouse embryonic fibroblasts (Ganuza et al., 2012). Thus Cdk7 is essential for the activation of the cell cycle by phosphorylation of T-loop residues of the Cdks.

The active kinases and the activation process are conversely suppressed by the binding of cyclin-dependent kinase inhibitors (CKIs). CKIs consist of two families: INK4 proteins (p15,p16,p18 and p19), and the Cip/Kip family ($p21^{Cip1}$, $p27^{Kip1}$ and $p57^{Kip2}$) (Vidal and Koff, 2000). The INK4 family generally inhibit cyclin D-type Cdk activity by competitively binding to the Cdk subunit. The Cip/Kip family shares a homologous inhibitory domain, which is responsible for the inhibition of Cdk4- and Cdk2-containing complexes by direct binding. The Cip/Kip family acts on Cdk2 preferentially *in vivo*, though they can target all G1 cyclin complexes *in vitro*. (Parry et al., 1999; Ortega et al., 2002; Soos et al., 1996). Mammalian p21 transcription is primarily induced by p53, a transcriptional regulator in response to DNA damage (Harper and Elledge, 1996). However, this is not conserved in other organisms such as in *Drosophila*, where the sole Cip/Kip-type CKI, dacapo (dap) expression is correlated with a cessation of cell proliferation during tissue development and controlled by developmental signaling (de Nooij et al., 1996; Lane et al., 1996; Sukhanova and Du, 2008). p21 inhibits cyclin/Cdk2 complex activity during G1 and S phases, leading to cell cycle arrest (Wade Harper et al., 1993). The closely related paralogs, p27, is high in G0 cells and binds to and

preferably inhibits CycE/Cdk2 as cells progress into G1. The destruction of p27 by the E3 ubiquitin ligase Skp2 allows the Cdk2 complex to be active and to promote the G1-S transition (Sherr and Roberts, 1999). Consequently, disruption of p27 in mice leads to an increase in the fraction of S phase cells in the thymus, demonstrating that p27 functions as a negative regulator of cell proliferation (Kiyokawa et al., 1996).

**Controlled proteolysis in cell cycle progression**

The proteolysis of cyclins and their regulators ensures the proper temporal order of cell cycle events. The two major protein degradation complexes involved in cell cycle regulation are Skp-Cullin-F-box (SCF) complexes for G1-S phase progression and the APC/C (the Anaphase-Promoting Complex/Cyclosome) for the completion of Mitosis and quiescence entry. The SCF complex consists of four subunits: Skp1 (scaffold protein), Cul1 (scaffold protein), RING-finger component (Rbx1), and a variable adaptor protein or F-box protein. The F-box protein targets a discrete number of specific substrates through protein–protein interactions. The F-box proteins Skp2 and Fbw7 target multiple cell cycle regulators. Skp2 mediates the degradation of the CDK inhibitors $p21^{Cip1}$, $p27^{Kip1}$ and $p57^{Kip2}$, the origin recognition subunit hOrc1, the replication initiation factor Cdt1, as well as the Rb-related tumor suppressor p130, ensuring that G1-S progression and DNA replication occur in a timely manner and only one per cycle (Tedesco et al., 2002; Willems et al., 2004; Cardozo and Pagano, 2004). Fbw7 targets several proto-oncogenes, including CycE, MYC, JUN and Notch (Welcker

and Clurman, 2008; Koepp et al., 2001). Mutations in Fbw7 have been found in several human cancers. Importantly, Fbw7 specifically targets phosphorylated CycE which is high during the G1-S transition due to self-phosphorylation and induces its degradation (Moberg, Bell, Wahrer, Haber, & Hariharan, 2001; Strohmaier et al., 2001). In *Fbw7* mutant mice and *Drosophila*, multiple cell types exhibit additional proliferation and disruption of G0 (Onoyama et al., 2007; Moberg et al., 2001), indicating Fbw7 is needed for timely cell cycle exit. However, loss of Archipelago (ago), ortholog of Fbw7 in *Drosophila*, did not disrupt normal cell cycle exit timing in wing development, and only delayed cell cycle exit in the eye by one cell cycle (Buttitta et al., 2007). This suggests the importance of Fbw7 at the proliferation-quiescence transition varies in different tissues and in some contexts may not be required.

APC/C is an E3 ubiquitin ligase complex whose activation requires the phosphorylation of specific subunits and the binding of a cofactor, Cdc20 (or Fizzy; Fzy) or Cdh1 (or Fizzy-related; Fzr) for full activity. APC/C complex is important to coordinate mitotic exit and quiescence (Sigrist and Lehner, 1997; Clijsters et al., 2013). During mitosis, APC/$C^{Cdc20}$ complex promotes mitotic exit by degrading key substrates such as the mitotic cyclins and Geminin, which usually accumulate during the S, G2, and early mitotic phases (Penas et al., 2011; McLean et al., 2011). In contrast, APC/$C^{Cdh1}$ plays a major role after mitotic exit in maintaining quiescence and preventing early onset of DNA replication. During quiescence, APC/$C^{Cdh1}$ prevents the assembly of pre-replicative

complexes by degrading CDC6 (Mailand and Diffley, 2005). Functions for APC/C in the establishment and maintenance of quiescence will be discussed in detail later.

## 1.2 Quiescence and G0

$G_0$ is a term broadly used to refer to a prolonged cell cycle arrest, or a sustained non-dividing state. $G_0$ can encompass distinct states, distinguished by their range of reversibility: from easily reversible to non-reversible (Fig.1.1). The term reversible quiescence has sometimes been used to describe cells that are not actively cycling, but may re-enter the cell cycle upon external stimuli. An example would be stem cells that respond to signals upon wounding to maintain tissue homeostasis or cancer cells that can re-enter the cell cycle to seed recurrent tumors. This term also is commonly used to describe cells that are not dividing due to nutrient or growth factor starvation, for example in cell culture. In contrast, cells that acquire their final fate and undergo terminal differentiation during development, often enter a prolonged or sometimes permanent cell cycle arrest, which is also referred to as $G_0$. This is a feature characteristic of neurons, mature epithelia and muscle to name a few examples. In some organisms however, certain mature, differentiated cell types maintain a reversible $G_0$ and can re-enter the cell cycle upon damage. This includes examples such as mature muscle from amputated axolotl limbs (Sugiura et al., 2016), the extraocular

muscles of zebrafish (Saera-Vila et al., 2015), Müller glia of the zebrafish retina (Wan and Goldman, 2016), and the sensory epithelium of the avian inner ear (Tsue et al., 1994). A third state of cell cycle arrest, senescence, is also often referred to as $G_0$. In senescence, cells exit from the cell cycle in response to telomere loss, stress, accumulation of DNA damage or aberrant oncogenic activity, and undergo permanent arrest accompanied by metabolic, nuclear and morphological changes associated with DNA damage (Salama et al., 2014). Senescence often represents a general response to aging and stress (Chandler and Peters, 2013), but recent work has shown that senescence also occurs during normal development (Storer et al., 2013; Muñoz-Espín et al., 2013).

## 1.3 Potential molecular markers of quiescence

Molecular markers that can distinguish G0 from G1 are of great interest in the cell cycle field. Most cell cycle assays such as immunostaining for markers of proliferating cells or flow cytometry cannot distinguish G0 from early G1 cells since both G0 and G1 cells contain 2C DNA contents and there is no obvious change in cell morphology (Zambon, 2010; Pozarowski and Darzynkiewicz, 2004). In some cell types, specific molecular markers can be correlated with G0, but these often don't translate to other cell types. Without a universal marker for G0, it has been very challenging to reliably identify G0 cells both *in vitro* and *in vivo*. Below is a discussion of existing molecular approaches used to distinguish G0 from G1 cells (Fig.1.2).

**Cyclin-dependent kinase inhibitors as markers of G0**

The CKIs p21 and p27 are often considered to be putative markers of quiescent cells in cell culture for the following two reasons. First, the expression levels of p21 and p27 are highest in G0 cells (Coller et al., 2006; Oki et al., 2014). Second, p21 and p27 bind to G1-Cdk complexes and suppress their activity to promote cell cycle arrest at G0 (Wade Harper et al., 1993; Polyak et al., 1994) .

In particular, the degradation of p27 is regulated by a two-step process: translocation-coupled cytoplasmic ubiquitination by KPC (Kip1 ubiquitination-promoting complex) at G1 phase and nuclear proteolysis by Skp2 at S and G2 phases. KPC, an E3 ligase complex, consists of KPC1 and KPC2. KPC-mediated p27 proteolysis depends on the nuclear export of p27, which takes place only at G1 phase entry. But depletion of either KPC1 or Skp2 does not delay cell cycle progression from G0 to S phase, the deficiency of both factors results in the accumulation of p27 and a delay in cell cycle progression (Kamura et al., 2004). KPC and Skp2 thus play redundant roles in p27 degradation which is essential for G0-G1 progression. Based on this, a novel fluorescent cell cycle reporter was generated to separate G0 and G1 cells by fusing a fluorescent protein to an inactive form of p27 protein. With this reporter and live, time-lapse imaging, I investigated the cell cycle behaviors at the proliferation-quiescence decision without cell synchronization and details will be discussed in chapter 3.

**Using the pRb family to identify cells in G0**

The retinoblastoma protein (pRb), the first identified tumor suppressor, functions to promote cell cycle exit *in vivo* and to slow down the G1-S progression *in vitro* (van den Heuvel and Dyson, 2008). The prevalent model of G0-G1 progression proposes that CyclinD:Cdk4/6 complex progressively phosphorylates Rb resulting in an inactive, hypo-phosphorylated Rb form, which drives G1 entry. However, recent biochemical studies in mouse embryonic fibroblasts (MEFs) showed that Rb is exclusively mono-phosphorylated by CyclinD:Cdk4/6 on any one of 16 putative Cdk phosphorylation sites that are spread throughout the protein at early G1 phase. Surprisingly, the mono-phosphorylated Rb still functions as a suppressor of E2F activity, in direct contrast to the prevalent model. At late G1 phase, mono-phosphorylated Rb is further hyper-phosphorylated by active CyclinE:Cdk2 complex thereby allowing G1/S progression (Narasimha et al., 2014). Importantly, in quiescent, differentiating cells, Rb remains in a repressive, un-phosphorylated form, which suggests that appearance of mono-phosphorylated Rb could be an early mark of the G0-G1 transition. Any one of the potential 16 phospho-sites may be phosphorylated to generate the “active” form of Rb, and therefore it is impossible to predict which one of the sites out of 16 will be mono-phosphorylated, and it is not feasible to generate an antibody. Moreover, the mono-phosphorylated Rb and un-phosphorylated Rb co-migrate on 1D SDS-PAGE and

cannot be separated, without a two-dimensional isoelectric focusing (2D IEF) gel. Thus, the mono-phospho Rb as a molecular marker of the G0-G1 transition cannot be monitored in individual cells or fixed tissue samples.

Another Rb family member, p130 is the primary E2F complex repressor in quiescent cells (Takahashi et al., 2000; Sadasivam and Decaprio, 2013). The highly conserved p130 complex termed DP, RB-like, E2F, and MuvB (DREAM) is thought to be responsible for cell-cycle dependent gene repression in certain G0 cells, including human glioblastoma cells and human primary fibroblasts (Litovchick et al., 2007). Chromatin immunoprecipitation (ChIP) and Multidimensional Protein Identification Technology (MudPIT) have revealed that DREAM complex directly binds to 800 human promoters, and that most E2F cell cycle targets are repressed by p130. The binding of p130 is significantly stronger in G0-arrested cells than in proliferating cells. This again confirms the finding that p130 is the predominant RB family protein bound to E2F- and E2F4- promoters in quiescent MEFs (Balciunaite et al., 2005). At G0-G1 transition, the G1 Cdks phosphorylate p130, which triggers ubiquitination of p130 via Skp2 and decay of the E2F-p130 repressive complex (Tedesco et al., 2002; Smith et al., 1996). It is likely that p130 is required to repress gene expression in quiescent cells, and unphosphorylated p130 may be a potential marker of quiescence in certain cell types.

**Using a T-loop phosphorylation cascade to monitor the G0-G1 transition**

During G1 phase, CycD-Cdk4/6 kinase activity is responsible for mono-phosphorylation of Rb to progressively promote the progression into G1 phase. Therefore, the activation of the Cdk4/6 complex will be critical for cells at the G0-G1 transition. CycD is constitutively expressed throughout the cell cycle, so how is the Cdk4 or Cdk6 activated other than binding to CycD? Previously, it has been shown that Cdk7, the only known CAK in metazoans, activates Cdk2 or Cdk1 in the S,G2 phases by phosphorylating their activating T-loop sites *in vivo* (Ganuza et al., 2012).

It was recently uncovered that at early G1, Cdk4 or Cdk6 activation is also largely dependent upon Cdk7 kinase activity *in vivo* (Schachter et al., 2013). Upon mitogenic signals, the Cdk7 activity is induced via the phosphorylation of its T-loop site by unknown endogenous kinase, enabling Cdk7 to act in a T-loop cascade towards Cdk4/6. Once Cdk4 or Cdk6 are phosphorylated on their T-loop sites and bound to CycD, they become active, but require continued Cdk7 activity to combat an unknown endogenous phosphatase that targets the unprotected T-loop site. This is quite different from the activation of Cdk2 or Cdk1 complex. Cdk7 plays an essential role in the activation and maintenance of Cdk4/6 activity to promote the G0-G1 transition. T-loop phosphorylation of Cdk7 and Cdk4 both increase at G0 exit *in vivo*, which suggests a CDK activation cascade via sequential T-loop phosphorylation could underlie the G0-G1 transition.

This brings up the question of what initiates Cdk7 activation at the G0-G1 transition. Is there another CAK? Or as *in vitro* studies have shown (Garrett et al. 2001), is Cdk7 a target of active Cdk2 in vivo? If so, Cdk2 activity will be critical for the proliferation-quiescence decision at a time much earlier in the cell cycle than its best known major role in the G1-S transition.

**Using CDC6 loading to the chromatin as a way to distinguish G0**

It is believed that origins of replication need to be licensed in G1 for DNA replication to occur in S phase of the cell cycle. Replication licensing involves the assembly of the pre-replicative complexes (pre-RCs) in a sequential order (Bell and Dutta, 2003). CDC6 is one of the pre-RC components, which plays a crucial role in recruiting the putative replicative helicase (Mcm2-7) to the replication origins. It has been reported that in quiescent cells, APC/$C^{Cdh1}$ dependent CDC6 proteolysis prevents pre-RC assembly (Petersen, 2000). Other pre-RC proteins are also down-regulated in G0 (Kingsbury et al., 2005). During G1 phase, Cdk phosphorylation blocks APC/C-mediated proteolysis and stabilizes CDC6, which promotes the assembly of pre-RC at the replication origins (Mailand and Diffley, 2005). It has therefore been proposed that the absence of CDC6 from the chromatin could be a potential marker of G0.

**Using transcriptional profiles to distinguish G0**

Quiescent cells have a distinct transcriptional profile from that of proliferative cells (Coller et al., 2006; Liu et al., 2007; Oki et al., 2014). With the application of a novel cell cycle reporter which is able to separate G0 and G1 cells, it was recently found that genes enriched in G0 are largely involved in tumor suppression, inflammatory response and wound healing. Whereas genes with enriched expression in G1 are mostly cell cycle regulators involved in G1-S progression as well as mitosis (Oki et al., 2014). Moreover, quiescence is not a uniform state. In human fibroblasts, different signals (such as mitogen withdrawal, loss of adhesion and contact inhibition) induce distinct gene expression changes in the establishment of quiescence, indicating that cells may exhibit variable states of G0 in response to different environmental stress (Coller et al., 2006).

Importantly, in the long-term maintenance of G0, the gene expression changes become more similar among different conditions, and the genes that are consistently regulated involve regulators of cell growth and division, as well as genes that suppress differentiation and apoptosis (Coller et al., 2006). However, there is little overlap in the gene expression profiles identified from different studies of G0 in different cell types (Coller et al., 2006; Liu et al., 2007), which raises the possibility that different cell types have distinct G0 states, and brings us back to the original question: what are the universal molecular markers of quiescence?

## 1.4 Developmental regulation of the proliferation-quiescence decision

### The double –repression of E2F and Cyclin/Cdk activity

Despite the central role for the Rb family proteins in most models of cell cycle exit and quiescence, cell cycle exit can still occur without functional pocket proteins. In embryonic development, removal of all three Rb family members (triple knockout or TKO) in the epithelial or neuronal progenitor cells, does not prevent cell cycle exit and differentiation (Wirt et al., 2010). In the conditional Rb family triple knockout (cTKO) hepatocytes, the deletion of the Rb family causes a temporary cell-cycle re-entry, and finally cTKO hepatocytes stably exit the cell cycle (Ehmer et al., 2014). This is consistent with the finding that hyperactivation of E2F in *Drosophila* can only temporarily delay cell cycle exit, but cells still eventually arrest in G0 (Buttitta et al., 2007). Thus additional mechanisms must exist to promote quiescence in differentiating cells *in vivo*.

CKI expression is commonly associated with G0. Not surprisingly, TKO mouse embryonic fibroblasts still exit cell cycle under serum starvation, but with high $p27^{Kip1}$, $p21^{Cip1}$ levels. This implies that CKIs may act as central mediators of cell cycle arrest in the absence of functional pocket proteins (Foijer et al., 2005). In mouse models, it has been reported $p21^{Cip1}$ deletion induces proliferation in hippocampal neurons, indicating

that $p21^{Cip1}$ is required to restrain proliferation in differentiating neurons during development (Pechnick et al., 2008). The p27-null mice show increased body size and aberrant proliferation in enlarged organs, which suggests that p27 also represses cellular proliferation during development (Fero et al., 1996). However, loss of all three CKI proteins (p21,p27 and p57) in the spinal cord only delays cell cycle exit during neurogenesis (Gui et al., 2007). This is consistent with the finding in *Drosophila* that, the sole Cip/Kip-type CKI, dacapo (dap), is dispensable for most cell cycle exit in *Drosophila* tissue including eye and wing development (Firth and Baker, 2005; Buttitta et al., 2007). Therefore, Rb family and CKIs play overlapping roles in control of cell cycle exit *in vivo*. Consistently, the loss of both Rb family and CKIs leads to further proliferation in tissues that should be G0 in animals ranging from mice to *Drosophila* (Zindy et al., 1999; Firth and Baker, 2005; Buttitta et al., 2007).

**Looking beyond the pRb family and CKIs in quiescence**

Studies show that APC/$C^{Cdh1}$ is active and highly expressed in quiescent cells (Coller et al., 2006; Liu et al., 2007). Work from different groups also suggests the proliferation-quiescence transition requires the activity of APC/$C^{Cdh1}$ complex (Garcí-Higuera et al., 2008; Buttitta et al., 2010; Ruggiero et al., 2012; The et al., 2015; Cappell et al., 2016). What roles could the APC/C play to promote G0? One important target of

the APC/C is Skp2, which leads to the ubiquitination and degradation of the negative cell cycle regulators, $p27^{Kip1}$ and $p21^{Cip1}$. Thus high activity of APC/C not only leads to degradation of mitotic cyclins (Sigrist and Lehner, 1997), but also stabilizes CKIs to prevent cell cycle progression (Binné et al., 2007). Therefore, the cell cycle protein degradation machinery is yet another layer of G0 regulation (Fig.1.3).

Inhibition of the APC/C disrupts quiescence in the wing and eye in *Drosophila* (Buttitta et al., 2010; Ruggiero et al., 2012; Tanaka-Matakatsu et al., 2007). In addition, inhibition of the APC/C cooperates with the loss of other negative regulators such as Rb family. For example, repression of APC/C activity together with aberrant E2F activity is able to bypass permanent cell cycle exit in the wing in *Drosophila* (Buttitta et al., 2010). This indicates that APC/C activity is required to limit the accumulation of cyclins and other essential E2F targets that promote active proliferation. CycE/Cdk2 activity has been reported to inhibit APC/C activity (Moberg et al., 2001; Koepp et al., 2001) and thus, the high APC/C activity in quiescent, differentiating cells may also increase the threshold level of CycE required to suppress APC/C and initiate entry into G1.

In C. elegans, double mutants of Rb and the APC/C activator Cdh1 exhibit aberrant expression of S phase genes in differentiated muscle cells, suggesting that Rb-mediated transcriptional repression and $APC/C^{Cdh1}$-mediated protein degradation work in parallel to inhibit cell cycle progression in differentiated tissues (The et al., 2015). Interestingly, the CycD/Cdk4 kinase complex is able to phosphorylate both Rb and

APC/C $^{Cdh1}$ *in vitro*, resulting in their inactivation. Thus one model proposes that D-type cyclins phosphorylate and abolish Cdh1 activity towards Skp2, and thereby allowing SCF $^{Skp2}$ complex to degrade CKIs, resulting in high CycE/Cdk2 complex activity, which further inhibits the APC/C activity to push cell cycle re-entry from G0 (Bashir et al., 2004; Wei et al., 2004). Rb-mediated transcription repression, stable CKI expression protected by the APC/C complex all impinge upon the restriction of CycE/Cdk2 activity level to promote the entry into quiescence.

**Cdk2 activity thresholds at the proliferation-quiescence decision**

Recent work by Spencer *et al* suggests that cells with higher Cdk2 activity choose to proliferate and enter a new G1 phase immediately after mitosis, while cells with lower levels of Cdk2 activity enter a temporary G0-like state after mitosis. This model suggests right after mitosis, a threshold of Cdk2 activity level is the key determinant of the proliferation-quiescence decision.

The threshold of Cdk2 activity is regulated via cyclin binding, the presence of active and inhibitory phosphorylations (Morgan, 1995), and the levels of Cdk inhibitors such as p21 and p27 (Sherr and Roberts, 1999) (also known as CDKN1A and CDKN1B). The abundance and availability of a cyclin binding partner (Cyclin E in G1 or Cyclin A in S-phase and G2) together with the relative levels of phosphorylation at inhibitory Cdk2 sites (T14 and Y15) and activating sites (T160 in the T-loop) all converge to influence

Cdk2 activity levels (Morgan, 1995). In addition, there is a negative feedback loop, where Cyclin E/Cdk2 auto-phosphorylates and activates a phospho-degron to catalyze its own ubiquitination via the E3 ligase Fbw7 (Koepp et al., 2001; Moberg et al., 2001; Strohmaier et al., 2001). Phosphorylation of the inhibitory T14 and Y15 sites is regulated by the Wee/Myt kinases and counteracted by cdc25 phosphatases, however flies with knocking out these phospho-sites still exhibit essential functions, which suggests the inhibitory phosphosites play minimal or redundant roles in regulating Cdk2 activity thresholds *in vivo* (Lane et al., 2000; Zhao et al., 2012). In contrast, Cdk2 phosphorylation of the T-loop at T160 is a hallmark of active Cdk2, absolutely required for activity (Merrick et al., 2008). The Cdk2 T-loop is thought to be constitutively phosphorylated by CAK (Larochelle et al., 1998), but as described, earlier CAK activity itself can be regulated by phosphorylation. Two phosphatases have been suggested to be the T-loop phosphatase that could counteract CAK, and they are CDKN3 (also called KAP) and PP2A (Poon and Hunter, 1995; Song et al., 2001). Although functional evidence for these phosphatases on the Cdk2 T-loop *in vivo* remains lacking. As described in chapter 2, my thesis work has revealed a new role for PP2A complex in regulating the Cdk2 T-loop *in vivo*.

## 1.5 Protein Phosphatase 2A complex (PP2A)

### Composition of PP2A complexes in mammals and in *Drosophila melanogaster*

Protein Phosphatase 2A (PP2A) is a serine/ threonine phosphatase. PP2A plays roles in multiple cellular activities including cell metabolism, signal transduction, cytoskeleton dynamics, cell proliferation and apoptosis. The functional PP2A holoenzyme consists of a 36-kDa catalytic subunit (C) and a 65-kDa scaffold subunit (A), and one regulatory subunit (B) (Hendrix, Turowski et al. 1993; Shi 2009). The spatial and temporal control of PP2A mostly depends on the particular regulatory subunit in use, in other words, the regulatory subunits direct PP2A to its substrates (Slupe, Merrill et al. 2011). The catalytic and scaffold subunits are highly conserved, while the regulatory subunits are more diverse. In mammals, PP2A complexes possess two isoforms of the catalytic subunit, two of the scaffold subunit and about 20 different regulatory subunits categorized into four families. Therefore, 92 possible PP2A heterotrimeric phosphatase complexes can be assembled (Virshup and Shenolikar, 2009; Haesen et al., 2014). By contrast, in *Drosophila*, there is only one catalytic subunit, microtubule star (*mts*), one scaffold subunit, *Pp2A-29B*, and six different regulatory subunits (Table1.1, Janssens and Goris 2001). The simplicity of the *Drosophila* PP2A system facilitates genetic *in vivo* studies of PP2A functions.

**PP2A plays multiple roles in regulation of mitosis**

To date, the study of PP2A and its contributions to cell cycle progression have primarily focused on roles for PP2A in the entry and exit from mitosis. Mitotic progression depends largely on the coordinated activities of several kinases and phosphatases. CyclinB/Cdk1, mitotic promoting factor (MPF) serves as the central kinase in mitotic regulation. Entry into mitosis requires the activation of CycB/Cdk1 complex, while exit from mitosis requires its degradation and the rapid dephosphorylation of its substrates. CycB/Cdk1 activity is regulated by the balance of activity between Wee1/Myt1 kinase that phosphorylates Cdk1 for inhibition and Cdc25 phosphatase that dephosphorylates the Wee1/Myt1 sites for activation (Lew and Kornbluth, 1996). Studies in mammalian cell culture systems showed that during early mitosis the PP2A complex represses the activation of Cdc25, leading to the inactivation of CycB/Cdk1 complex, which prevents cells from precocious mitotic entry (Forester, Maddox et al. 2007). Once cells enter into mitosis, active CycB/Cdk1 complex will inhibit the PP2A-B55 complex by phosphorylating one of its key targets—Greatwall (Gwl), a nuclear localized kinase. The phosphorylation activates Gwl, which subsequently phosphorylates Endosulfine proteins (Endos). Phospho-Endos then binds and inhibits the PP2A-B55 complex by acting as a pseudo-substrate (Mochida et al., 2010; Gharbi-Ayachi et al., 2010; Williams et al., 2014). At mitotic exit, PP2A-B55 plays a key role in the timely dephosphorylation of the Cdk1 substrates, while the inactivation of Cdk1

complex is mediated by APC/C E3 ligase complex (Mochida et al., 2009; Schmitz et al., 2010). In *Drosophila*, mitotic roles for PP2A are also largely carried out by the B55 regulatory subunit called twins, which has peak expression in mitosis. Above all, PP2A-B55 is the predominant PP2A complex in mitosis (Fig.1.4).

**PP2A in tumor suppression**

PP2A has been recognized as a tumor suppressor for over two decades (Janssens, Goris et al. 2005), but the molecular mechanism for PP2A in tumor suppression remains unclear. Mutations of the genes encoding PP2A scaffold and regulatory subunits occur in several human cancers (Walter and Ruediger 2012,Janssens, Goris, & Van Hoof, 2005; Nobumori et al., 2013). For example, in human prostate cancer, it has been found that the expression levels of PP2A scaffold and one of the B56 regulatory subunits—B'γ are greatly reduced in prostate cancer compared to the benign prostate (Pandey et al., 2013). In *Drosophila* neural stem cells, loss-of-function of the catalytic subunit of PP2A complexes, called *mts* resulted in the over-proliferation of stem cells (neuroblasts), leading to a brain tumor phenotype (Wang, Chang et al. 2009). Thus, maintaining PP2A function is essential for tumor suppression.

Recent evidence suggested that a subset of PP2A holoenzymes that specifically contain B56 (B56-PP2A) have the potential to suppress tumor formation. In human lung

cancer, a point mutation in B56γ has been shown to impair PP2A/B56 phosphatase activity towards substrates. Indeed, 24 point mutations have been identified in B56 in cancers (Nobumori et al., 2013). Some of the identified mutations have been shown to disrupt the ability of PP2A/B56 to block cell proliferation. Thus, understanding how compromising PP2A-B56 function leads to excessive proliferation may elucidate its role in tumor suppression.

**PP2A roles in control of quiescence/cell cycle exit**

Several studies have suggested roles for PP2A in the proliferation-quiescence transition. For example, PP2A- B55α was suggested to promote chondrocyte cell cycle exit by dephosphorylating the Rb family protein p107 (Kurimchak et al., 2013; Kolupaeva et al., 2013). In a second proposed mechanism PP2A inhibition during G2 phase interferes with the quiescence establishment in the subsequent G1 phase (Naetar et al., 2014). It is reported that compromising PP2A function in G2 leads to hyperactivation of Ras signaling and thus leads to the induction of c-myc, a well-known oncogene essential for transformation. Accumulated CycE mRNA and protein level are also detected in the mitotic phase, likely due to the c-myc transcriptional activity. Specific depletion of one B-regulatory subunit—B56ϒ phenocopied the G0 defects caused by Okadaic Acid treatment. However, no hyperactivation of Ras signaling was

observed with depletion of B56γ alone. This indicates that B56γ is a critical component of PP2A complexes involved in G0 arrest but the molecular mechanism may be in alternative way.

The two models above indicate that PP2A complex is necessary for the decision of proliferation-quiescence, but their conclusions are inconsistent in the regulatory pathways how PP2A impacts the decision as well as when the decision occurs. This may be due to the different cell lines used in two studies, or may indicate another mechanism is at work. This also raises an intriguing question: whether PP2A will impact the proliferation-quiescence decision *in vivo* tissue development? If so, what will the molecular mechanism be? I will present data directly addressing these questions in Chapter 2.

## Figures

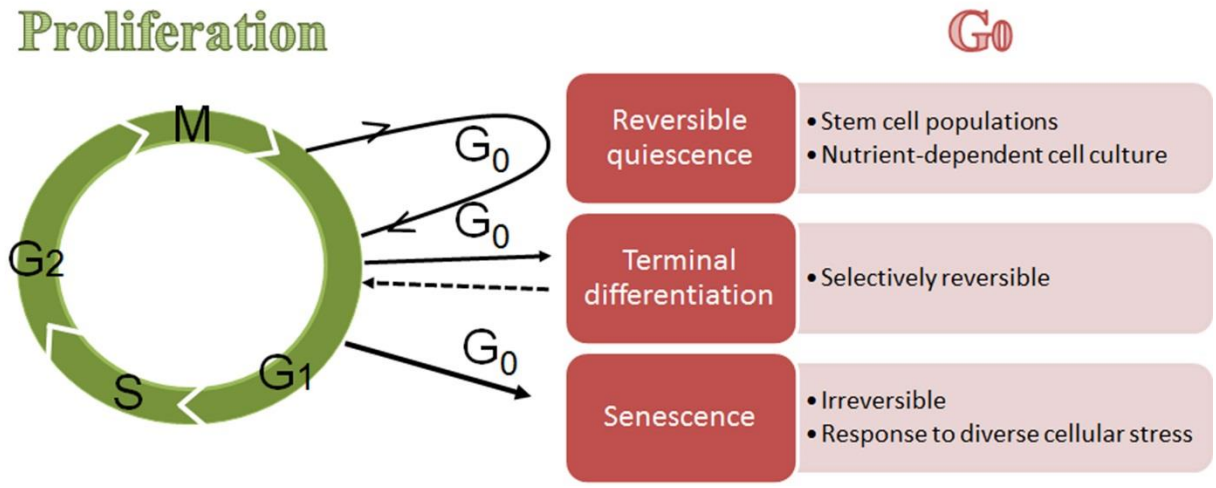


**Figure 1. 1 Distinct states of G0**

**There are at least 3 distinct states of G0 that vary in their reversibility.**

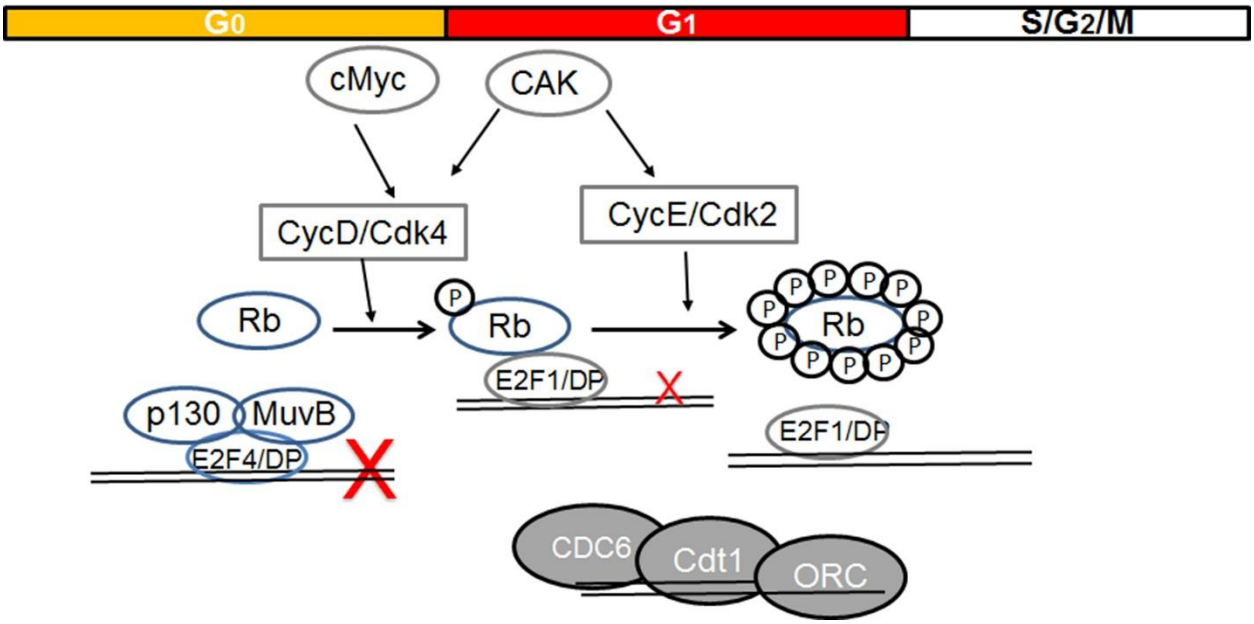


**Figure 1. 2 Molecular markers of G0-G1 progression.**

Upon G0 exit a cascade of kinase activity inhibits Rb-mediated repression, which once hyperphosphorylated allows cell cycle gene transcription. As cells enter into G1, licensing of origins for DNA replication starts.

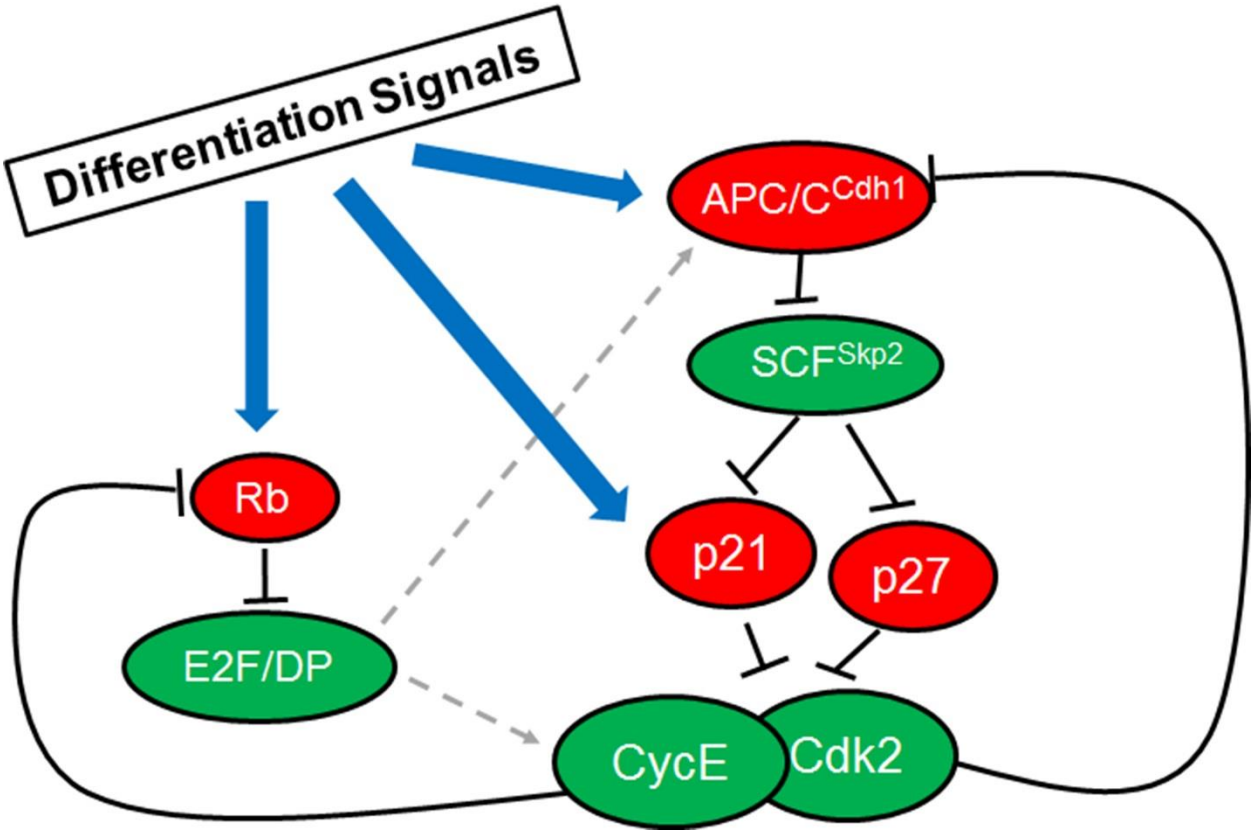


**Figure 1. 3 Regulatory pathways in control of the proliferation-quiescence decision**

Diagram shows the current studies of the regulations of the proliferation-quiescence decision in the developmental contexts. Differentiation signals triggers three redundant pathways that promotes quiescence entry while prevents cell proliferation. Regulation may act transcriptionally (grey dashed lines) as well as post-translationally (black lines) and includes both positive and negative feedback loops.

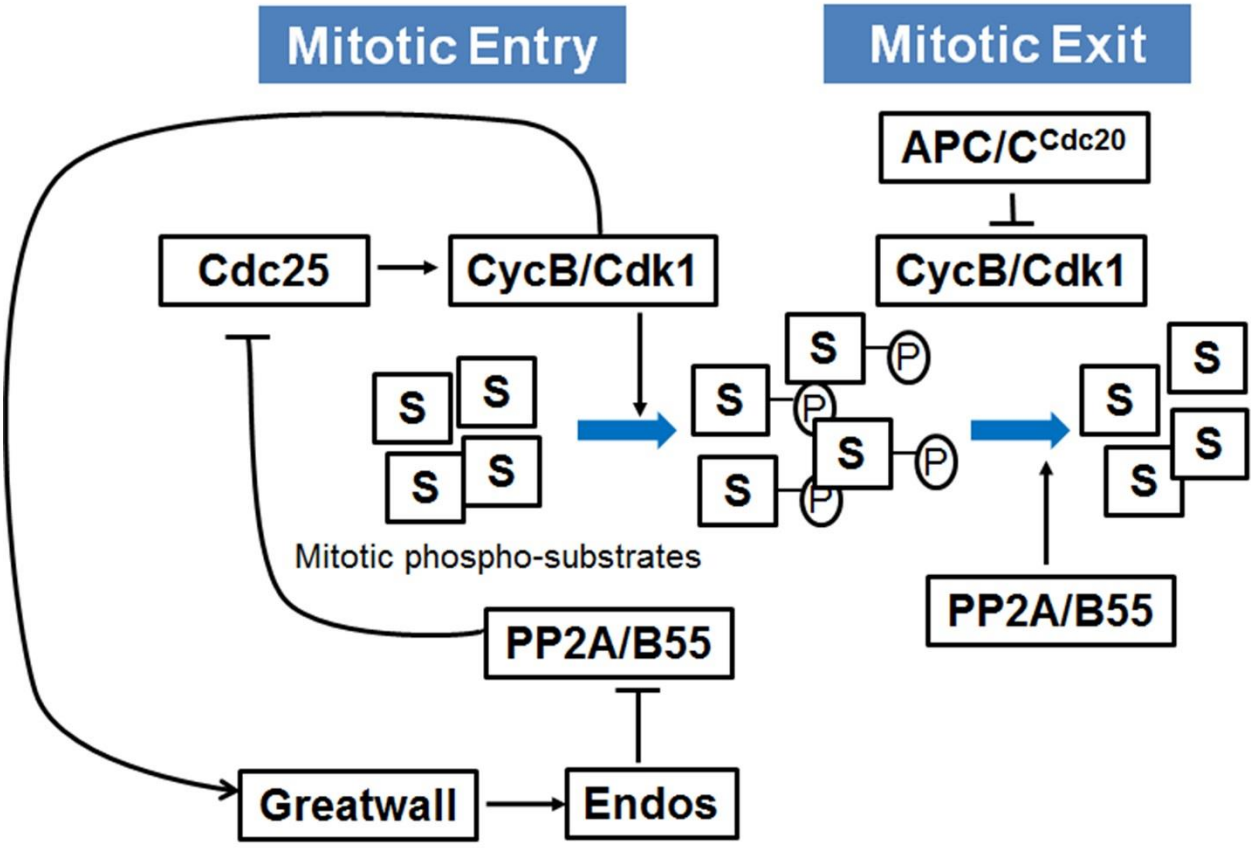


**Figure 1. 4 PP2A/B55 plays multiple roles in regulation of the mitotic entry and exit**

PP2A/B55 complex is critical to the regulation of both mitotic entry and exit. At mitotic entry, PP2A complex represses the early activation of CycB/Cdk1 complex, preventing cells from precocious mitotic entry. Upon mitotic exit, PP2A complex is responsible for the dephosphorylation of the Cdk1 substrates. Blue arrows indicate the progression of mitosis, while black lines depicts the post-translational regulations.

## Table

| Subunits | Description | Mammals | *Drosophila* |
|---|---|---|---|
| C | catalytic subunit | PP2A-Cα, PP2A-Cβ | mts |
| A | scaffolding subunit | PP2A-Aα(PR65α), PP2A-Aβ(PR65β) | Pp2A-29B |
| B | regulatory subunit | B55α B55β B55γ B55δ | twins/tws/aar |
| B' | regulatory subunit | B56α B56β B56ε B56$\gamma_1$ $\gamma_2$ $\gamma_3$ B56δ | PP2A-B'/wrd/B56-1 |
| | | | widerborst/wdb |
| | | | CG32568(sequence similarity) |
| B'' | regulatory subunit | PR72, PR48, PR130,PR59 | PP2A-B''/CG4733/dPR72 |
| B''' | regulatory subunit | striatin (PR110), SG2NA | Cka |

**Table 1.1 The composition of PP2A complexes**

**The components of PP2A complexes in mammals and *Drosophila melanogaster***

# Chapter 2. Protein Phosphatase 2A promotes the transition to G0 during terminal differentiation in *Drosophila*

This chapter was published in:

**Sun D, Buttitta L**. Protein phosphatase 2A promotes the transition to G0 during terminal differentiation in *Drosophila*. Development. 2015 Sep 1;142(17):3033-45.

## Abstract

Protein phosphatase type 2A complex (PP2A) has been known as a tumor suppressor for over two decades, but it remains unclear exactly how it suppresses tumor growth. Here we provide data indicating a novel role for PP2A in promoting the transition to quiescence upon terminal differentiation *in vivo*. Using *Drosophila* eyes and wings as a model, we find that compromising PP2A activity during the final cell cycle prior to a developmentally controlled cell cycle exit leads to extra cell divisions and delayed entry into quiescence. By systematically testing the regulatory subunits of *Drosophila* PP2A, we find that the B56 family member *widerborst* (*wdb*) is required for the role of PP2A in promoting the transition to quiescence. Cells in differentiating tissues with compromised PP2A retain high Cdk2 activity when they should be quiescent, and genetic epistasis tests demonstrate that ectopic CyclinE/Cdk2 activity is responsible for the extra cell cycles caused by PP2A inhibition. The loss of *wdb*/PP2A function cooperates with aberrantly

high Cyclin E protein, allowing cells to bypass a robust $G_0$ late in development. This provides an example of how loss of PP2A can cooperate with oncogenic mutations in cancer. We propose that the *wdb*/PP2A complex plays a novel role in differentiating tissues to promote developmentally controlled quiescence through the regulation of CyclinE/Cdk2 activity.

## Introduction

In adult metazoans, most terminally differentiated cells exit from the cell cycle and lie in a state of prolonged or permanent quiescence. The transition from active proliferation to quiescence *in vivo* is robust, often irreversible, and ensured by redundant cell cycle regulatory mechanisms (Buttitta et al., 2007; Firth and Baker, 2005; Nicolay et al., 2010; Pajcini et al., 2010; Wirt et al., 2010). By comparison, most studies of quiescence have been performed in cell culture where contact inhibition, drug treatments or withdrawal of mitogens induce a quiescent state which is most often readily reversible (Coller, 2011). While some of the key cell cycle regulators promoting quiescence in these contexts overlap (e.g. Retinoblastoma family members, Cyclin-dependent Kinase Inhibitors, CKIs), there must be critical differences between the reversible quiescence in cell culture and developmentally controlled robust cell cycle exit *in vivo*.

Recent work in mammalian cell culture has demonstrated that the level of Cdk2 activity after mitosis impacts the proliferation vs. quiescence decision for the next cell cycle, such that cells with low Cdk2 activity enter a quiescent “G0-like” state (Spencer et al., 2013). This suggests

that mechanisms regulating Cyclin/Cdk2 activity during the final cell cycle *in vivo* could impact the timing and robustness of cell cycle exit in tissues. Consistent with this hypothesis, the loss of CKIs which inhibit CyclinE/Cdk2 complexes or loss of the F-box protein Fbw7, which regulates Cyclin E stability, can partially delay proper cell cycle exit in certain tissues (Chen and Segil, 1999; de Nooij et al., 1996; Fero et al., 1996; Kiyokawa et al., 1996; Lane et al., 1996; Minella et al., 2008; Moberg et al., 2001; Tane et al., 2014). But even in the presence of aberrantly high CyclinE/Cdk2, cell cycle exit is most often only delayed by one or two cell cycles *in vivo*, demonstrating the robustness of developmentally controlled quiescence (Baumgardt et al., 2014; Buttitta et al., 2010; Loeb et al., 2005; Nakayama et al., 1996).

Determining which cell cycle regulators are required for developmentally controlled cell cycle exit *in vivo* has posed some challenges. The redundant functions of multiple paralogs for each cell cycle regulator makes genetic analysis complicated, with studies often encompassing double or triple mutants (Gui et al., 2007; Wirt et al., 2010; Zindy et al., 1999). In addition the late stage of development where cell cycle exit occurs and the asynchronous nature of cell cycle exit in many tissues requires conditional genetic manipulations and timecourse analysis of samples. *Drosophila* eyes and wings have been an advantageous system to study this process, as they undergo a relatively synchronized cell cycle exit during metamorphosis and have fewer paralogs with tools for precise conditional genetic manipulations. We used this system to examine cell cycle exit in terminally differentiating tissues and found that even in *retinoblastoma family 1* deficient cells, CyclinE/Cdk2 overexpression delays but cannot bypass cell cycle exit

(Buttitta et al., 2007), suggesting that additional downstream mechanisms ensure the transition from proliferation to quiescence *in vivo* (Ehmer et al., 2014; Nicolay et al., 2010; Simon et al., 2009).

To identify additional mechanisms ensuring cell cycle exit, we examined *Drosophila* homologs of several tumor suppressor proteins expected to play a role in promoting quiescence. PP2A has been recognized as a tumor suppressor for over two decades (Janssens et al., 2005), but the molecular mechanism for PP2A in tumor suppression remains unknown. PP2A de-phosphorylates RB family members to inhibit cycling (Kolupaeva and Janssens, 2013; Kurimchak and Grana, 2012), and removes an essential activating phosphorylation on the Cdk2 T-loop *in vitro* (Poon and Hunter, 1995). We therefore examined whether PP2A may play multiple, redundant roles to promote the developmentally controlled robust cell cycle exit *in vivo*.

Here, we show that cells with reduced PP2A function fail to transition to a quiescent state at normal developmental time. Loss of PP2A function specifically during the final cell cycle leads approximately 10% of cells to perform an extra cycle before entry into permanent quiescence. Cells with compromised PP2A exhibit increased Cdk2 activity and aberrant E2F transcriptional activity. In the presence of high, oncogenic Cyclin E the loss of PP2A function allows cells to bypass a robust $G_0$ mechanism during late stages in fly development. The PP2A enzyme is directed to distinct substrates via associations with different regulatory subunits, which can be highly dynamic during development. Here we show that the PP2A-B56 regulatory subunit *widerborst* (*wdb*) is specifically required for the PP2A- mediated transition between

proliferation and quiescence. Furthermore, this new function for PP2A-B56 occurs even in the complete absence of RB/E2F/DP function, suggesting it acts through downstream targets directly on the cell cycle machinery to promote quiescence *in vivo*.

## Results

### Loss of PP2A delays the transition to quiescence *in vivo*.

We performed a small-scale RNAi-based screen of approximately 500 randomly chosen Harvard Transgenic RNAi Project (TRiP) lines to identify new potential tumor suppressor genes involved in the proper timing of the developmentally controlled quiescence in the *Drosophila* eye. The primary screen was an adult eye-color based screen, an adaptation of the method described by Bandura and colleagues (Bandura et al., 2013). This was followed by a secondary, dissection-based screen to determine which hits from the initial screen effectively compromised cell cycle exit. Normally, the *Drosophila* eye becomes completely quiescent by 24h after pupa formation (24h APF) (Buttitta et al., 2007). We therefore looked for RNAis that compromised quiescence, leading to ectopic cell cycles at 24h APF. We used the *Glass Multimer Reporter (GMR)-Gal4* (Ellis et al., 1993) driver to express UAS-controlled RNAi lines, and assayed for ectopic S-phases by 5-ethynyl-2'-deoxyuridine (EdU) incorporation (Buck et al., 2008) and ectopic expression of a cell cycle transcriptional reporter *PCNA-GFP* (Thacker et al., 2003) in eyes after normal quiescence from 24-30h APF (Fig. S2.1). Importantly, the *GMR-Gal4* driver activates the UAS-RNAi specifically during the final cell cycle in the eye, thereby avoiding earlier deleterious effects. We found that two independent RNAi lines to the *Drosophila* PP2A catalytic subunit *microtubule star (mts)* and one to the sole PP2A scaffold A subunit, *Pp2A-29B,* caused ectopic S-phases and cell cycle gene expression, at timepoints when the *Drosophila* eye should be fully quiescent (Fig. S2.1 A-C).

To confirm the RNAi results, we overexpressed a dominant negative form of *mts* (*mts*$^{DN}$) during the final cell cycle in fly eyes and found that it fully recapitulated the RNAi phenotypes. The *mts* dominant negative is a truncation which interacts non-productively with PP2A scaffolding (A) and regulatory (B) subunits, and serves as an effective competitive inhibitor when overexpressed (Evans et al., 1999). To test whether the role for PP2A in quiescence is eye-specific, we overexpressed *mts*$^{DN}$ in the posterior wing during the final 1-2 cell cycles using *engrailed-Gal4,* modified with a temperature sensitive *Gal80*$^{TS}$ (*en*$^{TS}$, see methods for details). Similar to the eye, we observed ectopic S-phases by EdU incorporation and ectopic mitoses by staining for phosphorylation of Serine-10 on Histone H3 (PH3) at 24-28h APF, timepoints when few cell cycles are normally observed in the wing (Fig. 2.1A,B). Overexpression of a functional wild-type *mts* (*mts*$^{WT}$) however had no observable effect on quiescence in these tissues (Fig. 2.1C-D), confirming that the observed phenotype is due to the loss of PP2A function. We performed a timecourse and quantification of the mitoses in wings expressing *mts*$^{DN}$ (Fig.2.1E, S2.1D) or PP2A RNAis (Fig. 2.1F), which revealed continued mitoses in eyes and wings until 37h APF, 13h after the normal cell cycle exit in these tissues (Buttitta et al., 2007; Milan et al., 1996; Schubiger and Palka, 1987). To confirm the staining results, we measured the DNA content of pupal eyes expressing *mts*$^{DN}$ by flow cytometry. As expected from the ectopic cell cycle markers, an increased proportion of cells containing greater than 2C DNA content was observed in *mts*$^{DN}$ expressing eyes compared to stage matched controls without transgene expression (Fig.2.1G). However after 37hAPF, eyes expressing *mts*$^{DN}$ exit the cell cycle with a normal G1 DNA content. Altogether our data suggests that inhibition of PP2A during the final

cell cycle causes a temporary delay of the transition to quiescence in a compartment-autonomous manner.

**Inhibition of PP2A leads to an extra cell cycle during the delay of quiescence**.

We next investigated whether the delayed transition to quiescence caused by loss of PP2A leads to additional cell cycles or whether it is the result of a prolonged final cell cycle. To address this, we performed a clonal analysis to count the number of cells per clone, reflecting the number of cell divisions before quiescence, using the *heat shock (hs)-flp actin>stop>Gal4*/*UAS* "flip-out" system. In brief, with this system a precisely timed heat-shock leads to random cis-recombination between FRT sites (indicated by >) flanking a stop codon. Cells where recombination occurs "flip-out" the stop codon to allow Gal4-mediated gene expression, which continues permanently in all daughter cells (Pignoni and Zipursky, 1997). In this manner, the number of daughter cells can be counted after the delayed quiescence at 37h APF. Non-overlapping clones were induced at 0h APF (just prior to the final cycle) by a low-level of heat shock at 37°C. Transgenes to manipulate PP2A activity, as well as GFP to mark clones, and an apoptosis inhibitor (to prevent loss of daughters which confounds clonal cell counts) were expressed and cells per clone were counted blind for at least 100 clones in the wing blade at 42-44h APF (Fig. 2.2A, S2.1G). Most (95%) control clones expressing GFP and P35 contain 2 cells or less per clone, as the induction of the recombination occurs during or just prior the final cycle. However, 15% of clones expressing $mts^{DN}$ contain more than 2 cells per clone,

which indicates that approximately 10% of *mts*$^{DN}$ expressing cells undergo an extra cell cycle before entering G0. For comparison, when the G1 cyclin complex CyclinD/Cdk4 is directly overexpressed via Gal4/UAS, we observe 50% of cells performing an extra cell cycle, before becoming quiescent at 36h APF (Buttitta et al., 2007).

To determine whether PP2A inhibition also causes extra cell cycles in the eye, we examined the morphology of the fly eye at late pupal stages (40-42h APF). In a wild-type or control retinas (Fig. 2.2B), the apical ommatidial structure consists of four cone cells in the center surrounded by inter-ommatidial cells (IOCs) (Tomlinson and Ready, 1987). The IOCs are shared by adjacent ommatidial cores and the number of IOCs can be quantified within an ommatidial group (OG) that covers a defined hexagonal area (Figure 2.2D) (Ou et al., 2007). When PP2A is inhibited during the final cell cycle in the eye, extra IOCs are observed (17.4±0.3 cells/OG) consistent with approximately 1 extra cell cycle per OG. We confirmed the extra cycles are not due to disruption of programmed cell death in the pupal eye, as the cell number is further increased when apoptosis is inhibited (Fig. 2.2E,F). The size of the adult eye is also increased when PP2A is inhibited (Fig. 2.2H). Our cell count data suggests that PP2A inhibition enlarges the eye partly by ectopic cell proliferation, but we also consistently observed an increase in cell size. An increase in cell size is consistent with known functions of PP2A in the TOR/S6Kinase (S6K) pathway (Bielinski and Mumby, 2007; Hahn et al., 2010).

PP2A counteracts the phosphorylation of S6K, which we used as an assay to confirm the activity of our *mts* transgenes (Fig. S2.2A). To test whether the increase in active phospho-S6K

impacts the transition to quiescence, we overexpressed the GTPase, *Rheb*, which increases cellular growth, TOR signaling and phospho-S6K (Saucedo et al., 2003). We did not observe any delay in cell cycle exit in the pupal wing, nor extra IOCs in the retina when *Rheb* is overexpressed, despite increased phospho-S6K (Fig. S2.2). We therefore suggest the function of PP2A in the transition to quiescence is independent of its role in regulating phospho-S6K.

**Inhibition of PP2A leads to ectopic Cdk2 activity**.

Proper cell cycle exit in *Drosophila* eyes and wings is ensured by inhibition of E2F/DP-mediated transcription and suppression of Cyclin E/Cdk2 activity (Buttitta et al., 2007; Firth and Baker, 2005). To examine whether cells with inhibited PP2A retain high Cdk2 activity, we used anti-MPM2 staining as an *in vivo* readout for ectopic Cdk2 activity at timepoints after normal cell cycle exit. MPM-2 antibodies detect nuclear Cdk2 phospho-epitopes on the histone locus body (HLB) which occur normally only during S-phase in proliferating cells, in addition to the well-described cytoplasmic epitopes present during mitosis (White et al., 2011; White et al., 2007). We generated GFP marked clones in eyes and wings expressing CyclinE/Cdk2 as a positive control, $mts^{DN}$ or wild-type *mts* ($mts^{WT}$) during the final 1-2 cell cycles and examined MPM2 reactivity at 26h APF, two hours after normal cell cycle exit. We observed abundant nuclear HLB staining by MPM2 in cells expressing *CyclinE/Cdk2* and $mts^{DN}$, but no MPM2 staining in cells expressing $mts^{WT}$ (Fig. 2.3 A-C). This suggests that loss of PP2A leads to ectopic Cdk2 activity in normally postmitotic tissues.

We next tested whether loss of PP2A also leads to a failure to repress E2F/DP transcriptional activity during normal cell cycle exit. We used the E2F-responsive *proliferating cell nuclear antigen* (PCNA) promoter fused to GFP (Thacker et al., 2003) as a readout of ectopic E2F activity at timepoints after normal cell cycle exit. Compromising PP2A function in eyes during the final cell cycle led to ectopic E2F activity at 26h APF, a timepoint when little to no E2F activity should persist (Fig. 2.3D,E).

The repression of E2F/DP-mediated transcription upon cell cycle exit is modulated by RB binding, which is inhibited by RB phosphorylation via active Cyclin/Cdk complexes or promoted by de-phosphorylation via phosphatases. In mammals, PP2A can modulate the phosphorylation state of the RB- related pocket protein, p107, to promote cell cycle exit in chondrocytes (Jayadeva et al., 2010; Kolupaeva et al., 2008; Kurimchak et al., 2013). Thus, a plausible mechanism for PP2A regulation of the transition to quiescence could be through inhibition of *Drosophila* retinoblastoma family (Rbf)-mediated repression of E2F/DP transcriptional activity. To genetically test whether endogenous E2F/DP complexes are required for the delay of quiescence caused by PP2A loss, we used the MARCM system (Lee and Luo, 2001) to create *Dp* homozygous null mutant clones (Fig. S2.3), with and without PP2A inhibition. *Dp* null mutant cells exhibit defects in cell proliferation and *Dp* null mutant clones in larval wings are on average 3.27±0.21 times smaller than wild-type clones generated in parallel (Nicolay and Frolov, 2008). We confirmed a similar phenotype for *Dp* mutant clones in pupal wings, which are 3.06 times smaller than wild-type clones induced in parallel, Fig. 2.3G, Fig. S2.3) and *Dp* mutant

clones in the pupal wing lack Dp protein (Fig. 2.3H,I). *Dp* null mutant clones expressing $mts^{DN}$ in pupal wings exhibit ectopic mitoses in wings at timepoints after normal cell cycle exit, while no mitoses were observed in any stage-matched *Dp* null mutant clones (Fig. 2.3 G,H). This suggests that the delay of cell cycle exit upon inhibition of PP2A is epistatic to E2F/DP function, and reveals an additional role for PP2A in promoting quiescence independent of RB/E2F/DP complexes *in vivo*.

**Inhibition of PP2A function does not delay cell cycle exit by preventing APC/C activity**

The Anaphase Promoting Complex/Cyclosome (APC/C) promotes timely cell cycle exit in *Drosophila* eyes and wings by degrading residual Cyclin A and Cyclin B during the final G1 (Buttitta et al., 2010; Ruggiero et al., 2012; Tanaka-Matakatsu et al., 2007). Furthermore, the APC/C complex can cooperate with RB proteins to reinforce cell cycle exit by promoting degradation of Skp2, which targets CKIs for destruction (Binne et al., 2007). PP2A can impact the APC/C indirectly by counteracting Cyclin B/Cdk1 phosphorylations (Hunt, 2013) as well as regulating the binding and stability of the APC/C inhibitor Emi (Wu et al., 2007), which functions similarly to *Drosophila Regulator of Cyclin A1(Rca1)* (Grosskortenhaus and Sprenger, 2002). We therefore examined whether APC/C function may be inhibited when PP2A is compromised, leading to a delay in cell cycle exit. As a read-out for APC/C activity, we examined the levels of the known APC/C target, Cyclin B (CycB) by immunohistochemistry. GFP-marked clones

with transgene expression were induced by the "flipout" Gal4/UAS/Gal80$^{TS}$ system and shifted to permissive temperature during late larval stages (Fig. 2.4A-C). As a positive control, we inhibited APC/C activity by expression of *Rca1* and observed clear CycB accumulation in GFP positive cells in the posterior of larval eye imaginal discs (Fig. 2.4A, A'). However, we observed no change in CycB levels in eyes with either PP2A loss-of-function via *mts*$^{DN}$ expression or PP2A gain-of-function with *mts*$^{WT}$ (Fig. 2.4B-4C'). We also extracted protein samples from late larval eye imaginal discs and performed western blots to measure total levels of Cyclins A and B. We found that neither gain-of-function PP2A nor loss-of-function PP2A significantly increased CycA or CycB levels (Fig. 2.4D,E).

We next examined whether CycB/Cdk1 complex activation may be altered by PP2A inhibition during cell cycle exit *in vivo*. The activation of the CycB/Cdk1 complex is triggered by the removal of inhibitory phosphates on Cdk1 (at Y14 and T15) by the phosphatase cdc25c, termed *string* in *Drosophila*. The activity of *string* is rate-limiting for entry into mitosis in the wings and eyes *in vivo* (Neufeld et al., 1998) and persistent CycB/Cdk1 activity could delay proper cell cycle exit. However we did not observe significant effects on Cdk1 inhibitory phosphorylations under genetic manipulations of PP2A activity (Fig. 2.4F), in contrast to ectopic expression of *string,* which strongly reduces Cdk1 inhibitory phosphorylation as expected (Fig.2.4F).

**PP2A interacts with negative regulators of CyclinE/Cdk2 activity *in vivo*.**

Consistent with the evidence of ectopic Cdk2 activity when PP2A is compromised (Fig. 2.3 A-C), we also observed functional genetic interactions between known negative regulators of Cdk2 activity and PP2A in the fly eye (Fig. 2.5). The sole p21/p27 CKI in *Drosophila*, *dacapo (dap)*, is a major inhibitor of the CyclinE/Cdk2 complex upon cell cycle exit (de Nooij et al., 1996; Lane et al., 1996; Sukhanova and Du, 2008). We examined whether loss of *dap* cooperates with inhibition of PP2A to delay quiescence by quantifying IOCs in late pupal stages as described previously for Fig. 2.2. The loss of one copy of *dap* (using the $dap^4$ null allele) enhanced the effect of $mts^{DN}$ expression (driven by *GMR*-Gal4) on the number of IOCs (18.7±0.3), compared to PP2A inhibition alone (17.3 ±0.2) (Fig. 2.5A-5D). We also observed a 15% increase in adult eye size in *dap* heterozygotes expressing $mts^{DN}$ compared to siblings with normal *dap*, while $mts^{DN}$ expression alone caused ~8% increase in adult eye size (Fig. 2.5E). In addition, we used MARCM system to create *dap* homozygous null mutant clones, with and without PP2A inhibition via expression of $mts^{DN}$. In *dap* null mutant clones expressing $mts^{DN}$, we also observed an increase in extra cells including an increase in lens-producing cone cells, which is rarely seen in wild-type clones expressing $mts^{DN}$ (Fig.2.5G-I, S2.4I). In a reciprocal experiment, we overexpressed *dap* together with $mts^{DN}$ during the final cell cycle using the *GMR*-Gal4 driver, and observed a partial suppression of the enlarged eye phenotype caused by PP2A inhibition alone (Fig. 2.5F). This indicates that high Cdk2 activity is at least in part, required for the enlarged eye phenotype resulting from PP2A inhibition.

To confirm that the enhancement of the *dap* eye phenotypes by $mts^{DN}$ were due to impacts on CyclinE/Cdk2 function, we next examined a different negative regulator of CyclinE for genetic interactions with PP2A. Cyclin E (CycE) protein level is controlled by the SCF complex with the ubiquitin ligase Fbw7, termed *archipelago* (*ago*) in *Drosophila*. Loss of *ago* in the fly leads to aberrant accumulation of CycE protein and temporarily delays cell cycle exit of the bristle precursors in the eye (Moberg et al., 2001). Consistent with our results from loss of one copy of *dap*, we found that loss of one copy of *ago* (using the $ago^{1}$ allele) also enhanced the $mts^{DN}$ large eye phenotype (Fig. S2.4).

We next examined whether modulation of PP2A activity itself could impact CycE protein levels or stability during the final cell cycle. We used *GMR-Gal4* to drive expression of $mts^{DN}$ or $mts^{WT}$ during the final cell cycle in the eye and extracted protein from larval eyes for western blot analysis. We observed no significant increase in CycE protein levels when PP2A was compromised (Fig S2.4). Altogether our genetic data indicates that PP2A acts through a pathway independent of RB/E2F/DP, and possibly in parallel to *dap* or *ago* to regulate CycE/Cdk2 activity.

**PP2A inhibition cooperates with high Cyclin E to bypass robust cell cycle exit.**

High CyclinE /Cdk2 activity during the final cell cycle in fly tissues delays cell cycle exit, but after only a few extra cell cycles a robust cell cycle exit mechanism ensures permanent quiescence

(Baumgardt et al., 2014; Buttitta et al., 2010; Buttitta et al., 2007). We asked whether PP2A inhibition could promote cells with aberrantly high CycE expression to override the robust transition to quiescence and maintain proliferation during later stages in development, as suggested by its known role as a tumor suppressor. To test this, we used *GMR*-Gal4 to drive *UAS-CycE* expression together with the Baculoviral apoptosis inhibitor P35 (to minimize corrective apoptosis) with or without PP2A inhibition via $mts^{DN}$. We examined proliferation in the eye at late pupal stages, several hours after the normal robust exit that occurs even in the presence of de-regulated CycE (Fig. 2.6A-D). Pupal eyes expressing Cyclin E without any PP2A modulation exhibit few S-phases and mitoses at this late stage of development, while eyes expressing CycE together with $mts^{DN}$ maintain high proliferation even after the stage normally associated with robust permanent cell cycle exit. To further confirm this, we isolated late pupal eyes and performed flow cytometry to examine the DNA content in eyes at 46h APF. When eyes overexpress CycE, only about 9% of cells from the entire retina exhibit an abnormal S/G2 DNA content. By contrast, when PP2A is compromised in stage-matched eyes over-expressing CycE, 27% of cells exhibit abnormal S/G2 DNA contents (Fig. 2.6F). This suggests that PP2A normally functions as a barrier to limit the bypass of cell cycle exit when CycE is de-regulated *in vivo*.

**The PP2A B56 subunit *widerborst* regulates the transition to quiescence *in vivo***.

To identify the PP2A regulatory subunit responsible for promoting quiescence in differentiating tissues, we systematically tested each PP2A regulatory subunit in *Drosophila* for phenotypes in the eye (Table 2.1). We used RNAi to knockdown regulatory subunits during the final cell cycle, and compared the adult eye sizes of progeny (Fig. S2.5A). Inhibition of the *Drosophila* B56 epsilon homolog (also called PPP2R5E) *widerborst* (*wdb)* led to an enlarged eye phenotype, similar to what we observe with $mts^{DN}$ expression, whereas knockdown of the B55 homolog *twins* causes a decrease in eye size, perhaps due to defects in mitosis (Brownlee et al., 2011; Chen et al., 2007). To test directly whether *wdb* is required for cell cycle exit, we used a dominant negative form of *wdb, *$wdb^{DN}$ (Hannus et al., 2002). Expression of $wdb^{DN}$ driven by $en^{TS}$-Gal4 during the final 1-2 cycles in the wing or *GMR-Gal4* driving $wdb^{RNAi}$ during the final cell cycle in the eye, leads to ectopic S-phases and mitoses in tissues at developmental timepoints that are normally quiescent (Fig. 2.7A,A', Fig. S2.5C,D). We also observed ectopic E2F/DP transcriptional activity at normally postmitotic stages when *wdb* is knocked down (Fig. S2.5I). We quantified the mitotic index in pupal tissues expressing $wdb^{DN}$ at 26h APF (Fig. 2.7C), and found that the defect in cell cycle exit upon *wdb* inhibition is less dramatic than the defect caused by inhibition of *mts*. We suggest that either the dominant-negative *wdb* does not completely block *wdb* function, or *wdb* may not be the only PP2A regulatory subunit involved in the transition to quiescence and other subunits may provide some partially overlapping functions.

Consistent with our previous tests of genetic interactions between PP2A and negative regulators of CycE/Cdk2 activity, we observed that adult eye size is increased by15% in *dap* heterozygotes expressing $wdb^{DN}$ compared to $dap^{WT}$ siblings (Fig. 2.7E). Inhibition of *wdb* alone causes an ~8% increase in adult eye size, suggesting that loss of one copy of *dap* synergizes with inhibition of *wdb*, similar to the genetic interaction we observed with *mts*.

We next tested whether *wdb* contributes to the role of PP2A as a barrier to limit the bypass of cell cycle exit when CycE is de-regulated *in vivo*. We examined the morphology of the ommatidial structure in pupal retinas expressing CycE or CycE + $wdb^{DN}$ as described previously for Fig. 2.6. The expression of $wdb^{DN}$ and CycE expression together dramatically enhances the number of IOCs (Fig. 2.7F,G), indicative of continued cycling in the late pupal retina. By contrast, when the B55 family regulatory subunit (*twins*) is knocked down by RNAi in the CycE expressing background, there is no obvious difference in IOC cell number compared to CycE expression alone (Fig. S2.5J-L). Our data thus indicate that *wdb* contributes to the role of PP2A as a barrier to limit proliferation when CycE is de-regulated in terminally differentiating tissues.

**Inhibition of PP2A increases the T-loop phosphorylation of Cdk2.**

Our data suggest that PP2A may promote quiescence by limiting Cdk2 activity during the final cell cycle *in vivo* to restrict proliferation in terminally differentiating tissues. To test this hypothesis, we compromised PP2A function *in vivo* by expressing $mts^{DN}$ and CycE in the

posterior larval eye under the control of the *GMR-Gal4* promoter, followed by immunoprecipitation of CycE to measure effects on CycE/Cdk2 kinase activity. When $mts^{DN}$ is expressed in the posterior larval eye, we observe a 20-40% increase in CycE/Cdk2 kinase activity after normalization to the amount of CycE pulled down (Fig. 2.8A). One interpretation of this result is that PP2A knockdown leads to an increase in CycE/Cdk2 activity, however it is also possible that the observed increase in CycE/Cdk2 kinase activity is a result of the increased proliferation we observe when CycE is expressed under conditions where PP2A is compromised (e.g. Fig 2.6B,D) and not a direct effect of PP2A on CycE/Cdk2 activity. To distinguish whether the increased Cdk2 activity is due to an immediate effect of PP2A inhibition on CycE/Cdk2, we performed a kinase assay in *Drosophila* S2R+ cultured cells, where we can use short-term treatments with the pan-PP2A inhibitor Okadaic Acid (OA) to discern immediate versus indirect effects of PP2A inhibition on CycE/Cdk2 activity. We performed a timecourse and dosage test of OA treatment in S2R+ cells and confirmed that with 30 minutes of OA treatment, PP2A activity is inhibited as assessed by increased phosphorylation of S6Kinase. We therefore performed a timecourse of OA treatment on S2R+ cells transiently transfected with a CycE expression vector and performed CycE/Cdk2 kinase assays as described above. We found that with 30min of OA treatment, S2R+ cells exhibit a mild increase in CycE/Cdk2 activity (Fig. 2.8C), consistent with a direct effect of PP2A on CycE/Cdk2 activity. However upon longer OA treatments (2h shown), cells exhibit a reduction in CycE/Cdk2 kinase activity and a slower migrating form of CycE protein is immunoprecipitated (Fig. 2.8D). In mammalian cells, PP2A/B55$\beta$ can dephosphorylate the N- and C-terminal phosphodegrons of CycE1 (Tan et al.,

2014). Thus the slower migrating form of CycE we observe may be due to inhibition of PP2A/Twins (B55) by OA in *Drosophila* which impacts the measured CycE/Cdk2 activity. Altogether, our data suggests that short-term inhibition of PP2A can increase CycE/Cdk2 activity, while a prolonged loss of PP2A function impacts CycE/Cdk2 in a complex manner, due to differing functions of multiple PP2A complexes. We suggest there may be smaller contribution of PP2A/B55 complexes to the overall PP2A activity during the final cell cycle *in vivo*, compared to actively proliferating S2R+ cells *in vitro*.

PP2A can bind and remove an activating phosphate on the T-loop of human Cdk2 *in vitro* (Poon and Hunter, 1995) and the T-loop and critical activating phosphorylation sites are conserved between mammals and *Drosophila*. To test whether PP2A complexes limit CyclinE/Cdk2 activity after mitosis by removing the Cdk2 T-loop phosphorylation, we turned to murine cell lines where cells can be synchronized in M-phase and Cdk2 phospho-T-loop specific antibodies are available. We synchronized NIH 3T3 mouse embryonic fibroblasts (MEFs) in M-phase with a nocodazole treatment to de-polymerize microtubules. We then released cells from the mitotic arrest and performed a time-course analysis of Cdk2 T-loop phosphorylation in cells treated with the pan-PP2A inhibitor Okadaic Acid (OA) versus vehicle only. We observed that 8h after release from a mitotic arrest, treatment with OA for 30 minutes increases T-Loop phosphorylation 2-fold over a vehicle treated control (Fig. 2.8F). We next tested whether a similar OA treatment in asynchronously proliferating mouse fibroblasts could lead to an increase in Cdk2 T-loop phosphorylation. We observed a mild increase (20%) on

Cdk2 T-loop phosphorylation in 3T3 MEFs, while we detected no effect on Cdk2 T-loop phosphorylation in primary asynchronous MEFs. This suggests that redundant mechanisms may limit the effect of PP2A on the T-loop in primary cells. However, we observed a 50% increase in Cdk2 T-loop phosphorylation in p27-knockout ($p27^{KO}$) primary MEFs treated with OA (Fig. 2.8G), suggesting that PP2A may preferentially act on Cdk2 complexes that are not bound to Cdk inhibitors. We also observed increased levels of Cdk2 in $p27^{KO}$ MEFs suggesting the role of PP2A may be fully revealed under conditions where Cyclin E/Cdk2 levels are high, but need to be rapidly inhibited. This is consistent with the genetic interactions we observed in *Drosophila* between PP2A and the p27 homolog *dacapo*.

An interaction between *Drosophila* Wdb and Cdk2 in a yeast two hybrid assay has been reported (Stanyon et al., 2004). To confirm whether PP2A/Wdb complexes interact with CycE/Cdk2 complexes, we performed an immunoprecipitation of endogenous Cyclin E with a V5-tagged Wdb in proliferating $S2R^{+}$ cells (Fig. S2.6A). We observe a mild enrichment of Cyclin E in samples with Wdb-V5 pulled down, compared to controls and mock precipitations. The enrichment of CycE may be mild because PP2A/Wdb interacts with many substrates in a transient manner throughout the cell cycle. We propose that only a fraction of the precipitated Wdb-V5 complexes at a given time from asynchronously proliferating cells will therefore contain endogenous CycE. To examine this in more detail, we next transfected CycE and Wdb-V5 expression vectors in $S2R^{+}$ cells, and examined cells for co-localization of the proteins during the cell cycle. We found that Cyclin E and Wdb-V5 co-localize in the cytoplasm during mitosis

(Fig. S2.6B). Cyclin E is predominantly nuclear, but becomes dispersed in the cytoplasm during nuclear envelope breakdown in mitosis, while Wdb is predominantly in the cytoplasm. This suggests that PP2A/Wdb complexes most likely interact with Cyclin E/Cdk2 complexes transiently during or just after mitosis, before nuclear envelope re-formation. This is consistent with our results in 3T3 cells, which suggest that the maximal effect of PP2A on the Cdk2 T-Loop occurs about 8 h after a mitotic release. Altogether, our studies suggest that B56/PP2A can act to restrict CycE/Cdk2 activity after mitosis to promote quiescence *in vivo*.

## Discussion

We identify a new role for PP2A in promoting quiescence during the transition to a permanently postmitotic state in *Drosophila* wings and eyes. In our studies we observe that approximately 10% of cells undergo an extra cell cycle when PP2A functions are compromised. While this effect may appear small, the cell cycle exit mechanism *in vivo* is so robust that cells completely lacking major cell cycle regulators such as the RB family member *rbf1* or the sole p21/p27-type CKI *dacapo* only exhibit a mitotic or S-phase index of 9% or less in eyes and wings (Buttitta et al., 2007; Sukhanova and Du, 2008). As with other cell cycle regulators that act redundantly to promote cell cycle exit, we see synergism when PP2A is compromised under conditions de-regulating the G1-S Cyclin, Cyclin E (Firth and Baker, 2005).

Cells with reduced PP2A function exhibit ectopic cell cycle markers until 13h after normal exit timing, which is roughly consistent with the one extra cell division we measure by clonal lineage analysis. Importantly, the ectopic proliferation phenotypes we observe are the result of manipulating PP2A functions specifically during the final 1-2 cell cycles, without disturbance of prior PP2A mitotic functions during active proliferation.

### PP2A impacts the proliferation-quiescence decision *in vivo*

Recent studies on PP2A in the proliferation-quiescence decision have revealed that PP2A activates the retinoblastoma protein related family member p107 by dephosphorylation to

promote growth arrest in chondrocytes (Kolupaeva et al., 2008; Kurimchak et al., 2013). Another group recently found a second mechanism for PP2A to promote quiescence, whereby PP2A/B56 inhibits Ras signaling during G2 phase which limits subsequent Myc expression and reduces Cyclin E expression in the following G1 (Naetar et al., 2014). This promotes quiescence by limiting Cyclin E, which would otherwise disrupt the association of RB family members with E2F/DP complexes by phosphorylation. Our data however suggest there is yet another mechanism during the final cell cycle *in vivo*, independent of Ras/ERK signaling, dMyc (Fig. S2.7), Cyclin E levels (Fig. S2.4), and RB/E2F/DP function (Fig. 2.3), which promotes timely entry into quiescence. This additional mechanism acts directly on the cell cycle machinery, downstream or in parallel to RB/E2F/DP function, which appears to be critical for the extremely robust type of developmentally controlled $G_0$ observed *in vivo.*

**B56 regulatory subunits promote quiescence *in vivo*.**

The emergence of multiple pathways for PP2A to promote quiescence may be due to PP2A's broad functions, with impacts on various substrates in different cell cycle phases (Janssens et al., 2005; Mumby, 2007; Westermarck and Hahn, 2008; Yang and Phiel, 2010). In normal development, cells enter into quiescent state in response to developmental signals, while in cell culture serum deprivation is most often used for the synchronization in G0, via disrupted metabolic signals (Naetar et al., 2014). It may be that in these different biological contexts, PP2A acts upon different targets to influence the proliferation-quiescent decision. PP2A is

directed to distinct targets via the regulatory subunit, which has dynamic associations and localizations during the cell cycle. It is therefore important to note that consistent with the recent work of Naetar *et. al*., we also independently identified a B56 regulatory subunit (*wdb)* as the main PP2A regulatory subunit promoting quiescence *in vivo.* However our data demonstrates that *wdb* acts via a different mechanism to promote permanent cell cycle exit *in vivo*.

Most known cell cycle functions for PP2A in *Drosophila* involve the B55 regulatory subunit *twins* and its roles in regulating mitotic entry and exit (Brownlee et al., 2011; Chabu and Doe, 2009; Chen et al., 2007; Wang et al., 2013; Wang et al., 2011). Consistent with this, when we manipulate PP2A activity in early tissues such as the actively proliferating larval wing or eye, we also observe disruptions of mitosis. An inhibitory role for PP2A in the Hippo signaling pathway which regulates tissue growth, survival and proliferation has also been described (Ribeiro et al., 2010). However the role for PP2A inhibiting Hippo signaling acts via B''' regulatory subunits and exactly opposite to the growth and cell cycle phenotype we observe here. The requirement for *wdb* during the final cell cycle to promote quiescence implies that the PP2A enzyme complexes may switch from predominantly B55 (*twins*) to B56 (*wdb*) during the final cell cycle, mitotic exit and the subsequent G0 arrest. Understanding how the switches in PP2A regulatory subunits are regulated during the cell cycle and in response to developmental signals will be an important area for future study.

**PP2A inhibits CyclinE/Cdk2 activity during the final cell cycle to promote quiescence.**

A recent study monitoring single-cell cycle dynamics in cell culture demonstrated that thresholds of Cdk2 activity after the completion of mitosis regulate the subsequent proliferation-quiescence decision (Spencer et al., 2013). Our data suggest a role for PP2A in limiting Cdk2 activity during the final cell cycle *in vivo* to restrict proliferation in terminally differentiating tissues. Inhibition of PP2A during the final cell cycle leads to ectopic Cdk2 activity as detected by the anti-MPM2 epitopes at the HLB (Fig. 2.3) and genetically cooperates with Cyclin E inhibitors, *ago* and *dacapo*. In mammalian cells, PP2A inhibition after mitosis leads to an increase in the activating Cdk2 T-loop phosphorylation. It is possible that PP2A and Cyclin E/Cdk2 also share downstream targets in cell cycle regulation, similar to the role of PP2A/B55 complexes in reversing Cdk1 phosphorylation of mitotic targets. However, we could not confirm any effect of PP2A genetic manipulations on the phosphorylation of *Drosophila* Rbf, an important target of Cyclin E/Cdk2 activity for cell cycle exit in flies (Meyer et al., 2000) (Fig. S2.6C). We suggest that PP2A/Wdb acts to modulate Cyclin E/Cdk2 activity during the final cell cycle to help promote rapid and timely induction of G0 during development.

## Materials and Methods

### Fly stocks

$w^{1118}$

y w $hsflp^{122}$;+;UAS-CycE,UAS-Cdk2 (Buttitta et al., 2007)

y w $hsflp^{122}$;UAS-CycD,UAS-Cdk4;+ (Datar et al., 2000)

y w $hsflp^{122}$;UAS-CycA;+ (Jacobs et al., 2001)

y w $hsflp^{122}$; UAS-Stg/CyO-GFP; + (Neufeld et al., 1998)

y w $hsflp^{122}$;+;UAS-Dacapo (Neufeld et al., 1998)

y w $hsflp^{122}$; +; UAS-HA-Rca1/TM6B

y w $hsflp^{122}$;+;UAS-Rbf (Neufeld et al., 1998)

y w $hsflp^{122}$;+;UAS-Rbf $^{RNAi}$

w;tub>CD2>gal4,UAS-GFP;tub-$gal80^{TS}$,UAS-Diap (UAS-Diap from (Lohmann et al., 2002))

w;UAS-P35;act>CD2>gal4,UAS-$GFP_{NLS}$ (Neufeld et al., 1998)

FRT42D,$Dp^{a3}$/CyO-GFP;+ (Frolov et al., 2005)

w;FRT42D,$dap^{4}$/CyO-GFP (Lane et al., 1996)

w;FRT82B $ago^{1}$/TM6B (Moberg et al., 2001)

y w hsflp$^{122}$,tub-gal4,UAS-GFP;FRT42D tub-gal80

y w hsflp$^{122}$;GMR-gal4;PCNA-GFP (Bandura *et al*., 2013)

w; GMR-gal4, UAS-CycE; GMR-P35 (kindly provided by H. Richardson)

w; GMR-gal4; Dr/TM6B

w; en-gal4,UAS-GFP; tub-gal80$^{TS}$

UAS-P35;+;sb/TM6B

UAS-mts$^{DN}$ (Chabu and Doe, 2009)

UAS-mts$^{WT}$ (Wang et al., 2009)

UAS-wdb$^{DN}$ (Hannus et al., 2002)

**Histology and antibodies**

Pupae, staged from white pre-pupae (0 hr after pupa formation, hr APF) at 25℃, were dissected and fixed as described (Buttitta et al., 2007). Pupal cuticle was removed from wings post fixation. Note that the wing hinge and notum were excluded from our quantifications. Hoechst 33258 (Molecular Probes, 1 □g/ml) labels nuclei. Antibodies Used: Rabbit α-phospho-Ser10-histoneH3 (PH3, Upstate,1:4,000), mouse α-MPM2 (Upstate, 1:200), rabbit α-GFP (Molecular Probes, 1:1,000), mouse α -CycB (DSHB,F2F4, 1:100), mouse α-Discs Large (DSHB,4F3,

1:100), anti-*Drosophila* Dp (gift from Dr. M. Frolov). Appropriate secondary antibodies were Alexa 488, 568 or 633 conjugated (Molecular Probes) or HRP conjugated (Jackson ImmunoResearch) and used at 1:4,000. EdU incorporation was performed using Click-iT EdU Alexa Fluor 555 Imaging Kit from Life Technologies.

**IOC counting**

The IOCs are shared by adjacent ommatidial cores, and the number of IOCs is quantified within an ommatidial group (OG) that covers a defined hexagonal area (bordered by yellow dashed dots in Fig.2) with its apices being the adjacent ommatidial centers. Those secondary pigment cells crossed by the dashed lines were counted as half. At least 15 OG's were scored from independent samples for each genotype. (Method from (Ou, Wang, Jiang, & Chien, 2007))

**Clonal analysis**

Clones were induced by heat shock for 7 min. at 37℃ between 48-70hr AED in a *hsflp*; *tub>CD2>Gal4, UAS-GFP; tub-Gal80$^{TS}$,UAS-Diap* background. Animals were aged at 18℃ (permissive for Gal80$^{TS}$, Gal4 OFF), and shifted to 28℃ (non- permissive for Gal80$^{TS}$, Gal4 ON) at late L3 instar larval stage, collected at 0h APF and aged to different stages in metamorphosis. Experiments using *engrailed*-Gal4 with Gal80$^{TS}$ were carried out in the same way, except that experiments restricting transgene expression to the final cell cycle were shifted

to 28℃ at 0h APF. By phenotypic analyses and GFP visualization, we confirmed complete inhibition of Gal4 in the lines used here with $Gal80^{TS}$ at 18℃, and we detected activation of target genes within 6 hr of shifting to 29℃. Development at 28℃ proceeds 1.15 times faster than at 25℃, and 2.2 times more slowly at 18℃ (Ashburner, 1989). All incubation times were adjusted accordingly. Hours APF are presented as the equivalent time at 25℃ for simplicity. Loss-of-function clones were generated using MARCM (Lee and Luo, 2001). Larvae were heat shocked for 20 min at 37℃ at early third larval instar, collected for staging at 0 hr APF, aged at 25℃ and dissected at the indicated times.

**Clonal cell counts to quantify cell divisions**

Non-overlapping clones labeled with GFP, expressing the indicated transgenes, were induced at 0 h APF (white prepupae) with 2 min heat-shock at 37℃. Wings were dissected and fixed 40-42 h later, nuclei were labeled with 1 µg/ml Hoechst 33258, and GFP-positive cells per clone were scored blind on a Leica DMI6000 microscope. Cells per clone were counted blind for at least 100 clones in the wing blade and the average cell number per clone reflects the number of cell divisions that undergoes before exit. We excluded clones in the wing margin, hinge, notum area, and hemocytes in the veins. Transgenic expression of an apoptosis inhibitor (UAS-P35) was used in the clonal cell count experiments, including all controls.

**Flow Cytometry**

Dissociation of cells from staged, dissected pupae and FACS were carried out as described (Flegel et al., 2013). All experiments were carried out at least three times; representative examples are shown.

**Western Blotting and Kinase Assays**

Antibodies used: rabbit anti-CycE (Santa Cruz, sc-33748), goat anti-CycE (Santa Cruz, sc-15905), mouse α-CycA (DSHB,A12, 1:1000), mouse anti-CycB (DSHB, 1:1000), rabbit anti-phospho Cdc2(Cell Signaling, 1:1000), rabbit anti-Cdc2 (Upstate, 1:1000), anti-phospho S6K(Thr398)(Cell Signaling, 1:333), anti-dmyc (Santa Cruz, sc-28207), anti-dpERK (Sigma, M8159,1:500), anti-pERK (Cell Signaling, 1:1000), anti-HA probe (Santa Cruz, sc-805), anti-mouse phospho-Cdk2$^{T160}$ (Cell Signaling, 1:500), anti- mouse Cdk2(Santa Cruz, M2, 1:1000), anti-*Drosophila* Rbf (DX3), anti alpha-tubulin (DSHB,12G10, 1:1000), beta-tubulin (Sigma, 1:1000) or anti-mouse GAPDH (Cell Signaling, 14C10, 1:2000) were used as loading controls with the appropriate HRP-conjugated secondary antibody. Enhanced Chemiluminescence-detection (Amersham) followed by digital imaging (to prevent signal saturation, Bio-Rad) was performed and band signal intensity was quantified using NIH Image J. For kinase assays, cell lysates were collected either from late L3 imaginal discs or S2R$^{+}$ cells transfected with pMT-

Cyclin E. For the S2r cells, 30min or 2h OA (50nM) treatment was performed before cell harvest. See details in (Guest et al., 2011).

**Microscopy**

Images were obtained using a Zeiss LSM 510 confocal or Leica DMI6000 epifluorescence system with deconvolution (ImageQuant). All images were cropped, rotated and processed using Adobe Photoshop. For brightness/contrast the Auto Contrast function was used. All brightness/contrast adjustments were applied equally on the entire image. Adult eye images were obtained using Leica MZ10F microscope and a Nikon Ds-Vi1 digital camera. All adult eye images were measured using Nikon NIS Elements D software and processed with Adobe Photoshop.

**Cell culture**

*Drosophila melanogaster* S2R+ cells were cultured at 25°C in Schneider's insect medium supplemented with 10% fetal bovine serum (FBS). NIH3T3, $p27^{WT}$ and $p27^{KO}$ mouse embryonic fibroblast cells were cultured at 37°C, 5%$CO_2$ in Dulbecco's Modified Eagle Medium (DMEM) supplemented with 10% fetal bovine serum (FBS). For cell cycle synchronization, NIH 3T3 cells were treated with 200ng/uL Nocodazole for 18-20h. The constructs pMT-Wdb-V5 and pMT-

Cyclin E were transiently transfected using Fugene (Roche) and expressed by Copper induction (0.5mM) in S2R+ cells.

**Acknowledgements**

We thank Drs. M. Frolov, H. Richardson, S. Eaton, Y. Chabu, H. Wang, Y. Su, R. Duronio and the Bloomington Stock Center (NIH P40OD018537) for flies and Drs. J.E. Lee, C.Y. Lee, C. Duan and the Developmental Studies Hybridoma Bank for antibodies. We thank Drs. R. Smith-Bolton, K. Cadigan and C.Y. Lee for helpful comments on the manuscript and Dr. B. Edgar, in whose lab the initial pilot RNAi screen for cell cycle exit regulators was performed. We also thank Dr. J. Nandakumar and his lab members for their help and advice on kinase and pull-down assays. We thank Dr. A. Minella for providing $p27^{WT}$ and $p27^{KO}$ MEFs. We also thank Sapha Hassan and Kerry Flegel for technical assistance. This work was supported by the National Institute of Health grant R00GM086517 (LB), the Biological Sciences Scholars Program (BSSP) and startup funding from the University of Michigan. Author contributions: D.S. and L.B. developed the approach, performed the experiments, and prepared the manuscript.

## Figures

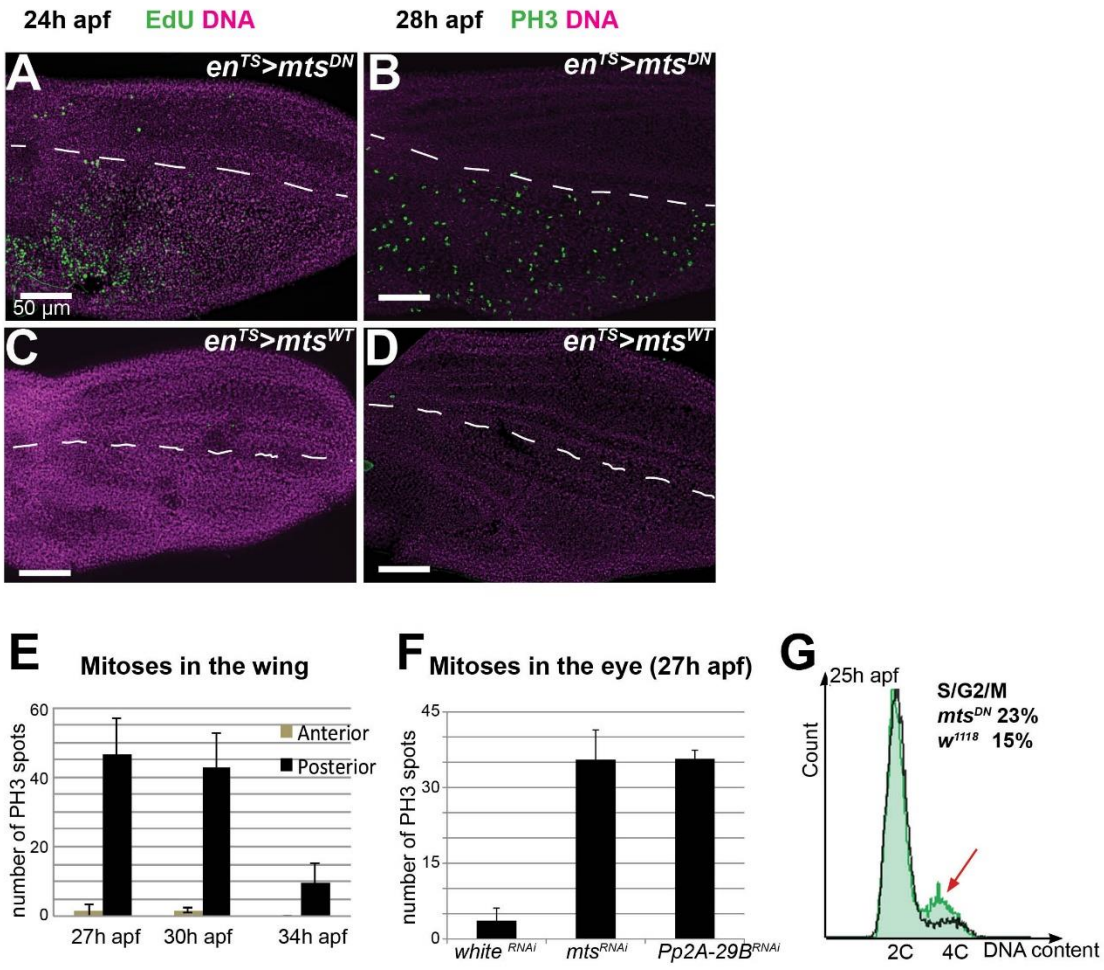


**Figure 2. 1 PP2A promotes the timely transition to quiescence *in vivo*.**

(A-D) Expression of a dominant negative *mts (mts*$^{DN}$ in A,B) or wildtype *mts* (*mts*$^{WT}$ in C,D) was restricted to the posterior wing during late larval stages using the *engrailed-Gal4/temperature-sensitive Gal80,UAS* system *(en*$^{TS}$). Pupal tissues were dissected at 24h APF and labeled with EdU for 1h to visualize S-phases (A,C) or labeled with anti-Phospho-histone H3 Ser10 (PH3) to visualize mitoses at 28h APF (B,D). In regions where PP2A function is compromised by *mts*$^{DN}$,

cells continue cycling when they should be postmitotic. (E,F) Quantification of ectopic mitoses in pupal tissues at different time points during normally postmitotic stages reveal a delay of cell cycle exit by about 10h. (G) Flow cytometry was used to assess the DNA content of 25h APF eyes with $mts^{DN}$ expression (green trace) or controls (black trace). The arrow indicates an increase in cells with non-G1 DNA content. Bar = 50um.

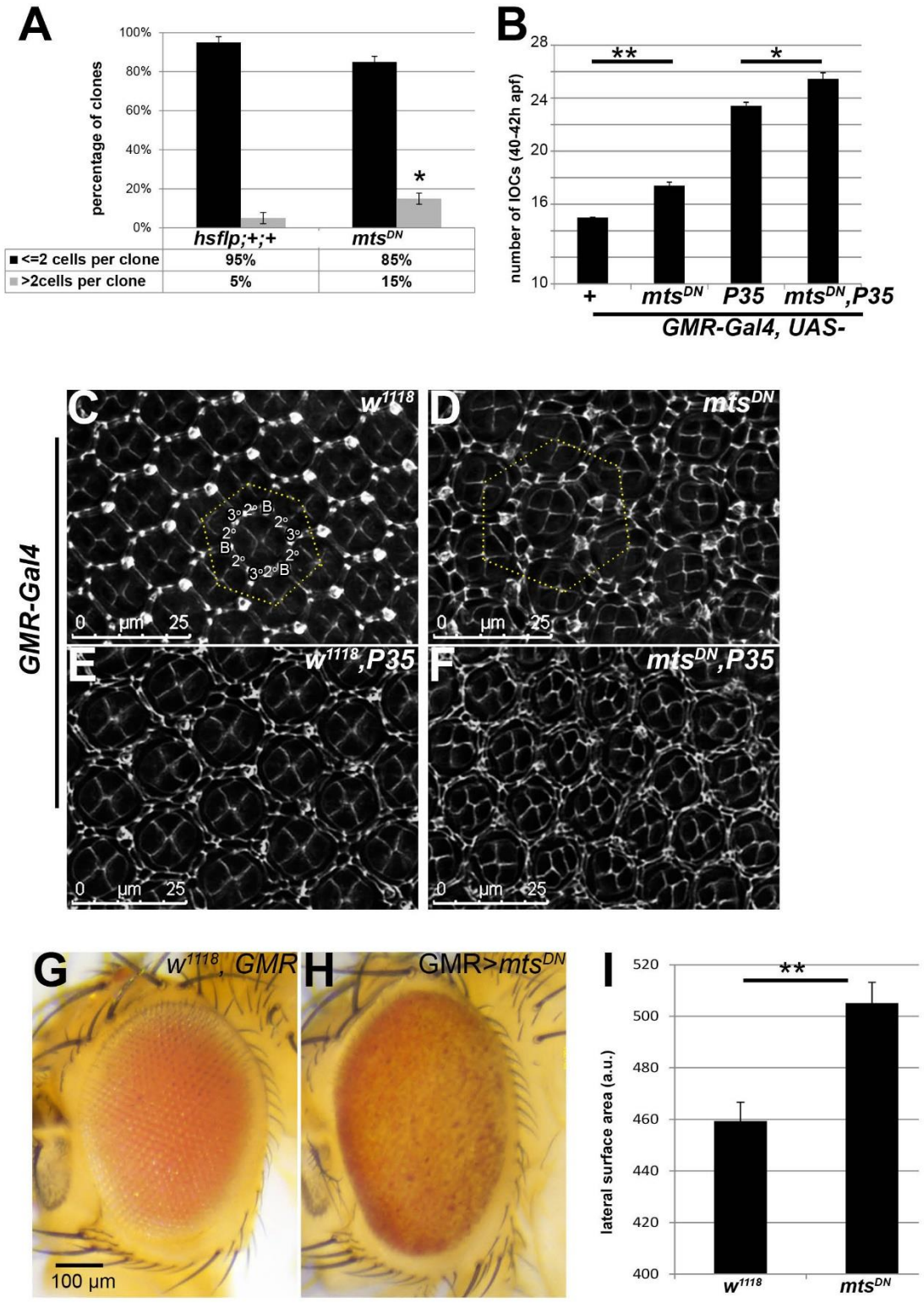


**Figure 2. 2 PP2A inhibition during the final cell cycle leads to extra cell divisions during tissue development.**

(A) Clonal-lineage analysis in the wing was used to measure the number of cell cycles before entry into quiescence. GFP marked clones were induced at the start of metamorphosis, 0h APF during the final cell cycle using the *hs*-Flp *actin>Gal/UAS* system. Wings were examined 42-44h later and cells/clone were quantified for at least 100 clones/genotype. Clones also express the apoptosis inhibitor P35 to prevent apoptosis. Approximately 10% of cells undergo an extra cell cycle when PP2A is inhibited during the final cell cycle to generate an increase in clones with >2 cells. (B-F) *GMR-Gal4/UAS* was used to drive expression of the indicated transgenes in the eye, specifically during the final cell cycle. Quantification of interommatidial cell (IOC) number was performed at 40-42h APF in retinas stained for Dlg to reveal cell morphology. Cell types of IOC were labeled as: B, bristles; $2^o$,secondary pigment cell; $3^o$, tertiary pigment cell. IOCs are shared by adjacent ommatidia and the number of IOCs was quantified within an ommatidial group (OG) that covers a defined hexagonal area (bordered by yellow dots in C,D). The secondary pigment cells crossed by the hexagonal boundary were counted as half. At least 15 OG's were scored from independent samples for each genotype (B). Representative examples are shown for $w^{1118}$(C), *GMR*>$mts^{DN}$ (D), *GMR*>P35 (E) and *GMR*>P35 + $mts^{DN}$ (F). (G-I) The lateral surface area of adult fly eyes were measured and compared between $w^{1118}$, *GMR* (G) and *GMR*>$mts^{DN}$ (H). N=8 for I. P-values were determined by Student's *t* test (**P< 0.01).

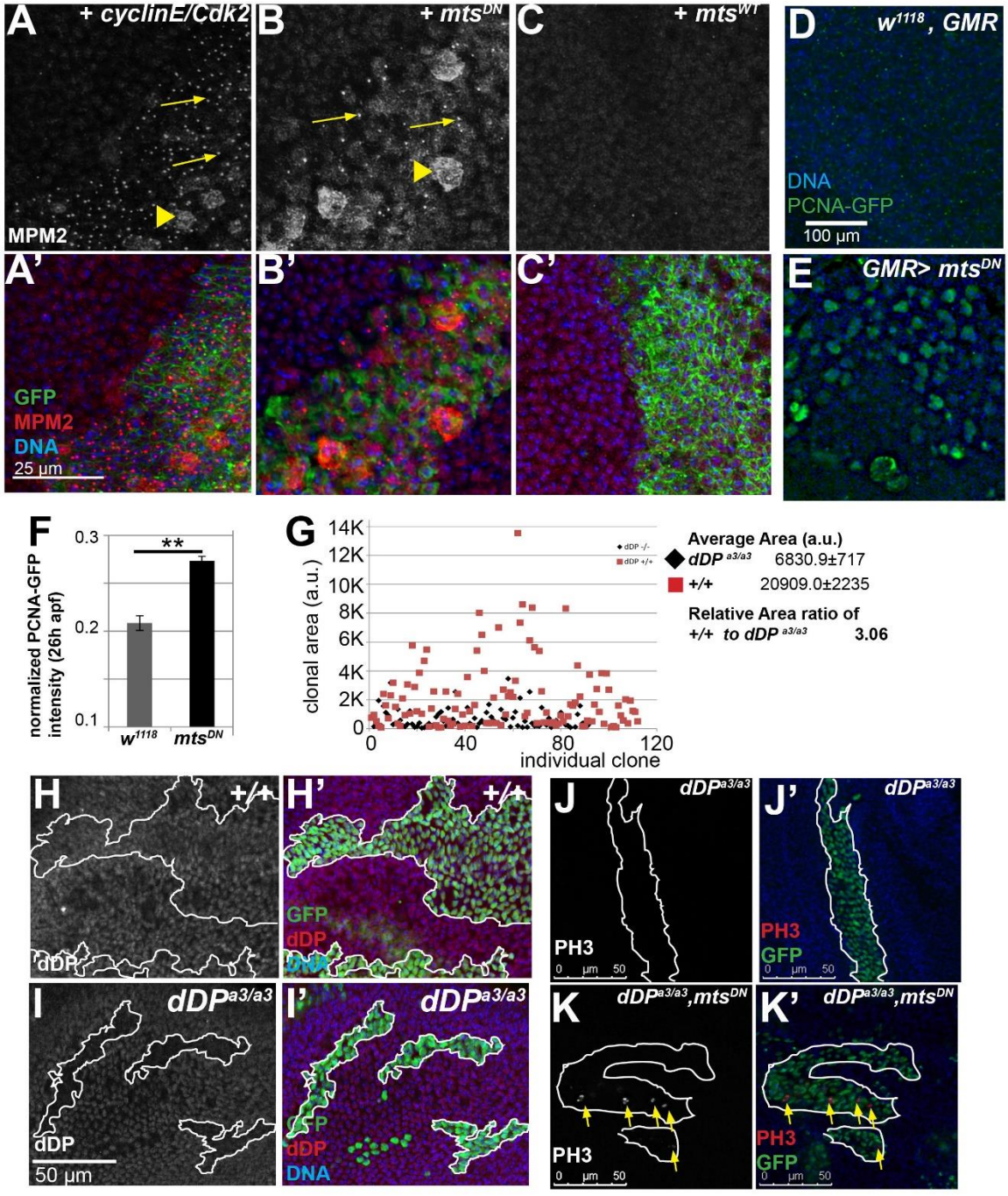


**Figure 2. 3 Inhibition of PP2A leads to ectopic Cdk2 and E2F activity during the final cell cycle.**

(A-C') Pupal wings containing clones expressing the indicated transgenes at 24h APF via the *hs-flp actin>Gal4/UAS* system, were stained with MPM2 antibody. MPM2 recognizes subnuclear foci (arrows) corresponding to Cdk2 phosphorylated epitope(s) at the Histone Locus Body. This is in contrast to the cytoplasmic staining (arrowhead) that indicates mitotic MPM2 phospho-epitopes. (A,A') *CyclinE/Cdk2* overexpression results in MPM2 foci within clones. (B,B') Inhibition of PP2A function via expression of $mts^{DN}$ leads to MPM2 subnuclear foci. (C,C') No ectopic MPM2 foci are observed in clones expressing $mts^{WT}$. (D,E) Pupal eyes were assessed at 26h APF, a stage normally postmitotic, for E2F transcriptional activity using the PCNA-GFP reporter transgene. (E) Expression of $mts^{DN}$ during the final cell cycle via *GMR-Gal4/UAS* leads to ectopic E2F activity, when tissues should be postmitotic. (F) Quantification of the PCNA-GFP reporter intensity was normalized to DNA content and compared between control ($w^{1118}$) and $mts^{DN}$. P-values were determined by Student's *t* test (**P< 0.01). Wild type or $Dp^{a3}$ null mutant clones were induced using the MARCM system by a 20 min heat shock at 37°C at early L3 stage. Clones were examined and measured at 24-26h APF. A scatter plot (G) of clone sizes reveals that the average area of $dDp^{a3}$ null mutant clones compared to wild-type control MARCM clones generated in parallel. (H-I') Wild type or $Dp^{a3}$ null mutant clones were stained with Dp antibody. $Dp^{a3}$ mutant clones lack Dp protein. (J-K') Loss of PP2A delays cell cycle exit independent of E2F activity. *Dp* null mutant clones (J,J') or *Dp* null mutant clones

expressing *mts*$^{DN}$ (K,K') were induced as above, and assayed for ectopic mitoses via anti-PH3 at a time normally postmitotic, 26h APF. Clones were marked by GFP. White lines outline the clones and yellow arrows indicate ectopic mitoses within the clones.

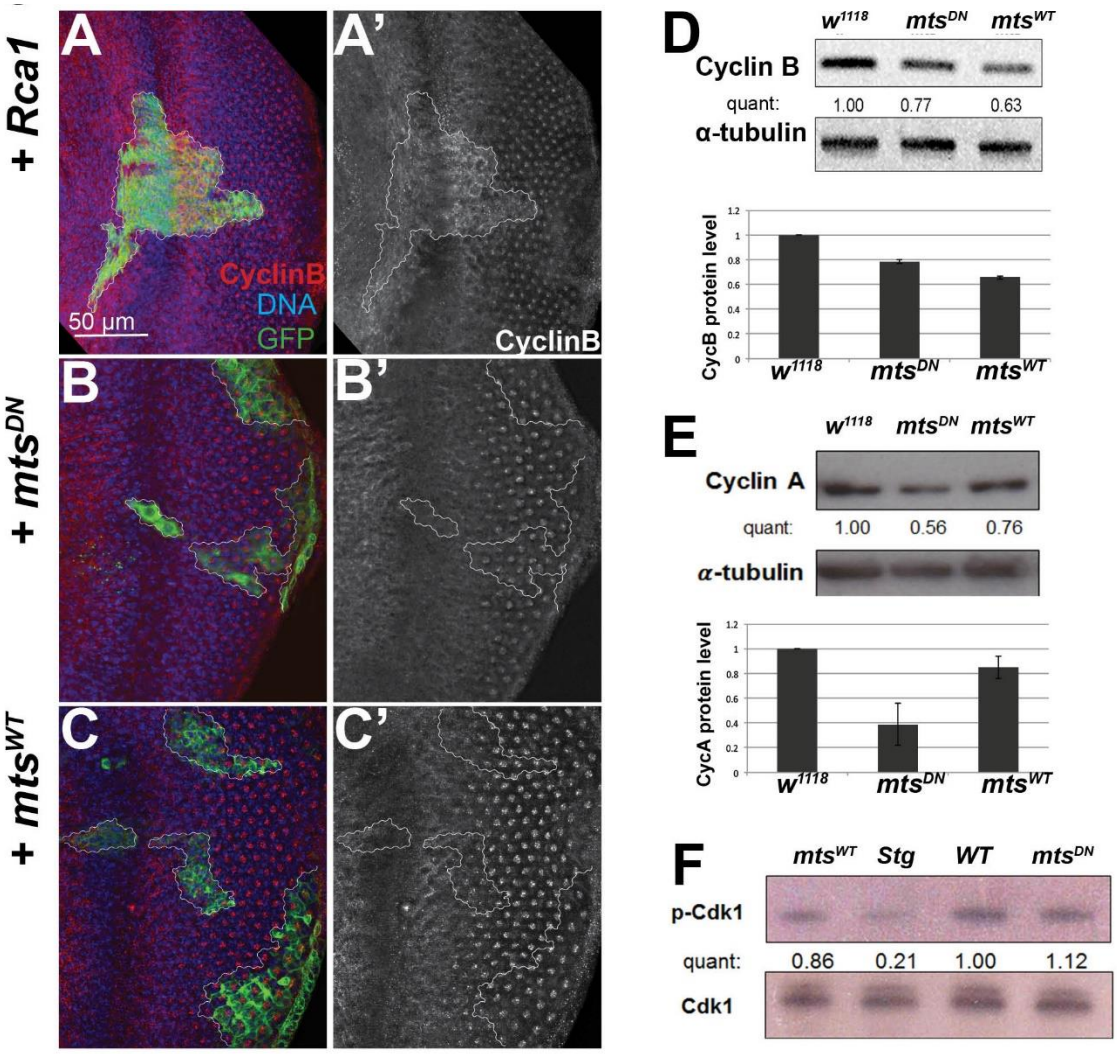


**Figure 2. 4 APC/C activity is not compromised by reduced PP2A function during the final cell cycle.**

(A-C') Late L3 instar larval eye imaginal discs were isolated and stained with anti-Cyclin B in red, DNA in blue. Clones were induced by the *hs*-Flp *actin*>Gal4/UAS system and marked by GFP. As a positive control, overexpression of *Rca1* (A,A') resulted in accumulation of Cyclin B protein via inhibition of the APC/C. By contrast, no obvious change in Cyclin B level was

observed for either *mts*$^{DN}$ overexpression (B,B') or wildtype *mts* overexpression (C,C'). Note that Cyclin B staining is observed in R8 photoreceptors as previously described (Ruggeiro *et al*., 2012). (D-F ) Western blots of Cyclin B, Cyclin A, or phospho-Cdk1 (p-Cdk1) levels with *mts*$^{DN}$ or wildtype *mts* overexpression. Protein samples were collected from either late L3 instar larval eye imaginal discs with transgene expression under control of *GMR-Gal4* (D,E) or late L3 instar larval heads with transgene expression induced by the *hs*-Flp *actin*>Gal4/UAS system (F). Altering PP2A activity did not increase Cyclin B or Cyclin A, nor strongly alter the ratio of p-Cdk1/total Cdk1. Note that expression of the Cdk1 phosphatase Stg significantly reduces pCdk1, and serves as a positive control. Bar graphs show the quantification of signal intensities from two independent experiments.

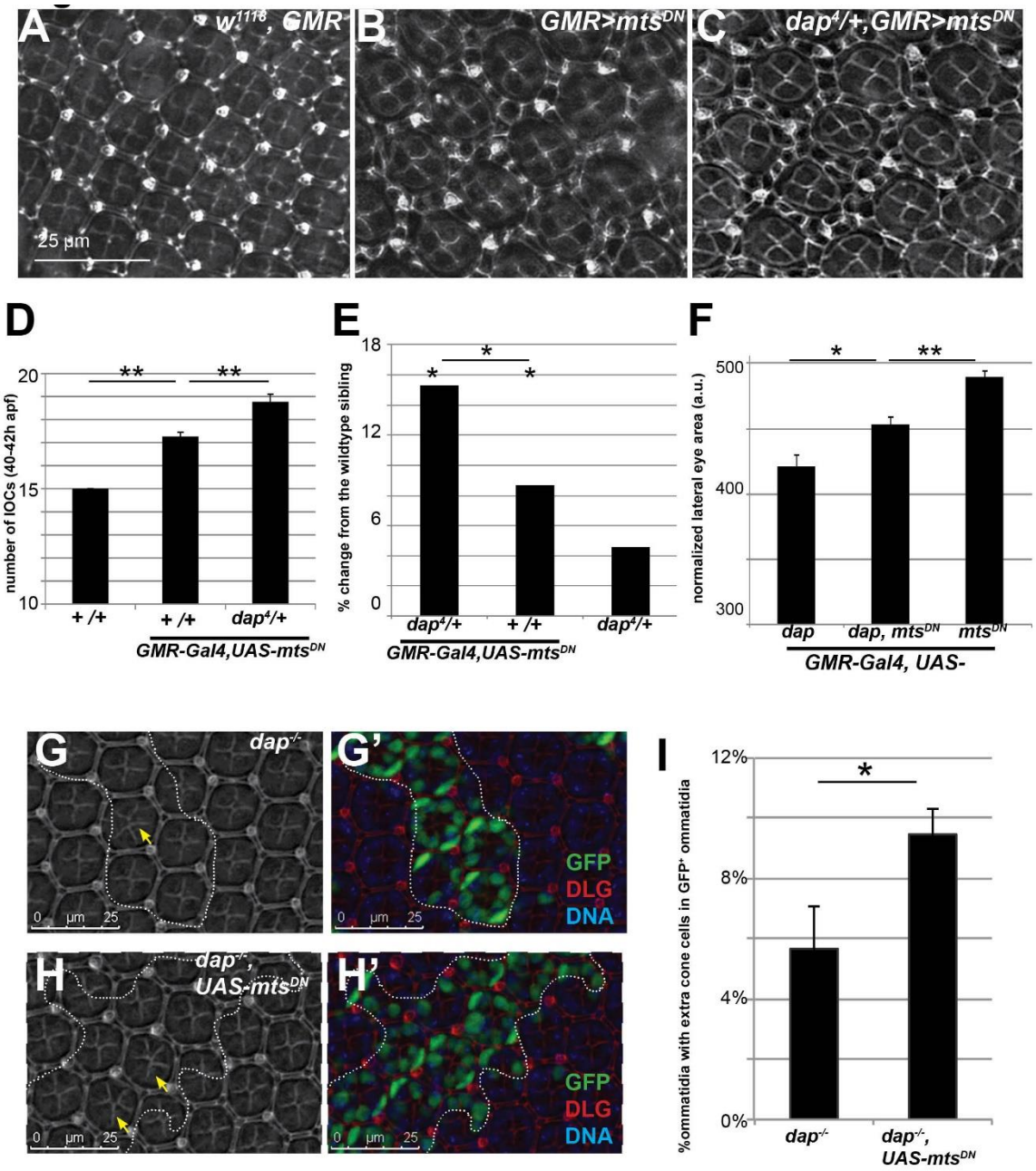


**Figure 2. 5 PP2A genetically interacts with negative regulators of CyclinE/Cdk2 activity *in vivo*.**

(A-D) The number of IOCs is modulated by PP2A and *dacapo* in pupal eyes. $w^{1118}$, *GMR* (A) *GMR>mts*$^{DN}$ (B) $dap^{4/+}$, *GMR>mts*$^{DN}$ (C) pupal retinas were isolated at 42h APF and stained for Discs Large protein (Dlg), to determine the numbers of IOCs. IOC quantification is shown in D.

Loss of one *dap* allele exacerbates the ectopic cell proliferation in pupal retinas caused by PP2A inhibition alone. (E) The lateral surface area of each adult eye was measured, and compared to the area of *dap+/dap+; GMR-Gal4/+* control siblings. The change in eye size is presented as the percentage change from the control siblings. All animals were raised under identical conditions within the same vials. Positive values represent increases in eye size. (F) The area of each adult eye for the indicated genotypes was measured at the lateral view, and normalized to total head size by measurements of the distance between fronto-orbital to postvertical bristles, as animals were raised in parallel but in separate vial crosses. (G-I) GFP labeled mutant clones were induced using the MARCM system at the early third instar larval stage. In *dap* mutant clones and *dap* mutant clones expressing $mts^{DN}$, extra cone cells were quantified at 41h APF (I). Yellow arrows indicate examples of ommatidia with extra cone cells. P-values were determined by Student's *t* test (**p*<0.05;***p*<0.01) N=10.

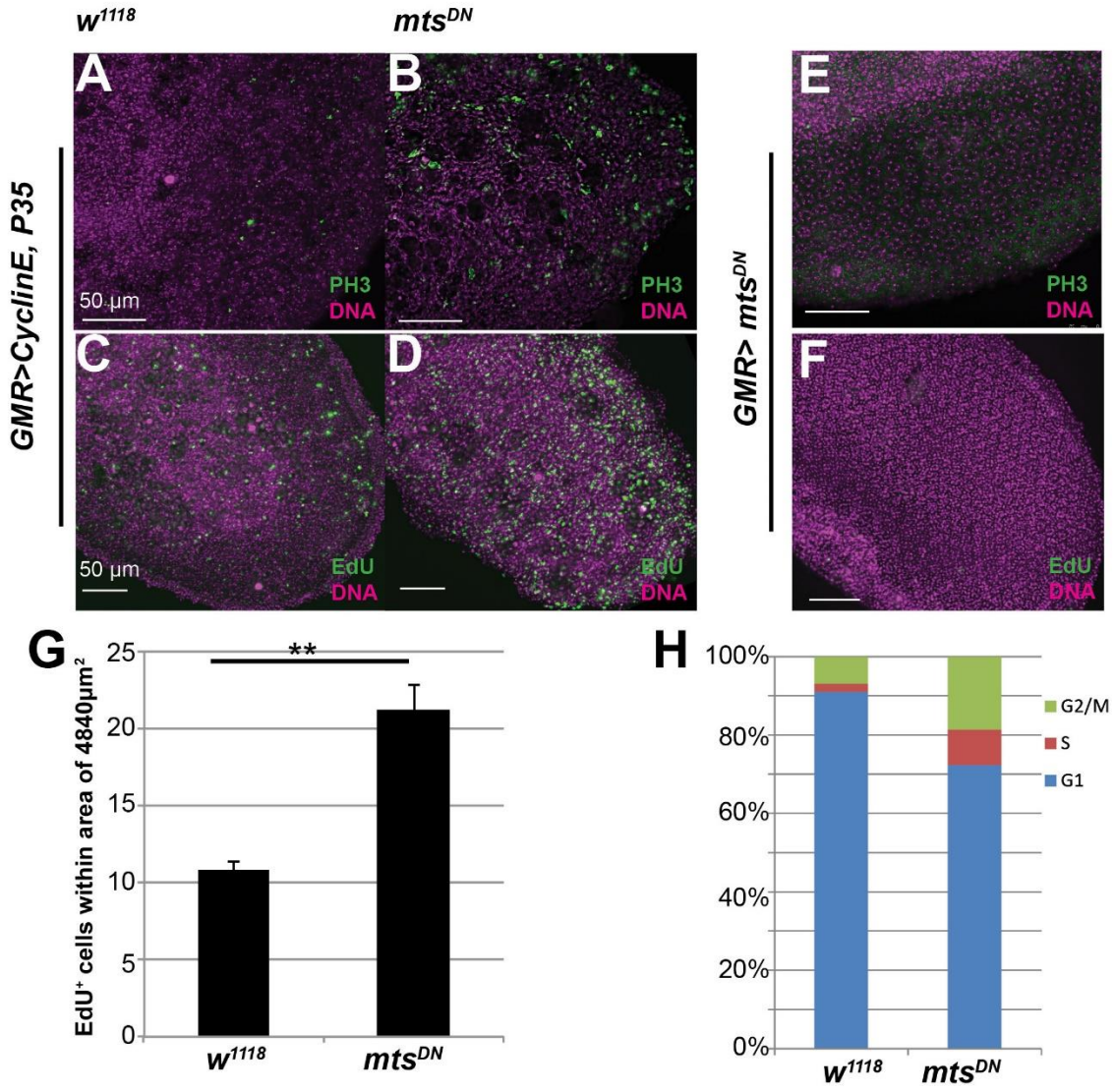


**Figure 2. 6 Loss of PP2A function cooperates with high CyclinE to bypass cell cycle exit.**

(A-D) Pupal eyes expressing Cyclin E and the apoptosis inhibitor P35 under control of *GMR-Gal4* were stained for mitoses (with anti-PH3) or S-phases (via EdU incorporation) at 40-44h APF. Eyes with $mts^{DN}$ expression in the presence of high Cyclin E exhibit an increase in both EdU and PH3 staining (B,D), compared to the high Cyclin E control (A,C). (E-F) pupal eyes expressing $mts^{DN}$ alone under control of *GMR-Gal4* were stained for mitoses or S-phases at 40-

44h apf. (G) EdU was quantified within a central area of the pupal eye and compared between genotypes (N=6 **P< 0.01 by Student's *t* test). (H) FACS analysis of DNA content was performed on 46h APF pupal eyes with high Cyclin E and $mts^{DN}$ expression and compared to controls with high Cyclin E. Cells with an S/G2 DNA content are increased when PP2A function is compromised.

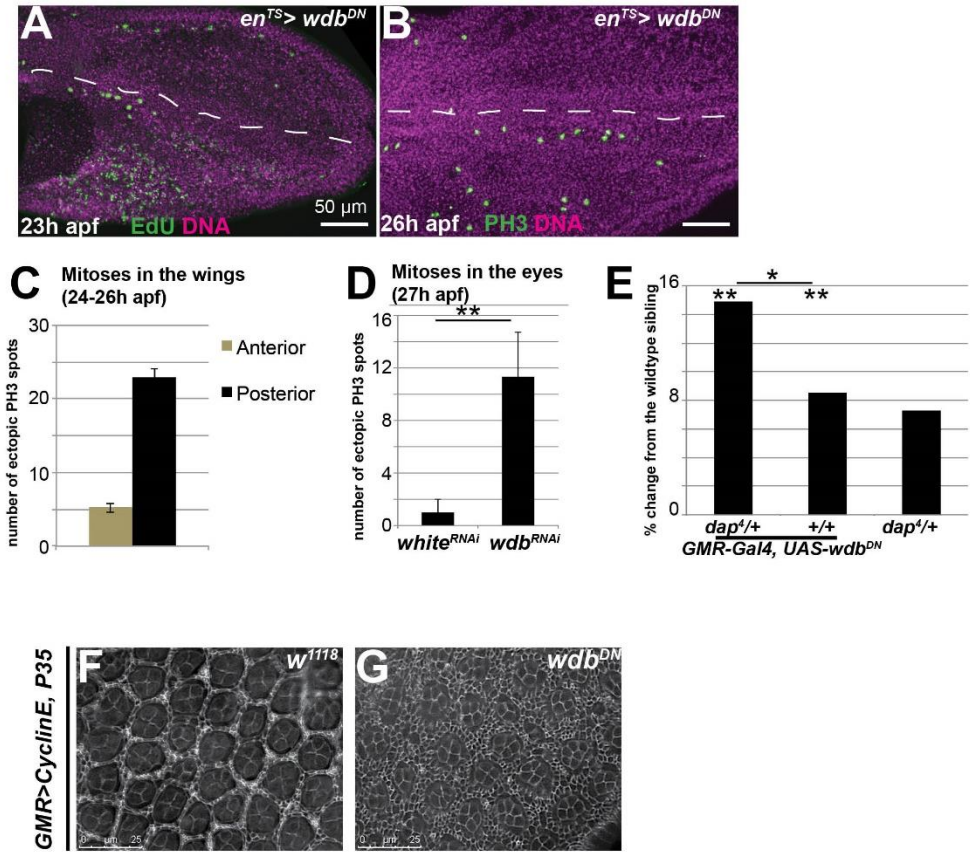


**Figure 2. 7 The B56/*wdb* regulatory subunit promotes the transition to quiescence in terminally differentiating tissues.**

(A-B) Dominant negative *wdb* (*wdb*$^{DN}$) was expressed in the posterior wing from mid-L3 using *en-Gal4/Gal80*$^{TS}$. Pupal tissues were labeled with EdU for 1h at 23h APF to visualize S-phases (A) or labeled with anti-PH3 at 26h APF to visualize mitoses (B). Bar = 50um. (C,D) Quantification of ectopic mitoses in pupal wings from 24-26h APF (C) and eyes at 27h APF (D). (E) Quantification of adult eye sizes show an increase of >8% when *wdb*$^{DN}$ is expressed during the final cell cycle using *GMR/Gal4*. Loss of one allele of *dap* enhances this phenotype, while

loss of one allele of *dap* alone increases eye size <8%. (F,G) Pupal retinas were isolated at 42h APF and stained for Dlg to visualize IOCs in the sensitized *GMR>CyclinE+P35* background (F) IOC numbers increase, forming multiple layers between cone cell clusters in this background when $wdb^{DN}$ is expressed (G).

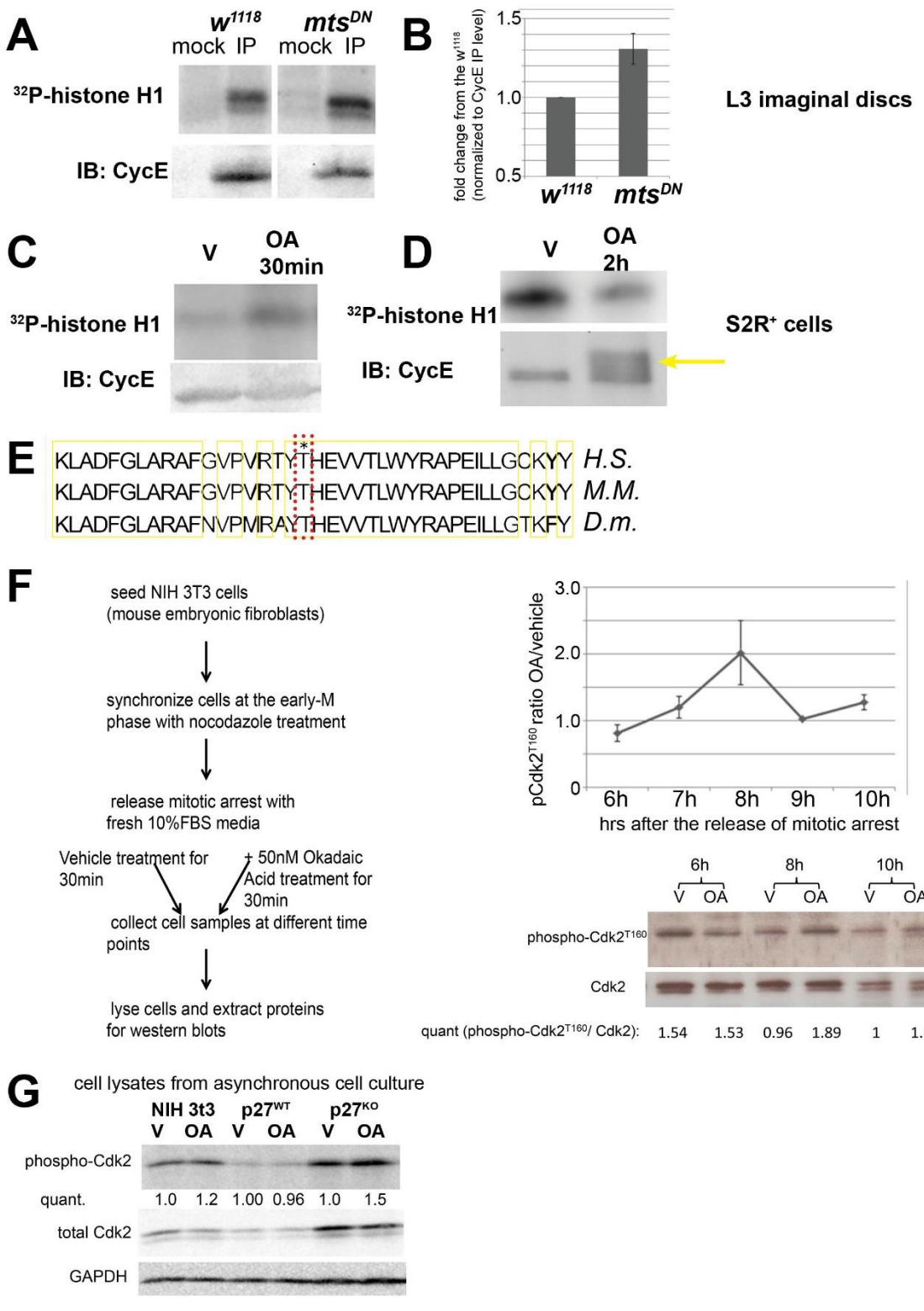


**Figure 2. 8 PP2A affects Cdk2 T-loop phosphorylation.**

(A,B) CycE/Cdk2 activity was measured via an *in vitro* kinase assay using Histone H1 as a substrate. Protein samples were collected from larval eyes co-expressing Cyclin E, the apoptosis inhibitor P35, with or without $mts^{DN}$ under control of *GMR-Gal4*. CycE was immunoprecipitated, while mock precipitations (without CycE antibody) were performed with the same lysate. (C,D) S2R+ cells transfected with a CycE expression vector were treated with 50nM OA for either 30min or 2h versus vehicle (DMSO) only. Kinase assays were performed on immunoprecipitated CycE. (E) The T-loop phosphosite of Cdk2 is conserved in human, mouse and *Drosophila*. (F) Murine 3T3 cells were arrested in G2/M using nocodazole and subsequently released from arrest. A timecourse was performed, to examine endogenous Cdk2-T-loop phosphorylation in samples treated with vehicle only or the PP2A inhibitor Okadaic Acid (OA) for 30 minutes at the indicated timepoint after nocodazole release. An outline of the experimental procedure is shown at left. A representative blot of total Cdk2 and phospho-Cdk2 after nocodazole release is shown at right. The line graph shows quantification of the OA treated/vehicle treated phospho-Cdk2 ratio with 2-3 independent biological replicates at each timepoint. Error bars indicate s.e.m. (G) In asynchronously proliferating murine 3T3s treatment with OA causes a 20% increase in Cdk2 T-loop phosphorylation, while primary $p27^{WT}$ MEFs show no increase. In contrast, asynchronously proliferating $p27^{KO}$ MEFs exhibit a 50% increase in Cdk2 T-loop phosphorylation upon OA treatment.

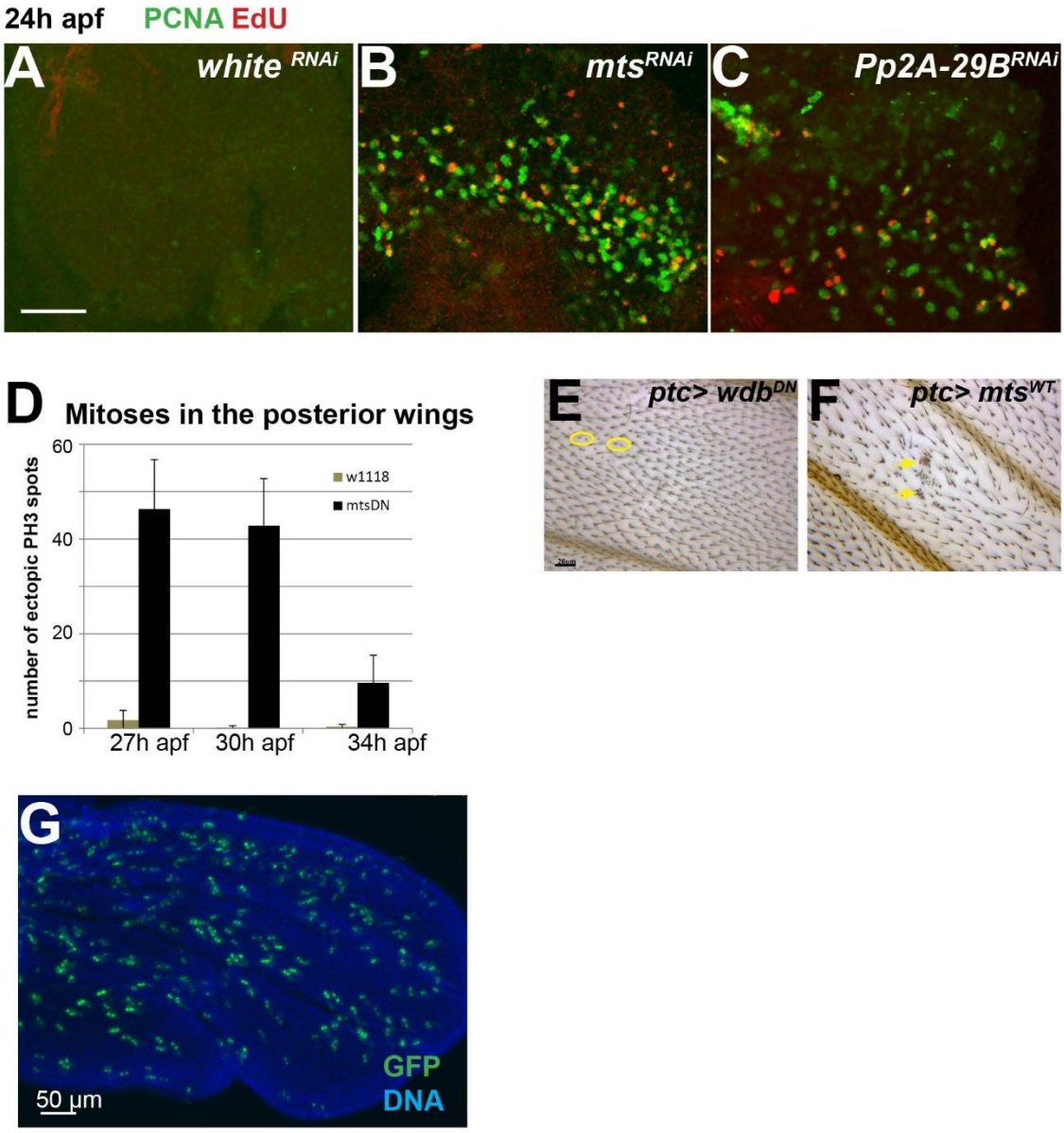


**Figure S2. 1 Loss of PP2A activity delays the transition to quiescence *in vivo*.**

(A-C) The catalytic subunit (*mts*) or the scaffold subunit (*Pp2A-29B*) of PP2A was knocked down with RNAi transgenes expressed in the eye during the final cell cycle using *GMR-Gal4/UAS* and compared to a control (*white*) RNAi. Pupal tissues were isolated at 24h APF and labeled with EdU for 1 h to visualize S-phase. Expression of a PCNA-GFP reporter was used as

a readout of ectopic E2F/DP transcriptional activity in eyes. Contrast and gain were increased in the control sample to show there is no reporter activity or EdU incorporation. (D) bar graph shows counts of mitoses posterior to posterior in pupal wings at developmental stages (E,F) The indicated transgenes were expressed along the anterior-posterior boundary of the wing under the control of *patched-Gal4/UAS* and adult wings were examined for wing hair phenotypes. Note that $wdb^{DN}$ causes a loss of wing hair (yellow circles), whereas overexpression of *mts* leads to a multiple wing hairs phenotype (arrows), consistent with (Hannus et al., 2002). Supplemental Table 1 shows the components of PP2A complexes in mammals and in *Drosophila.* (G) A representative image from the clonal lineage tracing experiment in Fig. 2A. GFP-labeled clones with $mts^{DN}$ expression were induced at 0h APF, and pupal wings were dissected at 42- 44h APF.

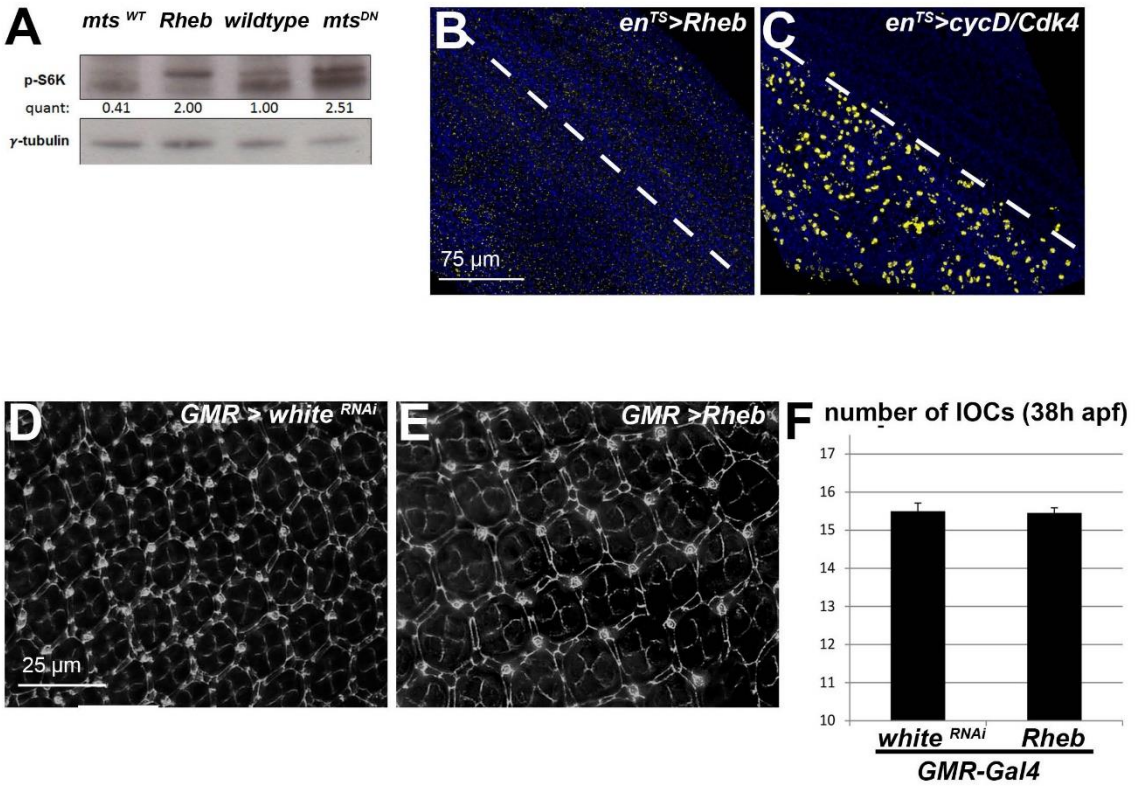


**Figure S2. 2 Activation of the TOR/S6K pathway does not delay the transition to quiescence.**

(A)The indicated transgenes were induced by the *hsflp actin>Gal4/UAS* system, with a 30min heat-shock to drive expression throughout the animal. Protein was extracted from larval heads and phospho-S6K levels were determined by western blots. (B-C) The indicated transgenes were expressed in the posterior compartment of pupal wings from 0h APF using *en-Gal4/Gal80$^{TS}$*. Tissues were collected at 26h APF and labeled with anti-PH3 to visualize mitoses. No mitoses were observed in the posterior wing when *Rheb* (an activator of TOR) is overexpressed. By contrast, overexpression of *CyclinD/Cdk4* serves as a positive control to demonstrate delayed quiescence. (D-F) Assessment of interommatidial cell (IOC) number in 38-h APF eyes in which *GMR-Gal4* drives expression of *white* RNAi (D) or *Rheb* (E). Pupal retinas

were stained for Dlg, and the numbers of IOCs were quantified in panel F (N=10). IOC number is not increased in eyes expressing Rheb compared to a control RNAi.

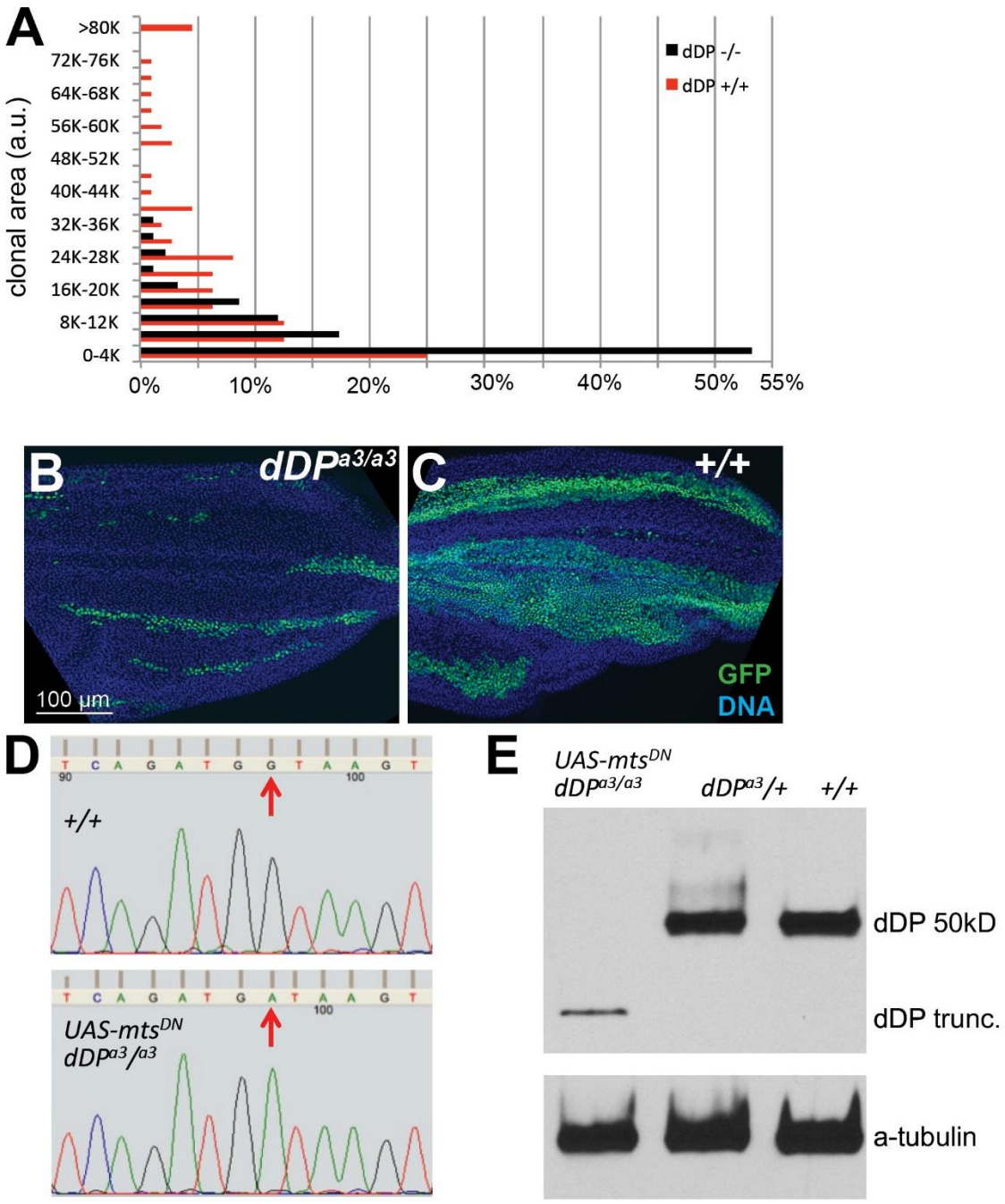


**Figure S2. 3 *Dp* null mutant clones have a proliferation defect.**

Wild type or $Dp^{a3}$ null mutant clones were induced using the MARCM system by a 20 min heat shock at 37°C at early L3 instar larval stage. Clones were examined and measured at 24-26h APF. (A) The majority of $dDp^{a3}$ null mutant clones (~95%) are below 20,000 (arbitrary unit) in

size, while almost 40% of wild type clones were above 20,000 in size. (B,C) Wild type or*dDp$^{a3}$* null mutant clones were induced in parallel and are marked by GFP expression. (D) Sequencing of the *dDp$^{a3/a3}$,UAS-mts$^{DN}$* fly line confirms the expected point mutation in previously reported in the *Dp$^{a3}$* allele (Frolov et al., 2005). (E) Western blots for Dp expression were performed on samples extracted from wild type, heterozygous or homozygous *dDp$^{a3}$,UAS-mts$^{DN}$* animals. *Dp$^{a3/a3}$,UAS-mts$^{DN}$* homozygotes express only a truncated form of Dp as previously reported (Frolov et al., 2005).

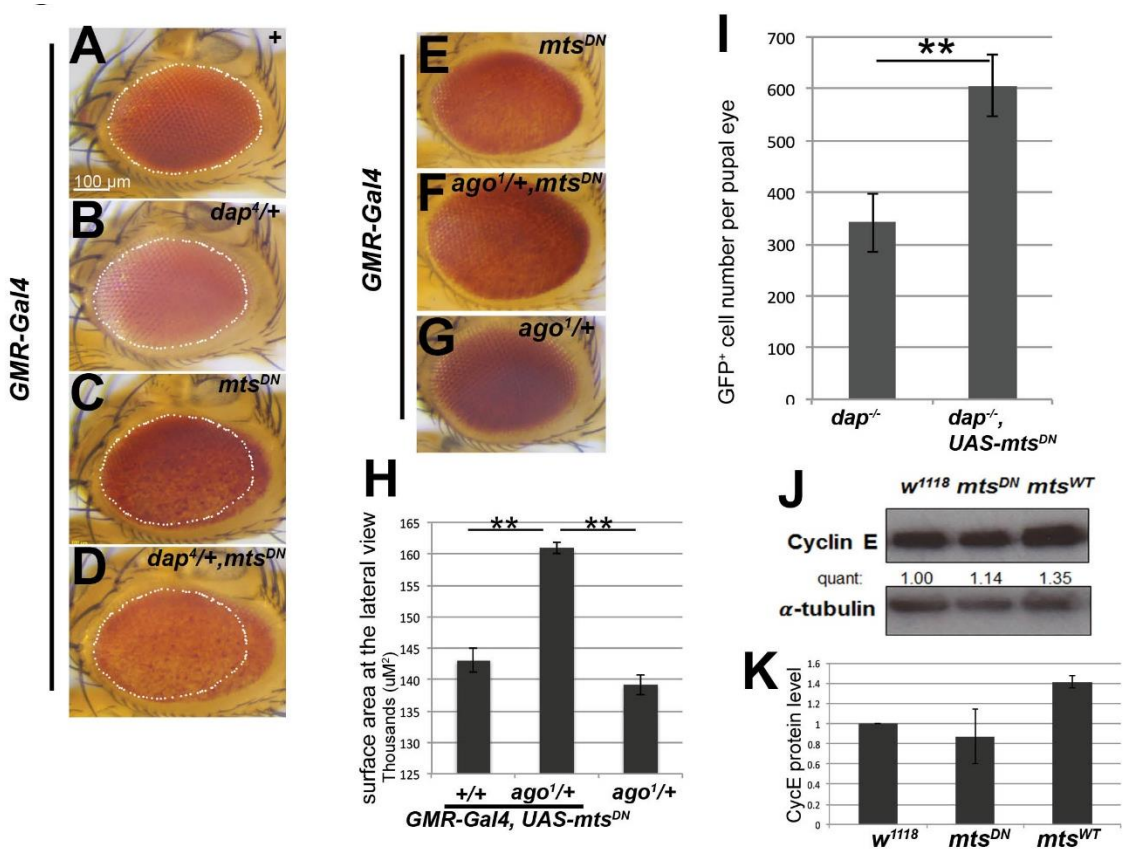


**Figure S2. 4 PP2A genetically interacts with negative regulators of Cyclin E/Cdk2 activity *in vivo*.**

(A-D) Representative adult eye images used for quantifications in Fig. 5E. The white dots outline the control eye size for comparison. *GMR-Gal4*-mediated $mts^{DN}$ expression causes a large eye phenotype (C) which is enhanced by the loss of one copy of *dap* (D). (E-H) Loss of one copy of *ago* enhances the $mts^{DN}$ large eye phenotype. P-values were determined by Student's *t*-tests (**, P< 0.01). (E-G) Adult eye examples used for quantification in Fig. S5H. (I) GFP labeled $dap^{4}$ clones were induced using MARCM at early third instar larval stage. *dap* mutant clones and *dap* mutant clones expressing $mts^{DN}$ were induced in parallel and examined at 41h APF. The total number of GFP positive cells per eye was compared between genotypes.

(J-K) Western blots were performed to measure Cyclin E protein levels upon manipulation of PP2A activity. Protein samples were extracted from late third instar imaginal discs with the indicated transgenes expressed via *GMR-Gal4/UAS*. Quantification of signal intensities from western blots of two independent experimental replicates are shown (K).

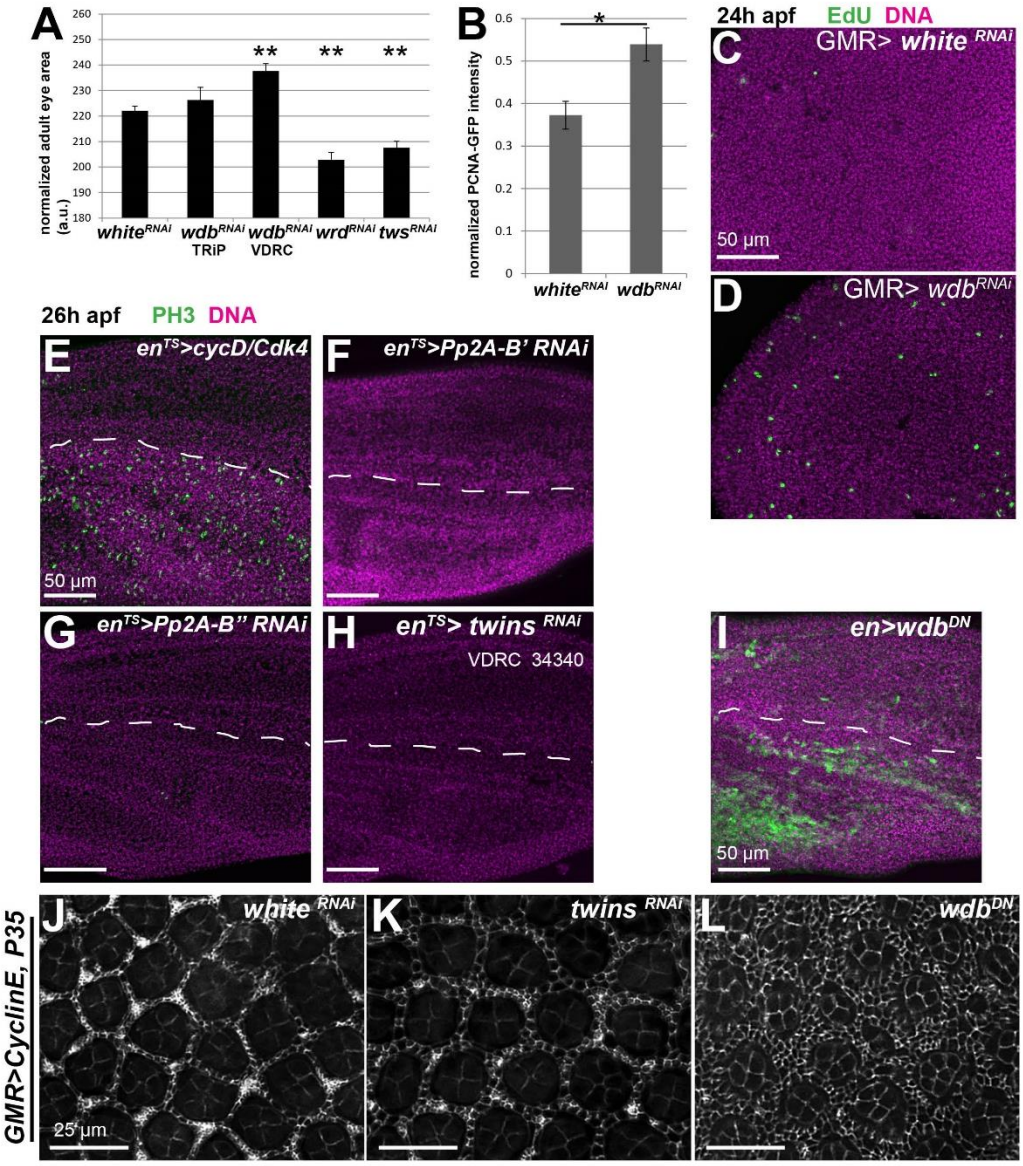


**Figure S2. 5 The B56/*wdb* regulatory subunit promotes the transition to quiescence in terminally differentiating tissues.**

Flies were raised at 31°C with *GMR-Gal4/UAS* expression of the indicated RNAi transgenes to regulatory subunits of PP2A. (A) Quantification of adult female fly eye size was normalized to total body size. Asterisks indicate *p*-values determined by a Student's *t* test (*$p<0.05$ **$p<0.01$). (B) Quantification of PCNA-GFP expression in *GMR-Gal4/UAS* control (*white* RNAi) or *wdb*

*RNAi* expressing pupal eyes at 24h APF. (C,D) Pupal eyes expressing the indicated transgenes driven by *GMR-Gal4/UAS* were labeled for 1 hour at 24h APF with EdU to visualize S phases. (E-H) Pupal wings expressing the indicated transgenes driven by *en-Gal4/Gal80$^{TS}$* at 26h APF were labeled with anti-PH3 to visualize mitoses (I) 24h APF pupal wings expressing *wdb$^{DN}$* in the posterior region driven by *en-gal4/UAS* display ectopic PCNA-GFP reporter activity. (J-L) Anti-Dlg staining was used to assess pupal eye morphology at 42-44h APF in a sensitized background with *GMR-Gal4/UAS* driving Cyclin E and P35 expression as well as the indicated transgenes.

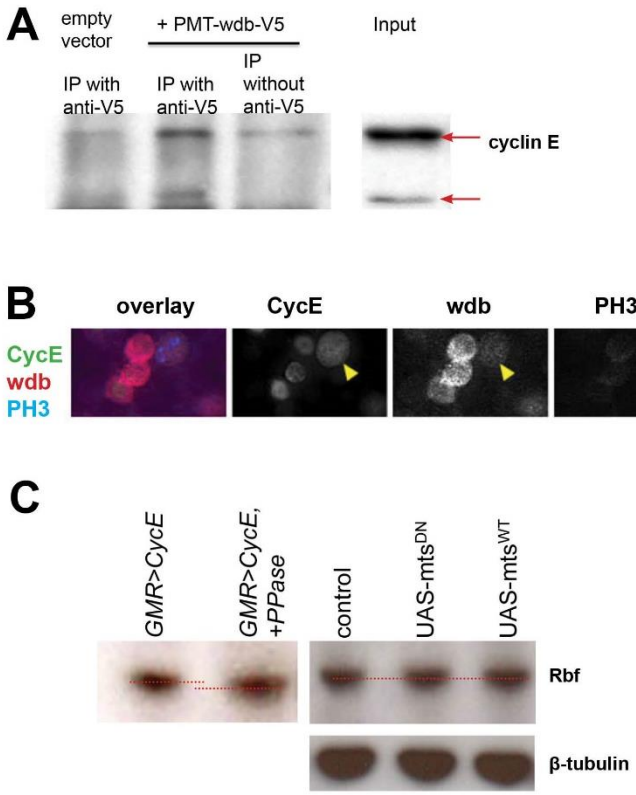


**Figure S2. 6 Wdb interacts with Cyclin E.**

(A) Lysates were prepared from S2R+ cells transfected with a pMT-Wdb-V5 expression plasmid, and an anti-V5 (or mock) pulldown was performed. Enrichment of endogenous Cyclin E was observed in the V5-pulldown. Note that in S2R+ cells two different size Cyclin E protein products are expressed (66 and 77 kDa). (B) S2R+ cells were transfected with a pMT-Wdb-V5 expression plasmid and a pMT-Cyclin E expression plasmid, and fixed and stained with anti-V5 to detect Wdb, anti-Cyclin E and anti-PH3 to detect cells in mitosis. The arrow indicates a cell in mitosis where Cyclin E becomes localized to the cytoplasm. (C) Lysates were collected from late third instar larval heads with PP2A transgene expression induced by the *hs*-Flp *actin*>Gal4/UAS system or from late third instar larval eyes expressing CycE and the apoptosis

inhibitor P35 under control of *GMR-Gal4*. Lysates were resolved on a NuPAGE Bis/Tris Gel as described (Lee et al., 2012) and blotted with anti-Rbf antibody (DX3). Lysate from larvae expressing Cyclin E was split, and one half was treated with lambda phosphatase (New England Biolabs) while the other half was not, to visualize the altered migration of phosphorylated Rbf. The phosphatase treated sample shows a subtle shift in migration, while no alteration of Rbf migration is observed in samples with genetic manipulations either increasing or inhibiting PP2A activity.

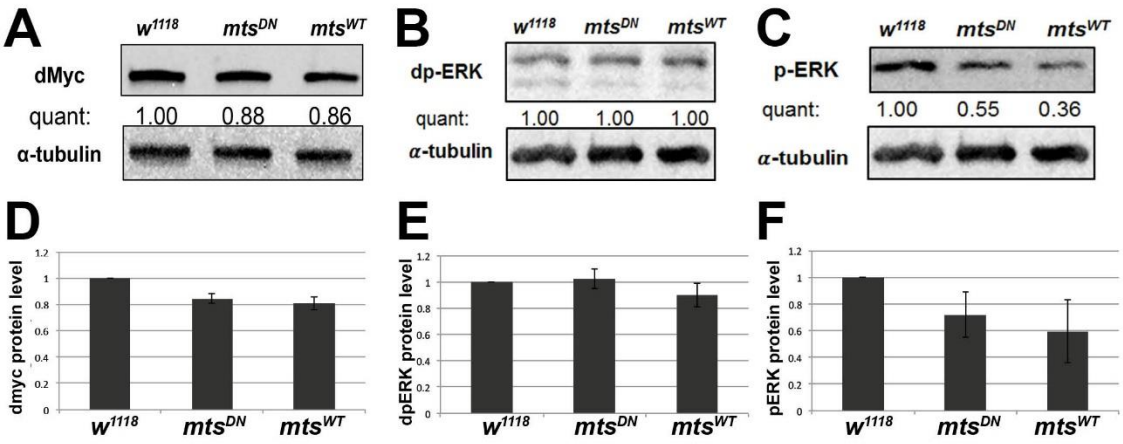


**Figure S2. 7 Inhibition of PP2A during the final cell cycle does not increase signaling through ERK, levels of dMyc.**

(A-C) Western blots were performed to measure Myc and phospho-ERK (p-ERK) protein levels upon manipulation of PP2A activity. Protein samples were extracted from late third instar larval eye imaginal discs with the indicated transgenes expressed via *GMR-Gal4/UAS* to manipulate PP2A activity specifically during the final cell cycle. Note that compromising PP2A activity does not up-regulate mono p-ERK or diphospho (dp) –ERK, nor alter the migration of Myc protein. Quantifications of protein signal intensity on western blots were shown in (D-F), which represents two independent experiments.

# Chapter 3 Live cell imaging to examine the proliferation-quiescence transition

## Abstract

In asynchronously growing cell culture, it is assumed that all cells are actively proliferating at similar rates, while the withdrawal of nutrients leads cells to stop cycling and to enter a state of reversible quiescence. By monitoring the asynchronously cycling mouse embryonic fibroblasts using G0/G1 cell cycle reporters and live, single-cell tracking, we have discovered that some cells can stay in a prolonged G0 as long as over 10 hours even under full serum conditions and that the length of the quiescent state is heterogeneous. Live-cell imaging revealed that cells can enter into either a transient or prolonged quiescent state after mitosis, prior to the next cell cycle even under conditions of abundant nutrients. Furthermore, we discovered that sister cells born of the same mitosis can make heterogeneous cell cycle decisions, that is, one cell enters quiescence while the other re-enters the cell cycle for the next round of division. This asymmetric decision phenotype implies a proliferation-quiescence cell cycle checkpoint occurs after completion of mitosis, distinct from other cell cycle checkpoints thought to regulate quiescence such as the Restriction point. Consistent with our work in *Drosophila*, we also found that PP2A plays a conserved role in promoting the entry

into quiescence after mitosis. We suggest this may contribute to PP2A's known tumor suppressor role.

## Introduction

Recent studies in mammalian cells found that even with abundant nutrients, many cells may enter a G0-like state in a cell culture (Spencer et al., 2013). The relative percentage of cells that enter G0-like state after mitosis varies in different cell types and culture conditions, suggesting many signaling inputs likely influence the proliferation-quiescence decision. This is consistent with findings in several cancer cell lines, suggesting some cells enter quiescence while others do not (Dey-Guha et al., 2011). This population heterogeneity in cell cycle activity, with one subpopulation actively cycling while another one staying in quiescence is termed proliferative heterogeneity. A study in search of the regulatory mechanism for proliferative heterogeneity suggested that the relative levels of p21 and Cdk2 are responsible for the decision to proliferate or to enter quiescence in a human breast epithelial cell line (Overton et al., 2014). This Cdk2-p21 model suggests that cells with high p21/low Cdk2 activity are more likely to remain in a steady quiescent state, while cells with low p21/high Cdk2 activity tend to rapidly commit to the next cycle after mitosis. Thus the threshold of Cdk2 activity set by its inhibitor p21 determines the proliferation-quiescence decision. But cells deficient in p21 still entered quiescence in low serum conditions. This suggests that mechanisms

independent of p21 also contribute to the decision to enter quiescence or proliferative cell cycle.

Indeed, another regulatory threshold model for the proliferation-quiescence decision, has been proposed (Yao et al., 2008). In this Rb-E2F bistable model, the two steady states (E2F-Off and E2F- On) define cellular quiescence and proliferation, respectively. The ‘barrier’ that separates the two states is the E2F activation threshold, and cells need to accumulate enough E2F activity to transit from quiescence to proliferation (Fig. 3.8). Cells under different environmental conditions or with different cell types are likely to have variable E2F activation thresholds. The model predicts that cells with a higher E2F activation threshold are in a deeper quiescence. This means that cells spend longer time to gain enough E2F activity in order to switch from E2F-Off/ quiescence to E2F-On/proliferation, whereas cells in shallow quiescence are more likely to re-enter cell cycle at a faster rate. Thus variying levels of quiescence may exist in asynchronous cell population, however evidence that demonstrates the existence of multi-state quiescence that is independent of serum starvation remains scarce. These observations raise the question that whether the multi-state quiescence is the source of the proliferative heterogeneity. These two models both suggest that the decision depends upon a bistable model with thresholds set by both positive and negative cell cycle regulators, which imply that within asynchronously growing cell populations, cells constantly make the proliferation-quiescence decision.

What are the characteristics of the proliferation-quiescence decision that are likely

to be quantitatively affected by the relative levels of cell cycle regulators? In order to better understand the proliferation-quiescence decision without artificial synchronization, we have implemented cell cycle reporters that distinguish G0 from G1 in live-cell imaging to monitor cell cycle behaviors at the proliferation-quiescence transition. The first generation of cell cycle reporters is the Fucci system (fluorescent ubiquitination-based cell cycle indicator) (Sakaue-Sawano et al., 2008), which is able to differentially label cells in G1/0, S and G2/M phases, thus allowing us to visualize the G1-M transition. The major drawback of this system is that it is unable to distinguish cells in quiescent/ G0 from cells in G1. Recently, a novel cell cycle indicator, mVenus-p27K$^{-}$, was generated to specifically label quiescent cells (Oki et al., 2014). This probe is a fusion protein consisting of a fluorescent protein mVenus and a Cdk binding defective mutant of p27. p27 accumulates in quiescence, and is degraded by two ubiquitin ligases: Kip1 ubiquitination-promoting complex (KPC)—an E3 ligase complex mediates cytoplasmic p27 degradation at G0-G1 transition, and SCF$^{Skp2}$ mediates its nuclear proteolysis at the S/G2/M phases (Kamura et al., 2004). Another cell cycle reporter—mCherry-hCdt1(30/120), is a fusion protein consisting of mCherry fluorescent protein and human Cdt1(hCdt1) degron— short amino acid sequence targeted by SCF$^{Skp2}$ complex at the S/G2/M phases. mVenus-p27K$^{-}$ together with mCherry-hCdt1(30/120) reporter label cells from after mitosis until early S phase in distinct colors, which allows us to examine the cell cycle behaviors of the proliferation-quiescence transition via live imaging or FACS analysis without chemical or nutrient-deprivation synchronization (Fig.

3.1A).

Since the proliferative heterogeneity mentioned earlier could be masked in bulk cell assays, it is important to monitor the proliferation-quiescence transition at single-cell resolution. However, time-lapse microscopy at the single-cell level produces large amounts of data, which could be tedious for the manual analysis. In order to quantitatively measure and analyze the proliferation-quiescence decision in live cells, we developed a new, automated cell cycle profiling platform to define, assign and quantify cell cycle behaviors after mitosis in the proliferation-quiescence decision.

## Results

### Validation of G0/G1 cell cycle indicators

To characterize the cell cycle behaviors in the proliferation-quiescence transition at single-cell resolution, I used a novel cell cycle indicator mVenus-p27K$^-$ combined with mCherry-hCdt1(30/120) probe to distinguish G0 cells from G1 cells (Fig. 3.1A).

Serum starvation is commonly used to synchronize cells in G0, or push cells into quiescence. First, to confirm that the mVenus-p27K$^-$ / mCherry-hCdt1(30/120) reporters are highly expressed in G1/0 phase, I performed either a short-term (24h,1%FBS) or a long-term (72h,1%FBS) serum starvation treatment, and the dot plots from flow cytometer analysis showed a gradual accumulation of double positive cells mVenus-p27K$^-$(+)/mCherry-hCdt1(30/120)(+) (Fig.3.1B,C). After 72h serum starvation, almost 90% cells are double positive (Fig. 3.1E). This data suggests that mVenus-p27K$^-$ / mCherry-hCdt1(30/120) expression accumulates in G0 cells. Surprisingly, I found that double positive cells accounted for almost 30% of the total cell population even when cells were cultured with abundant nutrients (Fig.3.1D,E). This suggests that under normal growth conditions, cells can enter a quiescent state, consistent with the findings of a recent study (Spencer et al., 2013).

To verify whether mVenus-p27K$^-$ / mCherry-hCdt1(30/120) reporters can distinguish G0 from G1 at the molecular level, I sorted cells into mVenus-p27$^{K-}$(+)/mCherry-

hCdt1(30/120)(+), mVenus-p27$^{K-}$(-)/mCherry-hCdt1(30/120)(+), mVenus-p27$^{K-}$(-)/mCherry-hCdt1(30/120)(-) three groups, and then performed western blot analysis (Fig. 3.2A,B) or real-time quantitative PCR (RT-qPCR) (Fig. 3.2C) from protein or RNA extracts to look for known markers of G0 vs. G1. For comparison, cells synchronized in G0 by serum deprivation were also sorted in a similar manner. p130, one of the Rb family members, is abundant in quiescent cells and largely involved in the repression of gene expression in G0 (Litovchick et al., 2007; Smith et al., 1996). As cells enter into cell cycle, p130 is phosphorylated, and is targeted for degradation (Tedesco et al., 2002). The protein detection via western blots showed an enriched level of un/hypo-phosphorylated form of p130 in quiescent cells compared to cycling cells. Quantitative analysis of the immunoblot signals showed that total expression level of p130 is greatly reduced in actively cycling cells (Fig. 3.2A). Cyclin-dependent kinase inhibitor— p27 expression also increases in G0 cells (Sherr and Roberts, 1999), and consistent with this, I observed a 4-fold enrichment in endogenous p27 in double positive cells under serum starvation, compared to mCherry single positive cells. I next examined an active cell cycle regulator that increases in G1, which is the phosphorylation of Cdk2 on the T-loop site – a readout of active Cdk2. Consistent with the proper separation of G0 and G1 cells, active Cdk2 accumulated in mCherry-hCdt1(30/120) single positive cells compared to double positive cells (Fig. 3.2B).

RT-qPCR results showed that in double positive mVenus-p27K$^-$(+)/mCherry-hCdt1(30/120)(+) cells, active cell cycle regulators are downregulated whereas tumor suppressors or genes protecting cells from accumulating damages are upregulated, such as Sod3(Fig. 3.2C), compared to the gene expression level from mCherry-hCdt1(30/120)(+) cells. This is consistent with the gene transcription profile of quiescent cells discovered in the previous studies (Coller et al., 2006; Oki et al., 2014; Liu et al., 2007). In summary, sorting of single positive and double positive cells with mVenus-p27K$^-$ & mCherry-hCdt1(30/120) reporters exhibit molecular markers consistent with the separation of quiescent cells from G1 cells.

**Automated computational analysis of live-cell imaging under normal unperturbed conditions**

To understand the kinetics of cell cycle behaviors at the proliferation-quiescence transition at a single-cell level, I took live, time-lapse images from asynchronously cycling population of cells expressing mVenus-p27K$^-$ & mCherry-hCdt1(30/120) reporters (movie attachment in GoogleDrive).

The time-lapse movie showed a successive fluorescent color change as cells pass through the mitosis-G1 transition: First, mVenus and mCherry fluorescence intensity increase simultaneously. In most cells this occurs for 3 hours. If both reporters continue

to accumulate beyond 3hr, we define this as cells enter into G0. Next, mVenus intensity drops down while mCherry signal increases, when cells progress from G0 to G1. Finally, as cells enter S phase, mCherry intensity goes down, indicating G1 exit and S-phase entry. Thus our reporters indicate G0 entry, G1 entry and S phase entry. These changes and cell cycle transitions correlate with the expected DNA content based on flow cytometry (Fig. 3.1F). Of note, cells spend different lengths of time in G0, suggesting a source of proliferative heterogeneity. We therefore quantitatively measured the probability of cells remaining in G0 as a function of time.

To monitor and quantitatively measure the dynamic transitions of cell cycle states—from cytokinesis to S phase entry, in collaboration with Dr. Qiong Yang's group in Biophysics and Dr. Alex Pearson in Dentistry, we developed an automated G0/G1 profiling platform that includes a computational framework for automated cell segmentation (identification of individual cells in an image), tracking and cell cycle state identification & quantification (Fig.3.3A). The cell segmentation and tracking allows us to record the fluorescent reporter intensity changes from individual cells in live, time-lapse imaging, even without the aid of a constitutive nuclear marker (Fig.3.4 A,B). While cell cycle state identification (G0,G1, or early S phase) & quantification provides us the quantitative calculations of the kinetics of the proliferation-quiescence transition. The trajectory of a single-cell trace using the automated system is consistent with what we observed in movies (Fig.3.3B).

$$\Delta Cherry / \Delta Venus = \frac{Cht+1-Cht}{Vt+1-Vt}$$

To quantitatively measure the relative change of two fluorescent reporters, we converted the pair of fluorescent intensity readings from each time interval into radian readings. In brief, this means that the ratio from the calculation above is converted to radian values over range from –π to π (pie) in the radial histogram (Fig. 3.3C). The length of the spikes depicts the frequency of individual cells with two fluorescent reporters exhibiting a specific behavior assigned to each radian. For example, a radian of -π/2 indicates cells enter into early S phase as mCherry signal decreases, while a radian of –π indicates cells exit G0 and enter G1 as mVenus signal drops down while mCherry is still high. In this way, we observe three distinct cell cycle behaviors at the proliferation-quiescence transition from the computational analysis of over 1000 single-cell traces in total, plotted onto a radial histogram to show the frequency and variability of three cell cycle behaviors in a population (Fig. 3.3C). Cells in G0 state with radian values from 0 to π/2, are grouped in blue state. Cells that exit G0 and progress into G1 phase with radian values from π/2 to π or $-\frac{2}{3}$ π to -π, are grouped in orange state. When cells enter into S phase with radian $-\frac{2}{3}$ π to 0, they are grouped in grey state (Fig.3.3D).

After data smoothing (described in methods & materials), we generated a dot plot to show all the radian assignment values for temporally adjacent t vs. t+1 cells over the

entire movie captured from asynchronous, cycling cells (Fig.3.3E). Each dot represents one single cell at any time interval. Therefore, cells remaining in the same state within an interval time lie on the diagonal of the plot, while cells that transit between two states will scatter to the left or right of the diagonal. Dots in blank squares are considered inconclusive or incorrect assignments, such as cells that undergo apoptosis. We find that each experimental data set has a correct assignment rate above 97% (Table 3.1), meaning over 97% of cell traces follow the expected order of reporter activity, which is G0-G1-S transition. This validates the accuracy of our cell cycle profiling platform and confirms the dynamic transitions we can observe via two reporters that reveal the proliferation-quiescence transition.

**Serum deprivation and PP2A inhibition impact the proliferation-quiescence transition in distinct manners.**

We next used the Kaplan-Meier (K-M) curves to estimate the time cells spent in a certain state (Fig.3.5). The Kaplan-Meier estimator is a common statistical analysis tool to approach the true survival function in a large enough sample pool in clinical trials (Kaplan and Meier, 1958). For our application, we took an advantage of it to estimate the probability of cells remaining in each state (blue/G0, orange/G1, grey/ early S phase) as a function of time. In the K-M curve, each step-down means cells exit that certain state. However, during the time-lapse imaging, due to the cell migration, cells

may move in or out of view in the middle of imaging, while others may be half tracked when the time-lapse image initiates or ends. In such cases, the total time of remaining in one state for the cell cannot be accurately determined, and thus the analysis considers them as “censored observations”. The censored traces are typically noted by "+" marks on the estimated K-M curve.

Under normal growth conditions (10%serum), the Kaplan-Meier curve of G0 state estimated that 9% cells can stay in G0 as long as over 10 hours, indicating that cells can enter a prolonged G0 under normal growth conditions. Also, the relative time span of G0 state covers a broad range indicating that quiescence can be heterogeneous.

To test our automated G0/G1 profiling platform, serum starvation was applied to promote G0 entry. Cells with serum deprivation exhibit significant difference in blue state (G0) and orange state (G1), but not grey state (early S phase) (Fig. 3.5A-C). As shown in the K-M curves, cells are more likely to enter a prolonged G0 upon serum starvation, suggested by the slower decline of the curve. This is consistent with many studies that serum starvation promotes and arrests cells in G0. However, cells also tend to have a longer G1 phase under serum starvation. This unexpected result may be consistent with a recent study showing that cells in G1 with high E2F activity can still delay S phase in response to serum starvation (Cappell et al., 2016). This study suggests that during early G1 a window of reversibility exists, when cells can return to quiescence under mitogenic stress. This means that cells may re-enter a quiescence

state in G1 phase to avoid the detrimental effects of cell division in response to the lack of nutrients. This suggests that there exists a quiescent state in G1 under serum starvation, which is not recognized by the mVenus-p27K$^-$ reporter.

Previously, I revealed a role for PP2A in restricting Cdk2 activity after mitosis to modulate the proliferation-quiescence decision in tissue development (Sun and Buttitta, 2015). My results showed compromising PP2A functions caused 10% cells to fail to enter G0. We showed this is due to that PP2A contributes to a mild increase of Cdk2 activity threshold to promote G0 entry. To examine the sensitivity of our assay to mild modulations of the proliferation-quiescence decision, I tested how PP2A impacts the proliferation-quiescence decision using short-term treatments with the pan-PP2A inhibitor Okadaic Acid (OA) PP2A inhibitor Okadaic Acid (OA).

In mammalian cells, PP2A/B55$\beta$ can stabilize CycE1 by removing the N- and C-terminal phosphodegrons (Tan et al., 2014). Our previous study also shows upon longer OA treatments (2h shown), cells exhibited a reduction in CycE/Cdk2 kinase activity and a slower migrating form of CycE protein, likely due to inhibition of PP2A/B55 function (Sun and Buttitta, 2015). Thus, short-term inhibition of PP2A can increase CycE/Cdk2 activity. 30min OA treatment was applied to specifically inhibit PP2A activity before time-lapse, live-cell imaging. As expected, the Kaplan-Meier curves showed that OA treatment results in a statistically significant decrease in the probability of cells entering a prolonged G0 whereas no significant difference in time spent in other two states (G1

and early S phase) (Fig. 3.5D-F). This indicates that PP2A plays a conserved role in promoting entry into prolonged G0 without affecting the G1 state. Our automated G0/G1 profiling platform was able to reflect a mild modulation by PP2A in the proliferation-quiescence decision.

**The asymmetric decision between sister cells in the proliferation-quiescence decision**

Using manual cell tracking (Fig.3.6A-C), I observed that two daughter cells derived from the same mitotic event can make asymmetric decisions at the proliferation-quiescence transition. In other words, for two sibling cells – one will enter into a prolonged G0 while the other will commit to the next cycle rapidly (Fig.3.6A). Although this occurred, it was more common to observe two daughter cells making symmetric decisions and simultaneously undergoing the next cycle (Fig. 3.6B) or entering into a prolonged G0 (Fig.3.6C). Due to lack of a constitutive nuclear marker, we were unable to perform the lineage tracing and to quantitatively measure the frequency of this asymmetric decision. Therefore, in a collaboration with Dr. Yu-Chih Chen, in the School of Electrical Engineering, we used a microfluidic array platform to both isolate and monitor single-cells, and their daughters in the subsequent cell divisions (Fig. 3.6D).

Our microfluidic device is a set of micrometer-size channels, using the hydrostatic pressure inside micro-channels to isolate and capture single cell from a fluid suspension. Once a cell enters a chamber, the captured cell serves as a flow restrictor to prevent other cells from flowing in. But occasionally more than one cell is captured in a single chamber, likely due to fluctuations in the fluid pressure.

Consistent with what I saw in the asynchronous cell culture for 3T3 cells, in the microfluidic device I found that two sister cells derived from the same mitosis made asymmetric decision: one of the two daughter enters the next cycle while the other stays in a quiescent state (Fig.3.6D). Cells in column 1 or 15 shows sister cells born of the same mitosis made heterogeneous decisions at the proliferation-quiescence transition. The occurrence of an asymmetric decision is about 15% from 20 mitotic divisions observed in about 100 single captured chambers in 40hr time-lapse movies. This suggests that the proliferation-quiescence decision is asymmetric after mitosis, and this asymmetry may be the reason for proliferative heterogeneity in asynchronous cycling cell populations.

## Discussion

### Automated, quantitative analysis via computational cell cycle profiling framework

The assessment of cell cycle behaviors in a population of cells commonly use traditional techniques, such as FACS and immunoblotting. However, single-cell assays reveal the heterogeneous behaviors that are masked by single time point (FACS) or bulk assays. Single-cell assays usually contain large amounts of data, which requires automated quantitative measurement and analysis. Here we developed large-scale, automated computational cell cycle profiling framework to assess cell cycle behaviors at single-cell level from time-lapse imaging. With the application of two fluorescent G0/G1 cell cycle indicators, I measured the dynamic cellular behaviors at the proliferation-quiescence transition. The advantage of our system is that we are able to characterize cell cycle behaviors via the measurement of two fluorescent cell cycle reporters in time-lapse imaging, without a constitutive nuclear marker. With proper modification of automated computational calculations, this framework could be applicable to assess active cell cycle progression via the traditional Fucci reporters. Thus, it will help us better understand the dynamic response of cell cycle behaviors to different physiological conditions or in various cancer models.

There are a few limitations of our system: first, we are unable to track multiple successive rounds of divisions due to the no color labeled S/G2/M phases. In other words, mother-daughter cell lineages cannot be assigned with the current cell cycle

indicators. Second, we uncovered that cells may enter into a quiescent state when they are in the early G1 state (the G1-G0 transition) under serum starvation, which is not recognized by mVenus-p27K$^-$ reporter. This implies the variability of quiescence under different conditions and indicates that no single cell cycle marker will be sufficient to cover all states of quiescence.

**Asymmetric decision at the proliferation-quiescence transition may lead to tumor dormancy**

A mixture of cycling and non-cycling cells is also likely to be an inherent property of many cancers that exhibit periods of dormancy and recurrence, such as breast and prostate cancer. Cellular dormancy refers to small groups of disseminated tumor cells (DTC) that separated from the primary tumor, spread through the circulation system to other distant locations of the body and stay in quiescence. It is believed that being quiescent allows residual DTCs to be refractory to the current chemotherapy which usually exclusively targets proliferating cells. Later, DTCs will cause the relapse of cancer by reverting back to proliferation when conditions are more favorable.

Research in human breast cancer cell lines has shown that inhibition of AKT signaling could induce asymmetric cancer cell division, which produces one actively cycling daughter and one slowly cycling G0-like cell (Dey-Guha et al., 2011). Such an

asymmetric division is consistent with my observation in untransformed mammalian cell culture, that two daughter cells born of the same mother can make heterogeneous decisions at the proliferation-quiescence transition. This suggests that the asymmetric decision upon the proliferation-quiescence transition could be a universal phenotype in a wide range of cell types, and investigation of the molecular mechanisms that underlie the asymmetric decision may elucidate how quiescent DTCs are generated from a proliferative primary tumor, to shed new light on cancer prognosis and treatment improvement.

**A checkpoint at the proliferation-quiescence decision**

Cell proliferation in culture is largely driven by environmental mitogenic stimuli in the culture medium. It is believed that cells are sensitive to extracellular serum growth factors in G1 phase prior to a time point, “restriction point” (R-point). After cells pass the R-point, even with serum deprivation, cells continue proliferation, and commit to the next cycle (Pardee, 1974). Back in the 1980s, time-lapse studies of Swiss 3T3 cells showed that a brief serum deprivation right after mitosis can arrest cells in quiescence /G0, accompanied by the reduction in protein synthesis. However, only cells within 3-4hr after last mitosis entered into quiescence in response to serum withdrawal, whereas cells more than 4hr after mitosis completed the rest of cell cycle even in the absence of serum (Larsson and Zetterberg, 1985). Therefore, G1 phase was subdivided into two

phases: “G1 postmitosis” and “G1 pre-DNA synthesis”, separated by the restriction point, serving as the decision boundary for cells to respond to growth factors.

Recent studies have suggested that the decision to enter quiescence actually occurs during G2 or immediately after mitosis, prior to the passage of cells through the restriction point (Spencer et al., 2013; Naetar et al., 2014; Sun and Buttitta, 2015) (Fig. 3.7). Thus, what regulates the proliferation-quiescence decision after mitosis? Studies in different cell types or model systems have suggested that different mechanisms for PP2A in modulation of the proliferation-quiescence decision prior to G1 entry. In human fibroblasts, it is suggested that PP2A/B56-mediated Ras inactivation in G2 phase influences the entry into quiescence (Naetar et al., 2014). However, our recently published data suggest a different role for the PP2A/B56 complex in promoting quiescent entry in developing tissues, which is independent of Ras/ERK signaling and RB/E2F/DP function (Sun and Buttitta, 2015). It is likely that the PP2A/B56 complex plays multiple roles in the proliferation-quiescence decision prior to R-point by acting upon different targets in cell types or developmental contexts.

Notably, our automated cell cycle reporter assay showed cells with compromised PP2A functions are 16% more likely to override a prolonged G0, compared to cells in control groups. In particular, PP2A inhibition for 30min before imaging only affects the probability of remaining in G0 phase but not G1 phase. This suggests that the proliferation-quiescence decision occurs immediately after mitosis and earlier than R-point. My data suggests that PP2A modulates this decision via suppressing Cdk2

activity after mitosis. Since the threshold of Cdk2 activity is responsible for the proliferative heterogeneity (Spencer et al., 2013), PP2A acts as an additional barrier to raise this threshold. Together, this indicates that after mitosis multiple cellular signal inputs impinge upon Cdk2 activity level at the proliferation-quiescence decision, directing cells to commit to a next cycle or to enter quiescence.

## Materials & Methods

### Cell culture

Mouse embryonic fibroblasts (MEFs) 3t3 were grown in Dulbecco's modified Eagle's medium (DMEM; Gibco) supplemented with 10% fetal bovine serum (FBS) and 1% penicillin-streptomycin. For PC3 cells, RPMI/ 10% FBS was supplemented with 1% penicillin-streptomycin.

### Flow Cytometry analysis and FACS

Cells were fixed with 4% paraformaldehyde, and then stained with the nuclear dye-- FxCycle Violet. Resuspended cells were analyzed by Attune flow cytometer to read the cell cycle profiles.

Prior to sorting, the transduced NIH3T3 cells were cultured in DMEM supplemented with either 10% FBS or 1%FBS for 24-72 hr, then subpopulation cells were sorted according to the intensity of their fluorescent reporters, mVenus-p27$^{K-}$(+)/mCherry-hCdt1(30/120)(+) NIH3T3 cells (G0) or mVenus-p27$^{K-}$ (-)/mCherry-hCdt1(30/120)(+)NIH3T3 cells (G1) or mVenus-p27$^{K-}$(-)/mCherry-hCdt1(30/120)(-) NIH3T3 cells (S/G2/M), using BD FACS Aria II system. Cells were sorted into sub-population for protein extraction or RNA isolation.

**Time-lapse, live-cell image**

Cells cultured on a 12-well plate in DMEM/10%FBS or 1%DMEM were subjected to time-lapse imaging by EVOS FL cell imaging system with an objective lens (20X) or IncuCyte Zoom live-cell imager under 37$^{o}$C , 5% CO2 environmental control. The imaging interval time was every 20 or 30 minutes, and the movie length was 24-30hr.  30min, 50nM OA treatment was done 1~2hr prior to the time-lapse imaging.

**Image process & analysis (program segmentation & tracking)**

Cell segmentation and tracking were performed using a MATLAB program that automates these processes as described below. The program interface provides interactive adjustment of the parameters used at each step in the segmentation process, allowing the user to tailor the segmentation process to accommodate the characteristics of each image under analysis. The output of this software is an Excel file containing the identified cells, the frame number(s) in which they appear, the size, approximate radius, and cell center location in each frame, and the average and maximum intensity values in the cell on both the red and green channels in each frame, as well as the segmentation settings used to obtain these results.

Cell segmentation

The segmentation process consists of four main steps: smoothing the image, conversion to black and white, splitting merged cells, and filtering potential cells by size. Initial smoothing is done using a circular averaging filter, where the filter radius is adjustable and is specified by the user for each image stack. The filtered image is then converted to a black-and-white image based on a threshold intensity level entered by the user. Pixels above this intensity are part of potential cell candidate areas and are white or value 1 in the resulting black-white image, while all remaining pixels are background (black, value 0). Connected sets of white pixels are considered candidate cells, and the resulting black-and-white image is cleaned up by removing any potential cells overlapping a border of the image and filling any holes within remaining potential cells. Since this simple threshold method often causes neighboring cells to be merged into a single spot, the next step splits these merged spots into separate cells. First the Euclidean distance transform of the inverse of the black-and-white image is calculated, giving the distance from each cell pixel to the background pixel. Those distances that are less than a user-specified threshold distance from background are then suppressed using an H-maxima transform; if the threshold entered is 0, this step is skipped. The resulting image, which ideally contains one local maximum per cell, is then segmented using the watershed algorithm. The dividing lines from this watershed output are overlaid with the black-and-white cell image; any pixel where a watershed line overlaps a cell spot is changed from a cell pixel to a background pixel, effectively dividing merged cells. Finally, each identified potential cell is compared to user-entered maximum and minimum cell sizes. Any potential cells with more pixels than the

maximum or fewer pixels than the minimum are discarded, and the remaining cell candidates are identified as cells.

Following automatic segmentation, the user has the option to manually delete cells that have been misidentified and/or draw additional cells that the automated process missed.

### Cell tracking

Once segmentation is complete, cell tracking is done with the Simple Tracker tool available on the MATLAB File Exchange. This tool uses the Hungarian algorithm to link cells from frame to frame into connected tracks using user-entered parameters for maximum movement distance allowed between frames and maximum gap in frames allowed between occurrences of the same cell track. Tracks were verified by hand to be sure that one track represented the same cell for the duration of the track.

## Statistical analysis

### Fluorescence Intensity smoothing

Analysis was restricted to cells tracked over at least 3 video frames (1~1.5hr). The mCherry and mVenous fluorescence signals were smoothed using a nearest neighbor proportion localized polynomial approach. The nearest neighbor value parameter was chosen using an Akaike

Information Criteria based optimization with leave one out cross-validation. Calculations were performed using the Locfit package in the software program R 3.0.1.

Transformation to survival time data

For each cell, the cell cycle state over each pair of time points was assigned as described in Fig. 3.3G. For each cell, the aggregated time spent in each state was calculated. The event class for the last time point in each state was assigned as either “correct cycle” or “censored”. Cells that were not assigned to progress forward in the cell cycle were excluded from the analysis.

Statistical calculations

Associations between experimental time and overall fluorescence intensity were calculated via the Pearson’s correlation coefficient and associated test. Survival curves were generated via the Kaplan-Meier method. Hazard ratios, median time to event, and time within a state comparisons were calculated using the Cox proportional hazards model. Survival time statistics were calculated using the survival package in R 3.0.1. Sample size calculations assumed equal number of cells per group, and equal event proportions between groups and were performed using the powerSurvEpi package in R 3.0.1.

**Western Blotting**

Antibodies used: anti-mouse Rb2/p130 (BD Biosciences, 610261,1:1000), anti-mouse phospho-Cdk2$^{T160}$ (Cell Signaling, 1:500), anti-mouse Cdk2(Santa Cruz, M2, 1:1000), anti-rabbit p27 (Cell Signaling, #2552, 1:1000) or anti-mouse GAPDH (Cell Signaling, 14C10, 1:2000) were used as loading controls with the appropriate HRP-conjugated secondary antibody. Enhanced Chemiluminescence-detection (Amersham) was performed and band signal intensity was quantified using NIH Image J.

**RT-qPCR**

For RT-qPCR, RNA was isolated from sorted cells per the TRIzol manual, resuspended in water, and then treated with TURBO™ DNase to remove contaminating DNA. Using 500ng of RNA per sample, cDNA was synthesized using oligo$(dT)_{20}$ and the Superscript III First-Strand Synthesis System (Invitrogen 18080051). qPCR using 0.5µL of cDNA per reaction was then performed using the 7500 Fast Real-Time PCR and StepOnePlus Real-Time PCR Systems (Applied Biosystems)

Primer sequences

| Primer name | Sequence |
|---|---|
| Forward-GAPDH | ATGTGTCCGTCGTGGATCTGA |
| Reverse-GAPDH | TTGAAGTCGCAGGAGACAACCT |
| Forward-PCNA | TTTGAGGCACGCCTGATCC |
| Reverse-PCNA | GGAGACGTGAGACGAGTCCAT |

| | |
|---|---|
| Forward-Mki67 | CCTTGGCTTAGGTTCACTGTCC |
| Reverse-Mki67 | TGCAGAATCCAGATGATGGAGC |
| Forward-Geminin | GGGAGCCCAAGAGAATGTGAA |
| Reverse-Geminin | CAAGCCTTTTGGCAACTCATTT |
| Forward-Sod3 | CCTTCTTGTTCTACGGCTTGC |
| Reverse-Sod3 | GCGTGTCGCCTATCTTCTCAA |
| Forward-Pdcd4 | CCACTGACCCTGACAATTTAAGC |
| Reverse-Pdcd4 | TTTTCCGCAGTCGTCTTTTGG |

**Acknowledgements**

Dr. Alex Pearson (University of Michigan, School of Dentistry) generated the statistical pipeline for the data analysis, data smoothing and graphing of the Kaplan-Meier curves using the R statistical software package. Zhengda Li (Yang Lab, University of Michigan, Biophysics) and Abbey Roelofs (University of Michigan, College of Literature, Science and the Arts IT) generated the scripts used for cell segmentation and tracking in MatLab software. I also thank Zhengda for his idea in converting fluorescent reporter intensity readings to the radian readings. In addition, I thank Dr. Yu-Chih Chen and the Yoon Lab (University of Michigan, Department of Electrical Engineering and Computer Science) for providing the microfluidic devices. Lulia Kana provided technical assistance.

## Figures

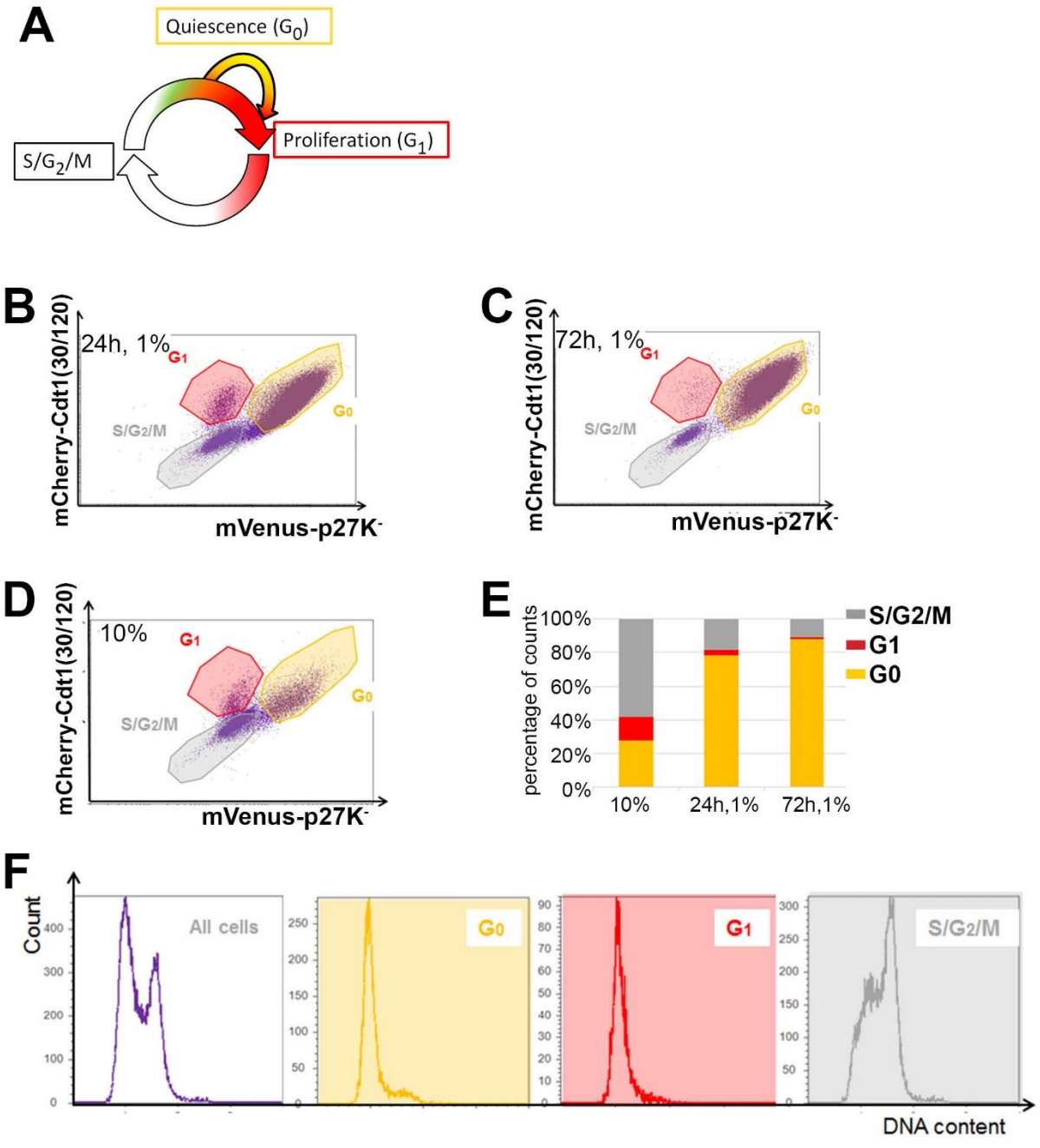


**Figure 3. 1 Expressions of mVenus-p27K$^-$ & mCherry-hCdt1(30/120) cell cycle indicators accumulate in G1/0 phase**

(A) Diagram of the fluorescence changes we observe with the G0/G1 mVenus-p27K$^-$ & mCherry-hCdt1(30/120) cell cycle reporters. (B-D) FACS dot plots are generated from 3T3 cells expressing mVenus-p27K$^-$ and mCherry-hCdt1(30/120) probes, cultured with 1% serum media for 24hr (B) or 72hr (C) or with normal 10% serum media (D). A sub-population of double positive cells increases as cells are treated with serum starvation. (E) Bar graph of FACS analysis is to show the composition of distinctively labeled cell sub-populations under different growth conditions. (F) Cell cycle profiles from sub-populations gated in Fig. 3.1D. Double positive cells with mVenus-p27K$^-$(+)/mCherry-hCdt1(30/120)(+) or single positive cells with mVenus-p27K$^-$(-)/mCherry-hCdt1(30/120)(+) labels contain 2C DNA contents. On the contrary, majority of S/G2/M cells with low mVenus-p27K$^-$ or mCherry-hCdt1(30/120) expression shows larger than 2C DNA contents.

.

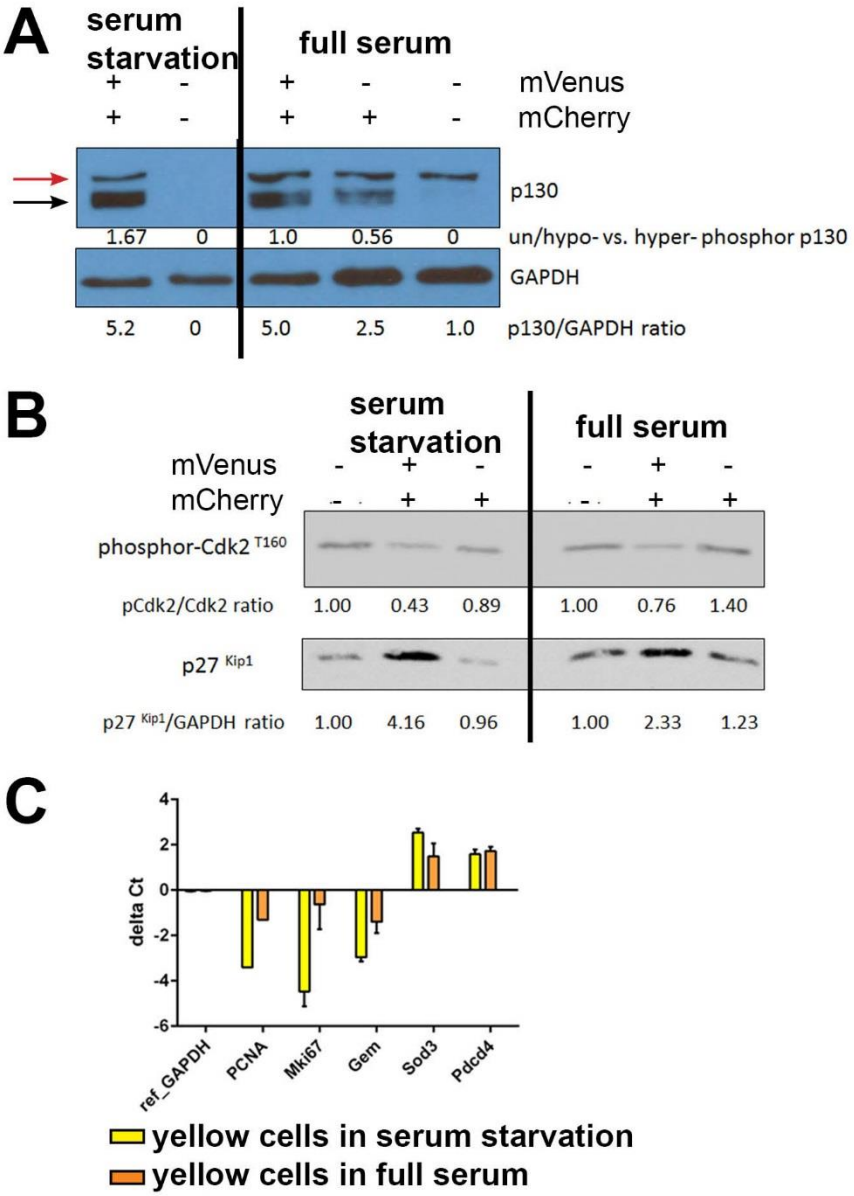


**Figure 3. 2 Molecular evidence to confirm G0/G1 cell cycle indicators**

(A-C) cells sorted into mVenus-p27K$^-$(+)/mCherry-hCdt1(30/120)(+), mVenus-p27K$^-$(-)/mCherry-hCdt1(30/120)(+), and mVenus-p27K$^-$(-)/mCherry-hCdt1(30/120)(-) three groups via FACS, and then protein or RNA extracts were prepared to perform western blot analysis (A,B) or real-time quantitative PCR(C). (A) The western blot showed that a 2-fold increase in the ratio of un/hypo-

phosphorylated to hyper-phosphorylated form p130 in double positive cells, compared to mCherry single positive cells. The un/hypo-phosphorylated form and hyper-phosphorylated form are indicated by the black and red arrows, respectively. (B) Cdk2 complex is a positive regulator in G1 phase, and the blots show the active form of Cdk2 is enriched in mCherry-hCdt1(30/120) single positive cells compared to double positive cells. In contrast, CKI protein-- p27 is highly expressed in double positive cells. (C) RT-qPCR shows that active cell cycle regulators are downregulated in mVenus-p27K$^-$(+)/mCherry-hCdt1(30/120)(+) yellow cells, whereas tumor suppressors or genes protecting cells from accumulating damages are enriched, compared to the gene expression level from mCherry-hCdt1(30/120) single positive cells. Δ CT = log2 of the fold difference from mCherry-hCdt1(30/120) single positive cell samples.

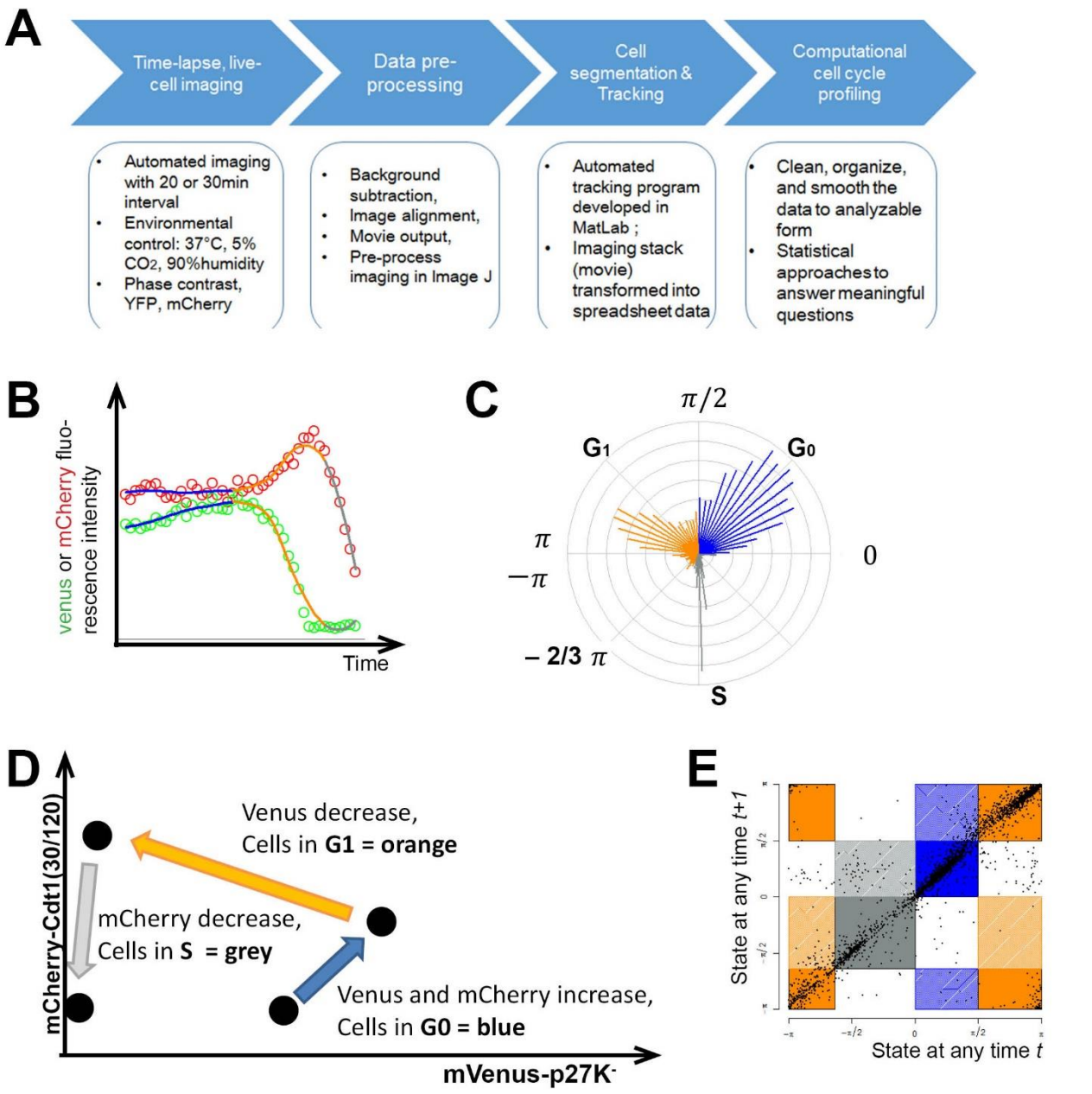


**Figure 3. 3 Automated computational analysis showing three distinct states under normal unperturbed growth conditions**

(A) A workflow of single-cell, automated computational cell cycle profiling platform (B) Representative single-cell trajectory of two fluorescent probes in time-lapse, live-cell imaging. Each circle depicts one fluorescent intensity reading at a given time in either green or red

channel. (C) The radial histogram shows the conversion of the two fluorescent intensity readings from each time frame to the radian readings between two time frames next to each other. The length of the spikes depicts the frequency of individual cells with two fluorescent reporters behaving at certain radian. (D) Three distinct cell cycle behaviors in order were observed from two cell cycle reporters fluorescent intensity changes in asynchronous cells. When cells in state G0, mVenus reporter as well as mCherry-Cdt1 accumulate together, colored in blue. Then cells transit into G1 when mVenus fluorescent signal decreases while mCherry still keeps high, which is colored in orange. The third state is S phase entry, when mCherry signal decreases, colored in grey. (E) The dot plot represents the post-smoother radian assignment values for all temporally adjacent t vs. t+1 over all captured cells in the movies from normal full serum growth conditions.

**Live, time-lapse movie attachments**.

Movie 1. 3T3 cells cultured in full serum media in a 30hr movie

Movie 2. 3T3 cells cultured in low serum media in a 30hr movie

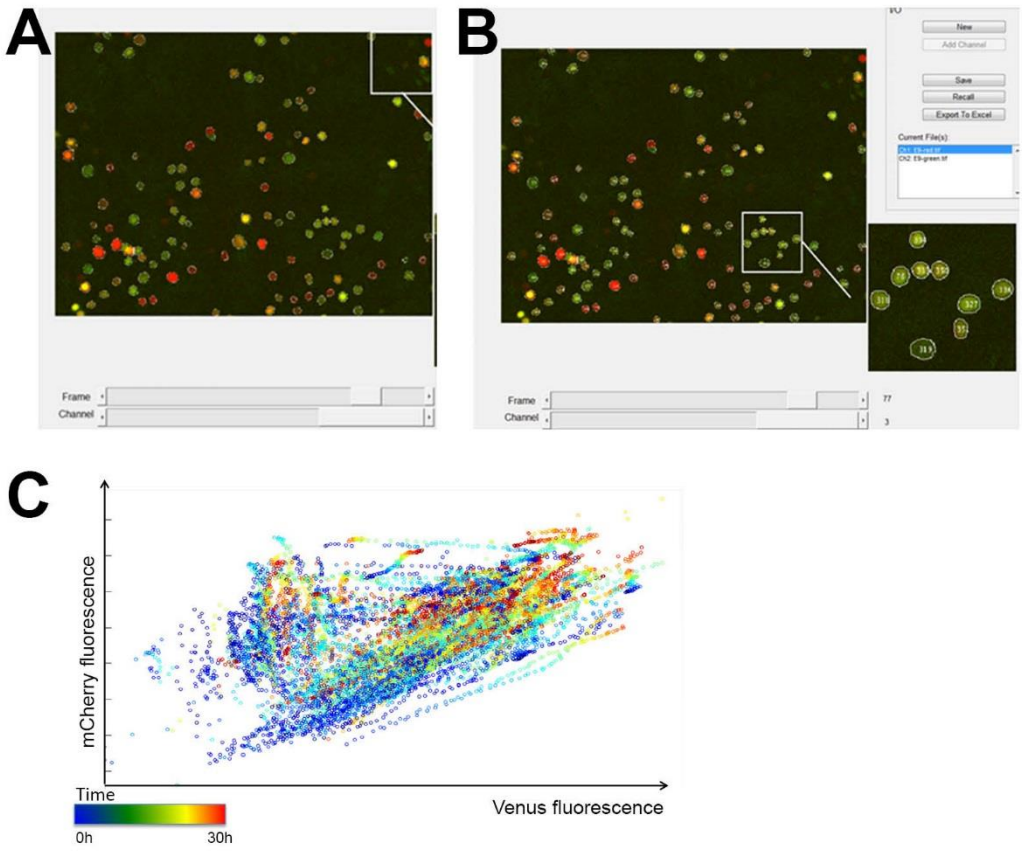


**Figure 3. 4 Live-cell image to show the cell cycle behaviors at the proliferation-quiescence transition**

(A-B) the interface of cell segmentation & tracking program in MatLab. (A) the result of cell segmentation (B) the result of cell tracking. (C) Raw outputs of the cell tracking program. Each cell is represented by a dot, and the color changes from blue to red over time. The plot was graphed according to the fluorescent intensity readings at any interval time in a 30h time-lapse movie.

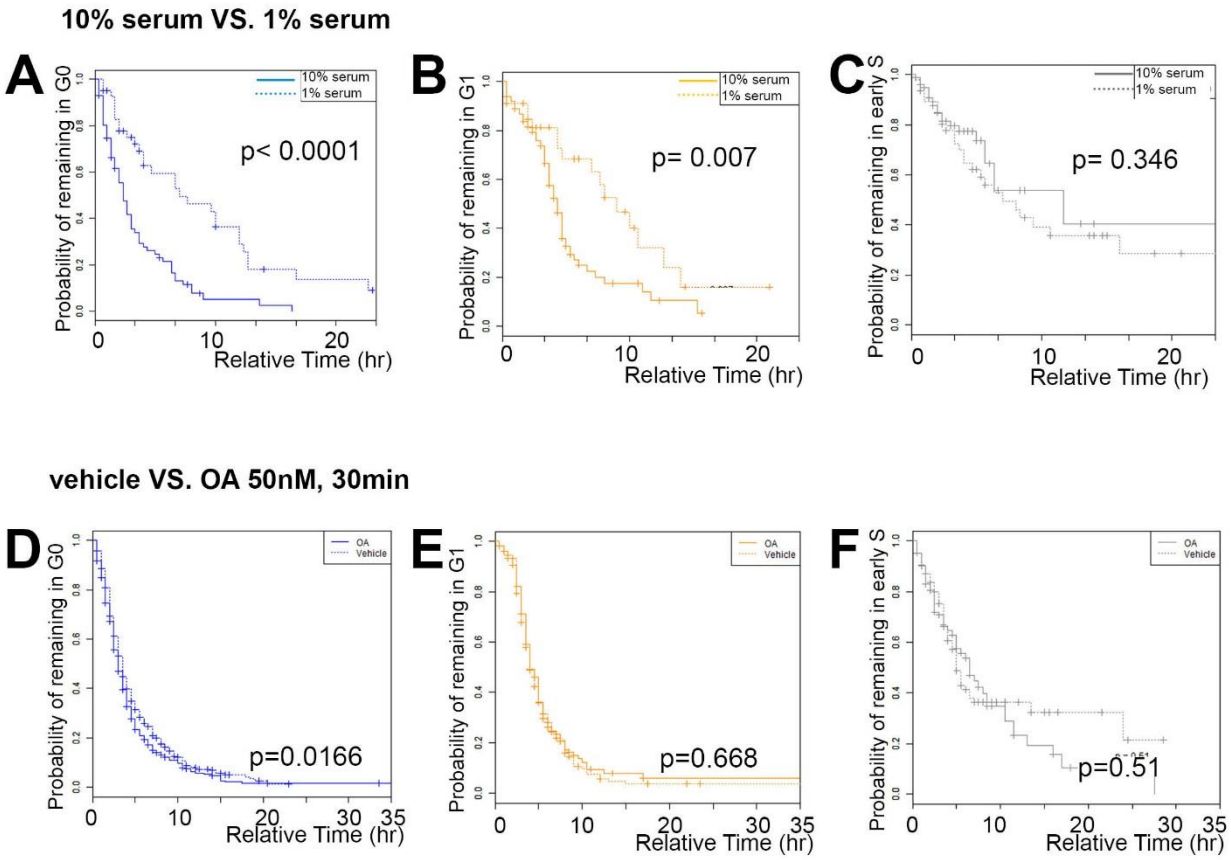


**Figure 3. 5 Serum deprivation and PP2A inhibition impact the proliferation-quiescence transition in distinct manners**

(A-C) The Kaplan-Meier curves of each state estimates the time cells remaining in each state under either full serum (10%) or low serum (1%) conditions. The analysis shows that cells tend to spend longer time in both G0 and G1 states in response to serum starvation (p value<0.05). (D-F) 50nM Okadaic Acid (OA) is used to inhibit PP2A functions for 30min prior to live, time-lapse imaging. The Kaplan-Meier curves showed cells with OA treatment tend to spend less time in G0 than cells in vehicle treatment. There is statistically significant decrease in the probability of cells entering a prolonged G0 whereas no significant difference in time spent in G1 state or S phase entry.

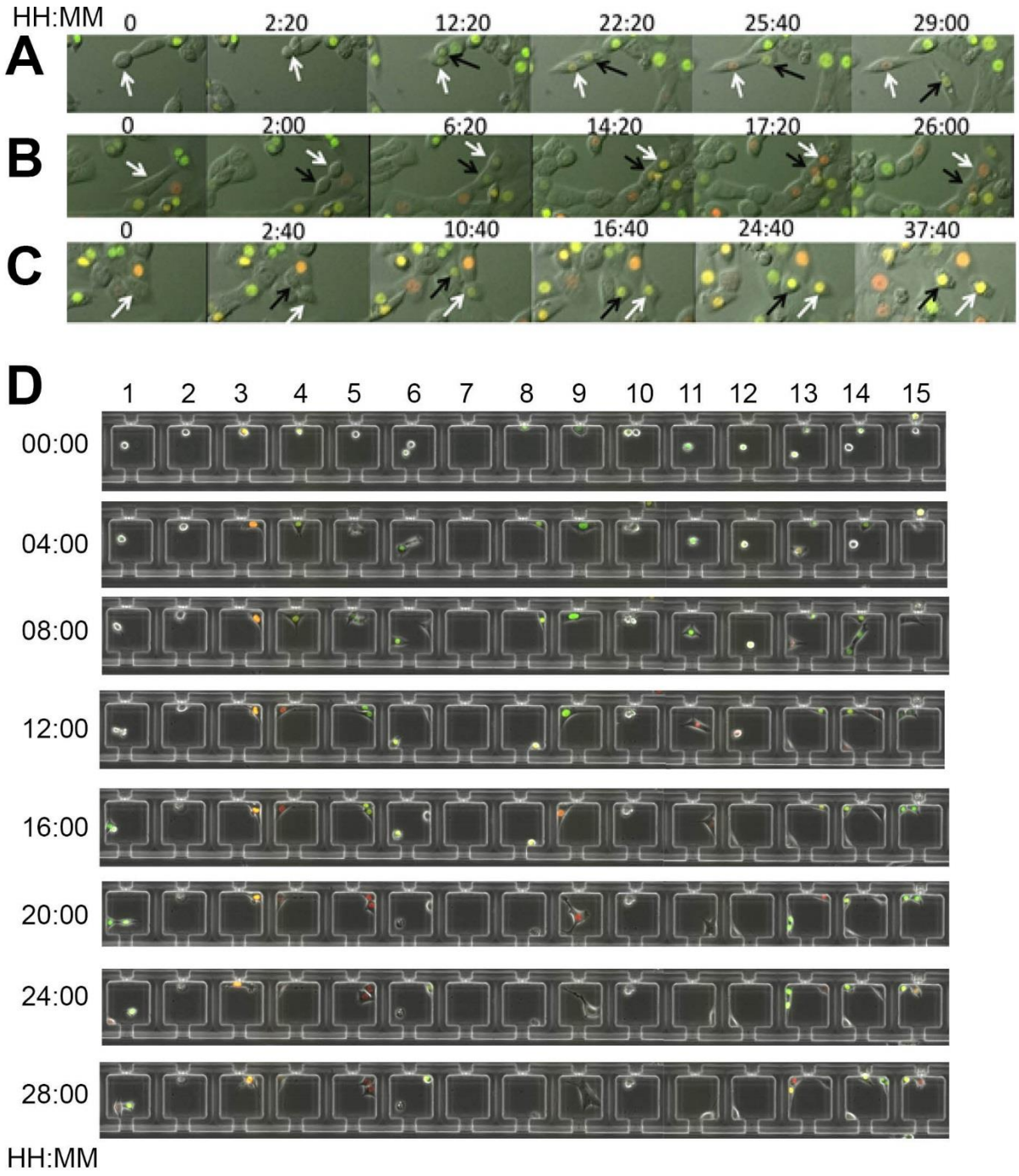


**Figure 3. 6 The asymmetric decision between sister cells born of the same mitosis at the proliferation-quiescence transition**

(A-C) Representative images from the live, time-lapse captured in asynchronous, cycling cells with mVenus-p27K$^-$ & mCherry-hCdt1(30/120) constructs. Daughters from the same mitosis are

indicated by black and white arrows. (A) two daughter cells born of the same mitosis made asymmetric decisions, while (B,C) daughter cells made symmetric decisions of the proliferation-quiescence in the same dish in normal full serum media. (D) Representative images of time-lapse, live-cell movie. Cells were captured and monitored via a microfluidic device prior to the time-lapse imaging. Chamber 1 and 15 show the asymmetric decision made between daughter cells. Chamber 5 shows a symmetric decision from two daughter cells. Cells in chamber 4,9 and 11 rapidly commit to the next cycle, while cell in chamber 3 stay in a prolonged G0. 5 out of 15 chambers shown here failed to capture single cells at the beginning of the movie, including chamber 6, 7,10,13 and 14.

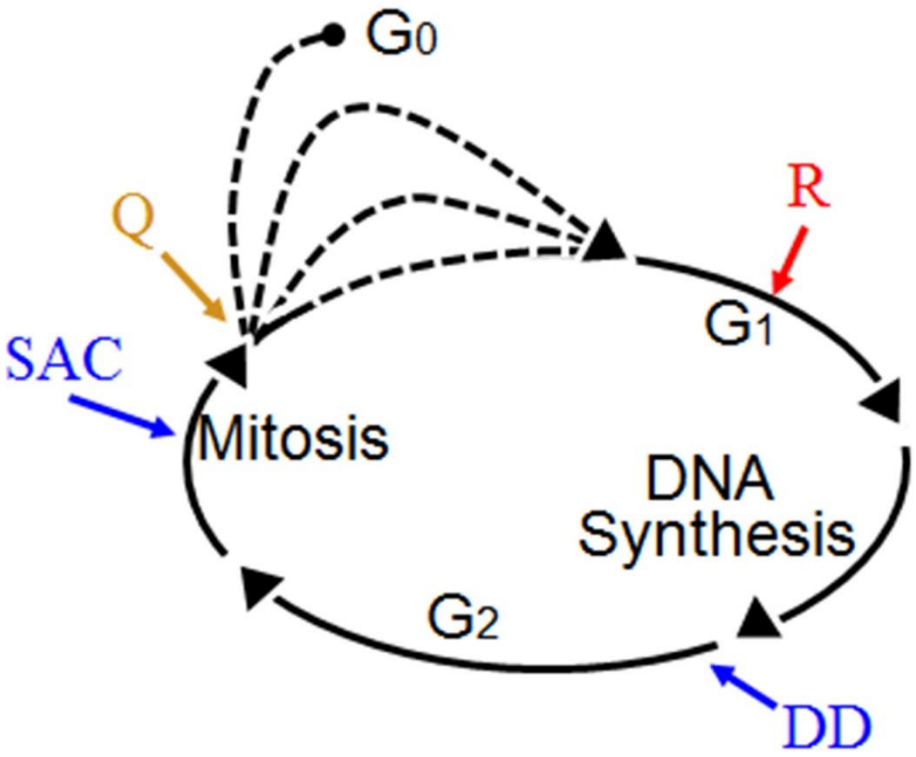


**Figure 3. 7 Checkpoints throughout the cell cycle.**

The red arrow denotes the Restriction Point (R), while the yellow arrow denotes the proliferation-quiescence decision point (Q). Other cell cycle checkpoints, such as the DNA damage checkpoint in G2 (DD, which may also occur in G1), and spindle checkpoint (SAC) are in blue. The variation in $G_0$ is depicted as dashed paths between M and G1 phases.

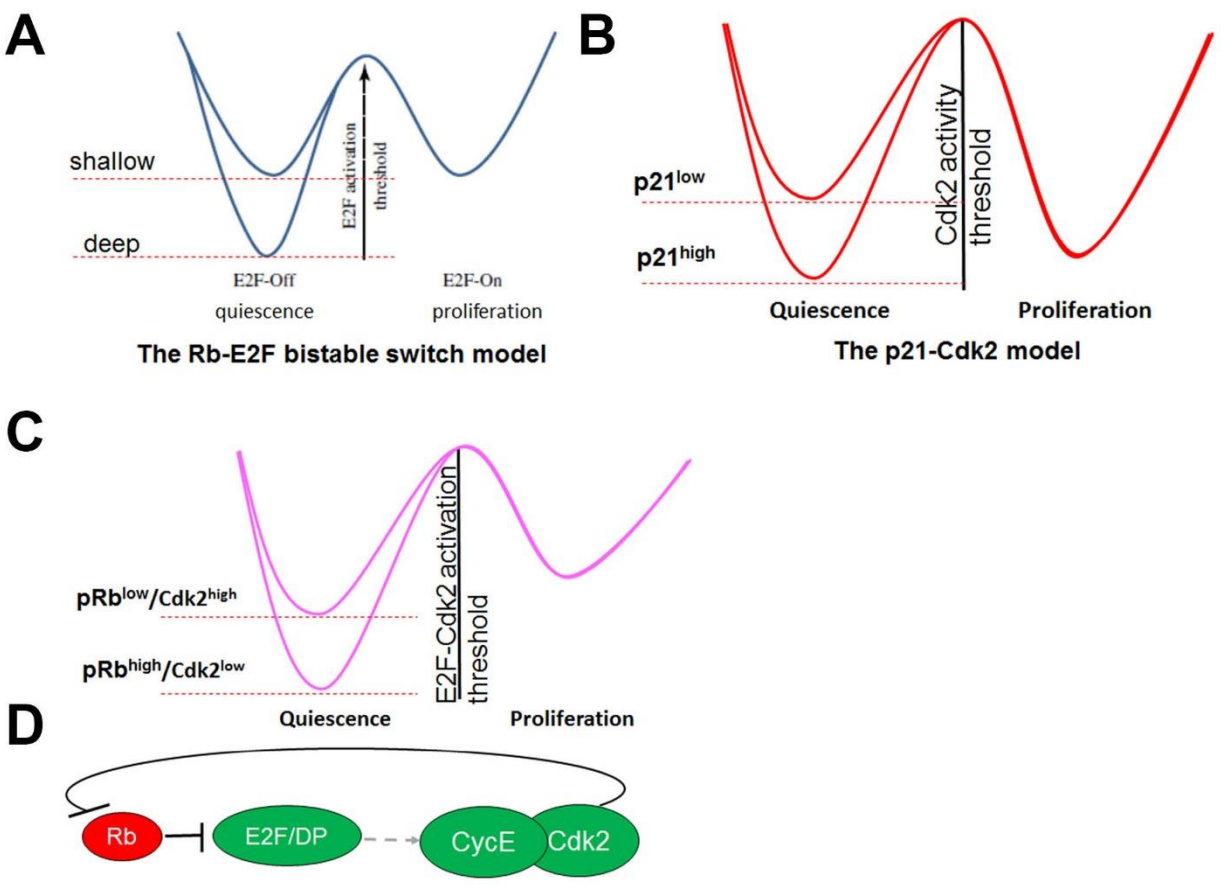


**Figure 3.8 The threshold models at the proliferation-quiescence decision**

(A)The Rb-E2F bistable switch model, modified from (Yao, 2014). (B) The p21-Cdk2 model, proposed from (Overton et al., 2014). (C) The connection between the Rb-E2F model and the p21-Cdk2 model is based on a feedback loop exists between the inhibitor Rb, the transcriptional activator E2F and the key G1 cyclin CycE (D).

## Tables

| Growth conditions | Error rate | Treatment | Error rate |
|---|---|---|---|
| Full serum (10%) | 1.94% | Vehicle | 2.37% |
| Serum starvation(1%) | 1.57% | 30min, 50nM OA | 3% |

**Table 3. 1 Table of error rates.**

The correct assignment rate is 1-error rate, and here shows the majority cells (97-98%) in real-time imaging follow the correct G0-G1-S/G2/M order.

Assuming 90% of cells observed to correctly exit cycle of interest

| | Hazard ratio = 1.2 | | Hazard ratio = 1.5 | | Hazard ratio = 2 | |
|---|---|---|---|---|---|---|
| α | β = 0.8 | β = 0.9 | β = 0.8 | β = 0.9 | β = 0.8 | β = 0.9 |
| 0.05 | 528 | 707 | 110 | 146 | 40 | 53 |
| 0.01 | 786 | 1001 | 163 | 207 | 59 | 75 |
| 0.001 | 1148 | 1406 | 238 | 291 | 86 | 105 |

Assuming 80% of cells observed to correctly exit cycle of interest

| | Hazard ratio = 1.2 | | Hazard ratio = 1.5 | | Hazard ratio = 2 | |
|---|---|---|---|---|---|---|
| α | β = 0.8 | β = 0.9 | β = 0.8 | β = 0.9 | β = 0.8 | β = 0.9 |
| 0.05 | 594 | 795 | 123 | 165 | 45 | 60 |
| 0.01 | 884 | 1126 | 183 | 223 | 66 | 84 |
| 0.001 | 1292 | 1581 | 267 | 327 | 97 | 118 |

**Table 3. 2 Table of the power calculation**

# Chapter 4. Conclusions & Future directions

## 4.1 The switch of PP2A functions after mitosis

Two major models regulate the proliferation-quiescence decision: first, Rb-mediated repression of E2F transcriptional complexes promotes quiescence, and second, CKI-directed suppression of G1 cyclin/Cdks activity promotes quiescence. My thesis work has revealed a parallel pathway for restricting Cdk2 activity through PP2A/B56 removing T-loop phosphorylation a couple of hours after mitosis. This promotes cell cycle exit upon differentiation in tissue development and entry into quiescence in mammalian cells (Fig.4.1). The threshold of Cdk2 activity level dominates the proliferation-quiescence decision, and my work shows PP2A/B56 is one of the upstream regulators of Cdk2 activity to modulate the proliferation-quiescence decision.

The involvement of B56 (wdb) in promoting quiescence following the completion of mitosis implies a regulatory subunit switch after mitosis impacts PP2A functions. The PP2A complex is a multisubunit protein phosphatase, and two factors influence PP2A activity towards substrates: the binding of specific B-type regulatory subunits and the levels of PP2A inhibitors (Williams et al., 2014). The expression pattern of the B-type subunits is often controlled in a cell- or tissue-specific manner, which can direct PP2A

functions to a specialized location in cells or tissues. B55 (*twins)* is widely expressed and perform its essential functions in mitosis. B55 protein level peaks in mitosis where it is required for mitotic entry, mitotic exit and chromosome segregation (Brownlee et al., 2011; Chen et al., 2007; Wang et al., 2016). This raises the question of how the regulatory subunits may switch from predominant B55 (twins) in mitosis to B56 upon mitotic completion and the entry into G0. One study has suggested that APC/C might target B55/tws for degradation at anaphase for the sister chromatid separation (Deak et al., 2003). This model is intriguing as the degradation of B55 by the APC/C may bias PP2A complexes toward B56 after mitosis.

Additionally, recent work characterized an inhibitor specific to PP2A/B56 complexes termed Bod1. Bod1 acts on the mitotic kinetochores late in mitosis (Porter et al., 2013), and its *Drosophila* ortholog CG5514 has been recently identified (Esmaeeli-Nieh et al., 2016). Therefore, an interesting future direction will be to examine whether Bod1 influences the proliferation-quiescence decision in opposition to PP2A/B56.

## 4.2 Proliferation is heterogeneous in clonal cell populations

Proliferative heterogeneity in clonal populations has been reported in multiple immortalized cell lines, such as MCF10A, Swiss3T3, as well as cancer cell lines, such as MCF7, and colon cancer-initiating cells (CCICs) (Spencer et al., 2013; Dey-Guha et

al., 2015; Srinivasan et al., 2016). The relative percentage of cells that enter quiescence is highly dependent upon the cell types and culture conditions, suggesting many signaling inputs likely influence the proliferation-quiescence decision. In the MCF10A cell line, this proliferative heterogeneity seems to be due to variable levels of the Cdk2 inhibitor p21, which acts as a rheostat to modulate Cdk2 activity above and below certain thresholds (Overton et al., 2014). In cancer cells such as HCT116 and MCF7, the β1-integrin/FAK/mTORC2/AKT1–associated signaling pathway has been suggested to promote asymmetric cell division and produce quiescent or slowly proliferating daughter cells (Fischer et al., 2015).

We also found that untransformed cells exhibit proliferative heterogeneity under growth conditions, and that the G0 state is heterogeneous. This means that cells spend variable lengths of time in G0/quiescent state, which leads to proliferative heterogeneity. A recent study has suggested that a transcriptional spike occurs heterogeneously at the mitosis-G1 transition, which could lead to cell-to-cell differences in mature mRNA expression (Hsiung et al., 2016). Hence, inherently heterogeneous mRNA levels may lead to the variability in quiescence.

Single-cell RNAseq analysis may allow us to examine the wide distribution of gene differential expressions, and this may further elucidate how cells enter into a prolonged quiescence instead of a transient one. In situations such as cancer, cells with random genetic mutations give rise to a vast heterogeneity in morphology, immunophenotype

and etc. Therefore, the traditional bulk population analysis may mask certain features that could provide novel unique diagnostic or therapeutic cues. Single-cell analysis is the way forward for understanding cancer cell heterogeneity in tumors.

## 4.3 Cellular quiescence in tumor dormancy

It is appreciated that most cancers are comprised of mixed populations, with some cells actively proliferating, while other cells are quiescent, depending on their micro-environmental cues (Hanahan and Weinberg, 2011). It is believed that tumor recurrence years after the primary treatment could be the result of the non-cycling, quiescent tumor cells re-entering cell cycle and developing into secondary tumors (Almog, 2010; Klein, 2011). A small group of disseminated tumor cells (DTCs) cells left from primary tumor removal or treatment are often resistant to chemotherapy, even small in size which turn out to be extremely different for clinical detection (Aguirre-Ghiso, 2007). The dormant DTCs exist in several human cancers, such as breast cancer, prostate cancer and colon cancer (Sosa et al., 2014; Yeh et al., 2015).

Prostate cancer (PCa) cells mainly metastasize to bone marrows, and stay dormant for years before switching back to proliferation and eventually causes tumor recurrence, reviewed in (Shiozawa et al., 2015; Morrissey et al., 2016). Recent studies in several prostate cancer cell lines *in vitro*, showed that a low frequency sub-population of cells

were in quiescence as assessed by a dye-retention assay (Wang et al., 2015). The idea that the quiescent tumor cells regain cellular proliferation triggers an interesting question whether disruption of quiescence will improve the primary cancer treatment outcomes *in vivo* cancer model. The mVenus-p27K$^-$ cell cycle indicator enables us to monitor the proliferation and quiescence properties of cells at single-cell resolution. Dr. Russ Taichman's group in University of Michigan generated a xenograft mouse model for human prostate cancer cell metastasis to the bone (Taichman et al., 2013). Combination of our G0/G1 cell cycle labeling techniques and their tumor dormancy model will provide us a great opportunity to test the hypothesis that DTCs are insensitive to chemotherapies designed to target proliferative cancer cells. Furthermore, we will be able to examine whether disruption of quiescence will sensitize DTCs to current chemotherapies and improve treatment outcomes.

## Figure

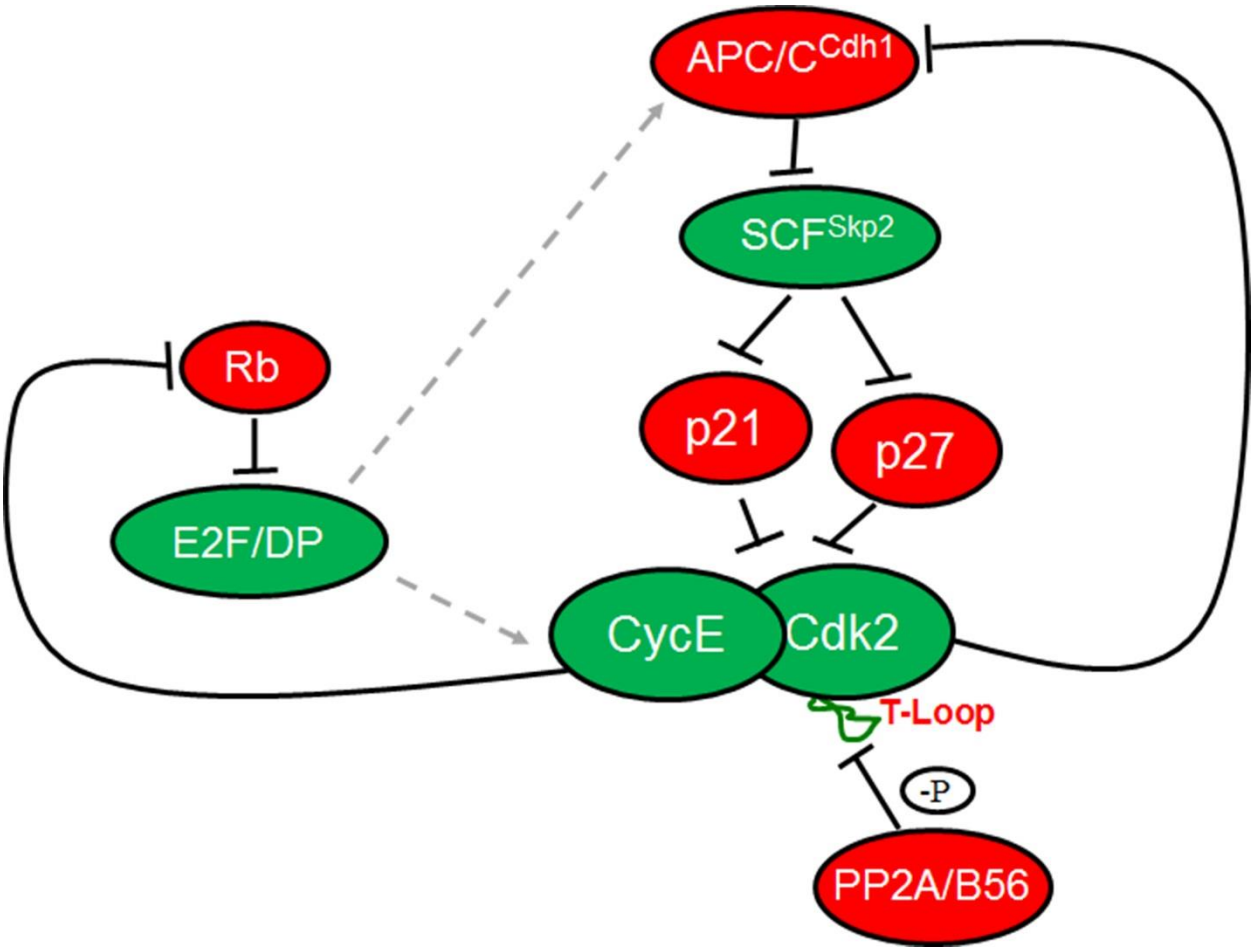


**Figure 4. 1 Molecular regulation of the proliferation-quiescence decision**

Molecular regulation of the proliferation-quiescence transition in development with negative (red) and positive (green) cell cycle regulators. Several studies suggest redundancy of negative regulators ensures robust cell cycle exit upon terminal differentiation. Regulation may act transcriptionally (grey dashed lines) as well as post-translationally (black lines) and includes both positive and negative feedback loops.

# References

**Aguirre-Ghiso, J.A.** (2007). Models, mechanisms and clinical evidence for cancer dormancy. Nat. Rev. Cancer **7**: 834–846.

**Almog, N.** (2010). Molecular mechanisms underlying tumor dormancy. Cancer Lett. **294**: 139–46.

**Balciunaite, E., Spektor, A., Lents, N.H., Cam, H., Te Riele, H., Scime, A., Rudnicki, M.A., Young, R., and Dynlacht, B.D.** (2005). Pocket protein complexes are recruited to distinct targets in quiescent and proliferating cells. Mol. Cell. Biol. **25**: 8166–78.

**Bashir, T., Dorrello, N.V., Amador, V., Guardavaccaro, D., and Pagano, M.** (2004). Control of the SCF(Skp2-Cks1) ubiquitin ligase by the APC/C(Cdh1) ubiquitin ligase. Nature **428**: 190–3.

**Bell, S.P. and Dutta, A.** (2003). DNA Replication in Eukaryotic Cells. http://dx.doi.org/10.1146/annurev.biochem.71.110601.135425.

**Binné, U.K., Classon, M.K., Dick, F.A., Wei, W., Rape, M., Kaelin, W.G., Näär, A.M., and Dyson, N.J.** (2007). Retinoblastoma protein and anaphase-promoting complex

physically interact and functionally cooperate during cell-cycle exit. Nat. Cell Biol. **9**: 225–32.

**Blais, A. and Dynlacht, B.D.** (2004). Hitting their targets: An emerging picture of E2F and cell cycle control. Curr. Opin. Genet. Dev. **14**: 527–532.

**Bracken, A.P., Ciro, M., Cocito, A., and Helin, K.** (2004). E2F target genes: unraveling the biology. Trends Biochem. Sci. **29**: 409–17.

**Brownlee, C.W., Klebba, J.E., Buster, D.W., and Rogers, G.C.** (2011). The Protein Phosphatase 2A regulatory subunit Twins stabilizes Plk4 to induce centriole amplification. J. Cell Biol. **195**: 231–43.

**Burkhart, D.L. and Sage, J.** (2008). Cellular mechanisms of tumour suppression by the retinoblastoma gene. Nat. Rev. Cancer **8**: 671–682.

**Buttitta, L. a, Katzaroff, A.J., and Edgar, B. a** (2010). A robust cell cycle control mechanism limits E2F-induced proliferation of terminally differentiated cells in vivo. J. Cell Biol. **189**: 981–96.

**Buttitta, L. a, Katzaroff, A.J., Perez, C.L., de la Cruz, A., and Edgar, B. a** (2007). A double-assurance mechanism controls cell cycle exit upon terminal differentiation in Drosophila. Dev. Cell **12**: 631–43.

**Cappell, S.D. et al.** (2016). Irreversible APCCdh1 Inactivation Underlies the Point of No Return for Cell-Cycle Entry. Cell **166**: 167–180.

**Cardozo, T. and Pagano, M.** (2004). The SCF ubiquitin ligase: insights into a molecular machine. Nat. Rev. Mol. Cell Biol. **5**: 739–51.

**Chandler, H. and Peters, G.** (2013). Stressing the cell cycle in senescence and aging. Curr. Opin. Cell Biol. **25**: 765–71.

**Chen, F., Archambault, V., Kar, A., Lio', P., D'Avino, P.P., Sinka, R., Lilley, K., Laue, E.D., Deak, P., Capalbo, L., and Glover, D.M.** (2007). Multiple protein phosphatases are required for mitosis in Drosophila. Curr. Biol. **17**: 293–303.

**Clijsters, L., Ogink, J., and Wolthuis, R.** (2013). The spindle checkpoint, APC/C(Cdc20), and APC/C(Cdh1) play distinct roles in connecting mitosis to S phase. J. Cell Biol. **201**: 1013–26.

**Cobrinik, D.** (2005). Pocket proteins and cell cycle control. Oncogene **24**: 2796–809.

**Coller, H.A., Sang, L., and Roberts, J.M.** (2006). A new description of cellular quiescence. PLoS Biol. **4**: e83.

**Deak, P., Donaldson, M., and Glover, D.M.** (2003). Mutations in mákos, a Drosophila gene encoding the Cdc27 subunit of the anaphase promoting complex, enhance centrosomal defects in polo and are suppressed by mutations in twins/aar, which encodes a regulatory subunit of PP2A. J. Cell Sci. **116**: 4147–58.

**Dey-Guha, I. et al.** (2015). A mechanism for asymmetric cell division resulting in proliferative asynchronicity. Mol. Cancer Res. **13**: 223–30.

**Dey-Guha, I., Wolfer, A., Yeh, A.C., G Albeck, J., Darp, R., Leon, E., Wulfkuhle, J., Petricoin, E.F., Wittner, B.S., and Ramaswamy, S.** (2011). Asymmetric cancer cell division regulated by AKT. Proc. Natl. Acad. Sci. U. S. A. **108**: 12845–50.

**Du, W. and Pogoriler, J.** (2006). Retinoblastoma family genes. Oncogene **25**: 5190–5200.

**Ehmer, U., Zmoos, A.-F., Auerbach, R.K., Vaka, D., Butte, A.J., Kay, M.A., and Sage, J.** (2014). Organ size control is dominant over Rb family inactivation to restrict proliferation in vivo. Cell Rep. **8**: 371–81.

**Esmaeeli-Nieh, S. et al.** (2016). BOD1 Is Required for Cognitive Function in Humans and Drosophila. PLoS Genet. **12**: e1006022.

**Firth, L.C. and Baker, N.E.** (2005). Extracellular signals responsible for spatially regulated proliferation in the differentiating Drosophila eye. Dev. Cell **8**: 541–51.

**Fischer, P., La Rosa, M.K., Schulz, A., Preiss, A., and Nagel, A.C.** (2015). Cyclin G Functions as a Positive Regulator of Growth and Metabolism in Drosophila. PLoS Genet. **11**: e1005440.

**Fisher, R.P.** (2005). Secrets of a double agent: CDK7 in cell-cycle control and transcription. J. Cell Sci. **118**: 5171–80.

**Foijer, F., Wolthuis, R.M.F., Doodeman, V., Medema, R.H., and te Riele, H.** (2005). Mitogen requirement for cell cycle progression in the absence of pocket protein activity. Cancer Cell **8**: 455–66.

**Ganuza, M., Sáiz-Ladera, C., Cañamero, M., Gómez, G., Schneider, R., Blasco, M.A., Pisano, D., Paramio, J.M., Santamaría, D., and Barbacid, M.** (2012). Genetic inactivation of Cdk7 leads to cell cycle arrest and induces premature aging due to adult stem cell exhaustion. EMBO J. **31**: 2498–510.

**Garcí-Higuera, I., Manchado, E., Dubus, P., Cañamero, M., Méndez, J., Moreno, S., and Malumbres, M.** (2008). Genomic stability and tumour suppression by the APC/C cofactor Cdh1. Nat. Cell Biol. **10**: 802–811.

**Gharbi-Ayachi, A., Labbé, J.-C., Burgess, A., Vigneron, S., Strub, J.-M., Brioudes, E., Van-Dorsselaer, A., Castro, A., and Lorca, T.** (2010). The substrate of Greatwall kinase, Arpp19, controls mitosis by inhibiting protein phosphatase 2A. Science **330**: 1673–7.

**Gui, H., Li, S., and Matise, M.P.** (2007). A cell-autonomous requirement for Cip/Kip cyclin-kinase inhibitors in regulating neuronal cell cycle exit but not differentiation in the developing spinal cord. Dev. Biol. **301**: 14–26.

**Haesen, D., Sents, W., Lemaire, K., Hoorne, Y., and Janssens, V.** (2014). The Basic Biology of PP2A in Hematologic Cells and Malignancies. Front. Oncol. **4**: 347.

**Hanahan, D. and Weinberg, R.A.** (2011). Hallmarks of cancer: The next generation. Cell **144**: 646–674.

**Harper, J.W. and Elledge, S.J.** (1996). Cdk inhibitors in development and cancer. Curr. Opin. Genet. Dev. **6**: 56–64.

**van den Heuvel, S. and Dyson, N.J.** (2008). Conserved functions of the pRB and E2F families. Nat. Rev. Mol. Cell Biol. **9**: 713–24.

**Hsiung, C.C.-S. et al.** (2016). A hyperactive transcriptional state marks genome reactivation at the mitosis–G1 transition. Genes Dev. **30**: 1423–1439.

**Huang, H.J., Yee, J.K., Shew, J.Y., Chen, P.L., Bookstein, R., Friedmann, T., Lee, E.Y., and Lee, W.H.** (1988). Suppression of the neoplastic phenotype by replacement of the RB gene in human cancer cells. Science **242**: 1563–6.

**Janssens, V., Goris, J., and Van Hoof, C.** (2005). PP2A: the expected tumor suppressor. Curr. Opin. Genet. Dev. **15**: 34–41.

**Kamura, T., Hara, T., Matsumoto, M., Ishida, N., Okumura, F., Hatakeyama, S., Yoshida, M., Nakayama, K., and Nakayama, K.I.** (2004). Cytoplasmic ubiquitin ligase KPC regulates proteolysis of p27(Kip1) at G1 phase. Nat. Cell Biol. **6**: 1229–1235.

**Kaplan, E.L. and Meier, P.** (1958). Nonparametric Estimation from Incomplete Observations. J. Am. Stat. Assoc. **53**: 457–481.

**Kingsbury, S.R., Loddo, M., Fanshawe, T., Obermann, E.C., Prevost, A.T., Stoeber, K., and Williams, G.H.** (2005). Repression of DNA replication licensing in quiescence is independent of geminin and may define the cell cycle state of progenitor cells. Exp. Cell Res. **309**: 56–67.

**Kiyokawa, H., Kineman, R.D., Manova-Todorova, K.O., Soares, V.C., Hoffman, E.S., Ono, M., Khanam, D., Hayday, A.C., Frohman, L.A., and Koff, A.** (1996). Enhanced growth of mice lacking the cyclin-dependent kinase inhibitor function of p27(Kip1). Cell **85**: 721–32.

**Klein, C.A.** (2011). Framework models of tumor dormancy from patient-derived observations. Curr. Opin. Genet. Dev. **21**: 42–9.

**Koepp, D.M., Schaefer, L.K., Ye, X., Keyomarsi, K., Chu, C., Harper, J.W., and Elledge, S.J.** (2001). Phosphorylation-dependent ubiquitination of cyclin E by the SCFFbw7 ubiquitin ligase. Science **294**: 173–7.

**Kolupaeva, V., Daempfling, L., and Basilico, C.** (2013). The B55α regulatory subunit of protein phosphatase 2A mediates fibroblast growth factor-induced p107 dephosphorylation and growth arrest in chondrocytes. Mol. Cell. Biol. **33**: 2865–78.

**Kurimchak, A., Haines, D.S., Garriga, J., Wu, S., De Luca, F., Sweredoski, M.J., Deshaies, R.J., Hess, S., and Graña, X.** (2013). Activation of p107 by fibroblast growth factor, which is essential for chondrocyte cell cycle exit, is mediated by the protein phosphatase 2A/B55α holoenzyme. Mol. Cell. Biol. **33**: 3330–42.

**Lane, M.E., Elend, M., Heidmann, D., Herr, a, Marzodko, S., Herzig, a, and Lehner, C.F.** (2000). A screen for modifiers of cyclin E function in Drosophila melanogaster identifies Cdk2 mutations, revealing the insignificance of putative phosphorylation sites in Cdk2. Genetics **155**: 233–44.

**Lane, M.E., Sauer, K., Wallace, K., Jan, Y.N., Lehner, C.F., and Vaessin, H.** (1996). Dacapo, a cyclin-dependent kinase inhibitor, stops cell proliferation during Drosophila development. Cell **87**: 1225–1235.

**Larochelle, S., Pandur, J., Fisher, R.P., Salz, H.K., and Suter, B.** (1998). Cdk7 is essential for mitosis and for in vivo Cdk-activating kinase activity. Genes Dev. **12**: 370–81.

**Larsson, O.. and Zetterberg, A.** (1985). Kinetic Analysis of Regulatory Events in G1 Leading to Proliferation or Quiescence of Swiss 3T3 Cells. Proc. Natl. Acad. Sci. U. S. A. **82**: 5365–5369.

**Lew, D.J. and Kornbluth, S.** (1996). Regulatory roles of cyclin dependent kinase phosphorylation in cell cycle control. Curr. Opin. Cell Biol. **8**: 795–804.

**Litovchick, L., Sadasivam, S., Florens, L., Zhu, X., Swanson, S.K., Velmurugan, S., Chen, R., Washburn, M.P., Liu, X.S., and DeCaprio, J.A.** (2007). Evolutionarily conserved multisubunit RBL2/p130 and E2F4 protein complex represses human cell cycle-dependent genes in quiescence. Mol. Cell **26**: 539–51.

**Liu, H., Adler, A.S., Segal, E., and Chang, H.Y.** (2007). A transcriptional program mediating entry into cellular quiescence. PLoS Genet. **3**: e91.

**Mailand, N. and Diffley, J.F.X.** (2005). CDKs promote DNA replication origin licensing in human cells by protecting Cdc6 from APC/C-dependent proteolysis. Cell **122**: 915–26.

**McLean, J.R., Chaix, D., Ohi, M.D., and Gould, K.L.** (2011). State of the APC/C: organization, function, and structure. Crit. Rev. Biochem. Mol. Biol. **46**: 118–36.

**Merrick, K.A., Larochelle, S., Zhang, C., Allen, J.J., Shokat, K.M., and Fisher, R.P.** (2008). Distinct activation pathways confer cyclin-binding specificity on Cdk1 and Cdk2 in human cells. Mol. Cell **32**: 662–72.

**Moberg, K.H., Bell, D.W., Wahrer, D.C., Haber, D. a, and Hariharan, I.K.** (2001). Archipelago regulates Cyclin E levels in Drosophila and is mutated in human cancer cell lines. Nature **413**: 311–6.

**Mochida, S., Ikeo, S., Gannon, J., and Hunt, T.** (2009). Regulated activity of PP2A-B55 delta is crucial for controlling entry into and exit from mitosis in Xenopus egg extracts. EMBO J. **28**: 2777–85.

**Mochida, S., Maslen, S.L., Skehel, M., and Hunt, T.** (2010). Greatwall phosphorylates an inhibitor of protein phosphatase 2A that is essential for mitosis. Science **330**: 1670–3.

**Morgan, D.O.** (1997). Cyclin-dependent kinases: engines, clocks, and microprocessors. Annu Rev Cell Dev Biol **13**: 261–291.

**Morgan, D.O.** (1995). Principles of CDK regulation..pdf.

**Morrissey, C., Vessella, R.L., Lange, P.H., and Lam, H.-M.** (2016). The biology and clinical implications of prostate cancer dormancy and metastasis. J. Mol. Med. (Berl). **94**: 259–65.

**Müller, H. and Helin, K.** (2000). The E2F transcription factors: key regulators of cell proliferation. Biochim. Biophys. Acta **1470**: M1–M12.

**Muñoz-Espín, D. et al.** (2013). Programmed cell senescence during mammalian embryonic development. Cell **155**: 1104–18.

**Naetar, N., Soundarapandian, V., Litovchick, L., Goguen, K.L., Sablina, A.A., Bowman-Colin, C., Sicinski, P., Hahn, W.C., DeCaprio, J.A., and Livingston,**

**D.M.** (2014). PP2A-Mediated Regulation of Ras Signaling in G2 Is Essential for Stable Quiescence and Normal G1 Length. Mol. Cell: 1–14.

**Narasimha, A.M., Kaulich, M., Shapiro, G.S., Choi, Y.J., Sicinski, P., and Dowdy, S.F.** (2014). Cyclin D activates the Rb tumor suppressor by mono-phosphorylation. Elife: e02872.

**Nobumori, Y., Shouse, G.P., Wu, Y., Lee, K.J., Shen, B., and Liu, X.** (2013). B56γ tumor-associated mutations provide new mechanisms for B56γ-PP2A tumor suppressor activity. Mol. Cancer Res. **11**: 995–1003.

**de Nooij, J.C., Letendre, M.A., and Hariharan, I.K.** (1996). A Cyclin-Dependent Kinase Inhibitor, Dacapo, Is Necessary for Timely Exit from the Cell Cycle during Drosophila Embryogenesis. Cell **87**: 1237–1247.

**Oki, T. et al.** (2014). A novel cell-cycle-indicator, mVenus-p27K(-), identifies quiescent cells and visualizes G0-G1 transition. Sci. Rep. **4**: 4012.

**Onoyama, I., Tsunematsu, R., Matsumoto, A., Kimura, T., de Alborán, I.M., Nakayama, K., and Nakayama, K.I.** (2007). Conditional inactivation of Fbxw7 impairs cell-cycle exit during T cell differentiation and results in lymphomatogenesis. J. Exp. Med. **204**: 2875–88.

**Ortega, S., Malumbres, M., and Barbacid, M.** (2002). Cyclin D-dependent kinases, INK4 inhibitors and cancer. Biochim. Biophys. Acta - Rev. Cancer **1602**: 73–87.

**Overton, K.W., Spencer, S.L., Noderer, W.L., Meyer, T., and Wang, C.L.** (2014). Basal p21 controls population heterogeneity in cycling and quiescent cell cycle states. Proc. Natl. Acad. Sci. U. S. A. **2014**: 1–8.

**Pandey, P., Seshacharyulu, P., Das, S., Rachagani, S., Ponnusamy, M.P., Yan, Y., Johansson, S.L., Datta, K., Fong Lin, M., and Batra, S.K.** (2013). Impaired expression of protein phosphatase 2A subunits enhances metastatic potential of human prostate cancer cells through activation of AKT pathway. Br. J. Cancer **108**: 2590–600.

**Pardee, a B.** (1974). A restriction point for control of normal animal cell proliferation. Proc. Natl. Acad. Sci. U. S. A. **71**: 1286–90.

**Parry, D., Mahony, D., Wills, K., and Lees, E.** (1999). Cyclin D-CDK subunit arrangement is dependent on the availability of competing INK4 and p21 class inhibitors. Mol. Cell. Biol. **19**: 1775–83.

**Pechnick, R.N., Zonis, S., Wawrowsky, K., Pourmorady, J., and Chesnokova, V.** (2008). p21Cip1 restricts neuronal proliferation in the subgranular zone of the dentate gyrus of the hippocampus. Proc. Natl. Acad. Sci. U. S. A. **105**: 1358–63.

**Penas, C., Ramachandran, V., and Ayad, N.G.** (2011). The APC/C Ubiquitin Ligase: From Cell Biology to Tumorigenesis. Front. Oncol. **1**: 60.

**Petersen, B.O.** (2000). Cell cycle- and cell growth-regulated proteolysis of mammalian CDC6 is dependent on APC-CDH1. Genes Dev. **14**: 2330–2343.

**Polyak, K., Kato, J.Y., Solomon, M.J., Sherr, C.J., Massague, J., Roberts, J.M., and Koff, A.** (1994). p27Kip1, a cyclin-Cdk inhibitor, links transforming growth factor-beta and contact inhibition to cell cycle arrest. Genes Dev. **8**: 9–22.

**Poon, R.Y.C. and Hunter, T.** (1995). Dephosphorylation of Cdk2 Thr160 by the Cyclin-Dependent Kinase-Interacting Phosphatase KAP in the Absence of Cyclin. Science (80-. ). **270**: 90–93.

**Porter, I.M., Schleicher, K., Porter, M., and Swedlow, J.R.** (2013). Bod1 regulates protein phosphatase 2A at mitotic kinetochores. Nat. Commun. **4**: 2677.

**Pozarowski, P. and Darzynkiewicz, Z.** (2004). Analysis of Cell Cycle by Flow Cytometry. In Methods Mol Biol (Humana Press: New Jersey), pp. 301–312.

**Ruggiero, R., Kale, A., Thomas, B., and Baker, N.E.** (2012). Mitosis in neurons: Roughex and APC/C maintain cell cycle exit to prevent cytokinetic and axonal defects in Drosophila photoreceptor neurons. PLoS Genet. **8**: e1003049.

**Sadasivam, S. and Decaprio, J.A.** (2013). The DREAM complex: master ccoordinator of cel cycle dependent gene expression. **13**: 585–595.

**Saera-Vila, A., Kasprick, D.S., Junttila, T.L., Grzegorski, S.J., Louie, K.W., Chiari, E.F., Kish, P.E., and Kahana, A.** (2015). Myocyte Dedifferentiation Drives Extraocular Muscle Regeneration in Adult Zebrafish. Invest. Ophthalmol. Vis. Sci. **56**: 4977–93.

**Sakaue-Sawano, A. et al.** (2008). Visualizing spatiotemporal dynamics of multicellular cell-cycle progression. Cell **132**: 487–98.

**Salama, R., Sadaie, M., Hoare, M., and Narita, M.** (2014). Cellular senescence and its effector programs. Genes Dev. **28**: 99–114.

**Schachter, M.M., Merrick, K. a, Larochelle, S., Hirschi, A., Zhang, C., Shokat, K.M., Rubin, S.M., and Fisher, R.P.** (2013). A Cdk7-Cdk4 T-loop phosphorylation cascade promotes G1 progression. Mol. Cell **50**: 250–60.

**Schmitz, M.H. a et al.** (2010). Live-cell imaging RNAi screen identifies PP2A-B55alpha and importin-beta1 as key mitotic exit regulators in human cells. Nat. Cell Biol. **12**: 886–93.

**Sherr, C.J. and Roberts, J.M.** (1999). CDK inhibitors: positive and negative regulators of G1-phase progression. Genes Dev. **13**: 1501–12.

**Shiozawa, Y., Eber, M.R., Berry, J.E., and Taichman, R.S.** (2015). Bone marrow as a metastatic niche for disseminated tumor cells from solid tumors. Bonekey Rep. **4**: 689.

**Sigrist, S.J. and Lehner, C.F.** (1997). Drosophila fizzy-related Down-Regulates Mitotic Cyclins and Is Required for Cell Proliferation Arrest and Entry into Endocycles. Cell **90**: 671–681.

**Smith, E.J., Leone, G., DeGregori, J., Jakoi, L., and Nevins, J.R.** (1996). The accumulation of an E2F-p130 transcriptional repressor distinguishes a G0 cell state from a G1 cell state. Mol. Cell. Biol. **16**: 6965–6976.

**Song, H., Hanlon, N., Brown, N.R., Noble, M.E.M., Johnson, L.N., and Barford, D.** (2001). Phosphoprotein–Protein Interactions Revealed by the Crystal Structure of

Kinase-Associated Phosphatase in Complex with PhosphoCDK2. Mol. Cell **7**: 615–626.

**Soos, T.J., Kiyokawa, H., Yan, J.S., Rubin, M.S., Giordano, A., DeBlasio, A., Bottega, S., Wong, B., Mendelsohn, J., and Koff, A.** (1996). Formation of p27-CDK complexes during the human mitotic cell cycle. Cell Growth Differ. **7**: 135–46.

**Sosa, M.S., Bragado, P., and Aguirre-Ghiso, J.A.** (2014). Mechanisms of disseminated cancer cell dormancy: an awakening field. Nat. Rev. Cancer **14**: 611–22.

**Spencer, S.L., Cappell, S.D., Tsai, F.-C., Overton, K.W., Wang, C.L., and Meyer, T.** (2013). The proliferation-quiescence decision is controlled by a bifurcation in CDK2 activity at mitotic exit. Cell **155**: 369–83.

**Srinivasan, T. et al.** (2016). NOTCH Signaling Regulates Asymmetric Cell Fate of Fast- and Slow-Cycling Colon Cancer-Initiating Cells. Cancer Res. **76**: 3411–21.

**Storer, M., Mas, A., Robert-Moreno, A., Pecoraro, M., Ortells, M.C., Di Giacomo, V., Yosef, R., Pilpel, N., Krizhanovsky, V., Sharpe, J., and Keyes, W.M.** (2013). Senescence Is a Developmental Mechanism that Contributes to Embryonic Growth and Patterning. Cell **155**: 1119–1130.

**Strohmaier, H., Spruck, C.H., Kaiser, P., Won, K.A., Sangfelt, O., and Reed, S.I.** (2001). Human F-box protein hCdc4 targets cyclin E for proteolysis and is mutated in a breast cancer cell line. Nature **413**: 316–22.

**Sugiura, T., Wang, H., Barsacchi, R., Simon, A., and Tanaka, E.M.** (2016). MARCKS-like protein is an initiating molecule in axolotl appendage regeneration. Nature **advance on**.

**Sukhanova, M.J. and Du, W.** (2008). Control of cell cycle entry and exiting from the second mitotic wave in the Drosophila developing eye. BMC Dev. Biol. **8**: 7.

**Sun, D. and Buttitta, L.** (2015). Protein phosphatase 2A promotes the transition to G0 during terminal differentiation in Drosophila. Development **142**: 3033–3045.

**Taichman, R.S., Patel, L.R., Bedenis, R., Wang, J., Weidner, S., Schumann, T., Yumoto, K., Berry, J.E., Shiozawa, Y., and Pienta, K.J.** (2013). GAS6 Receptor Status Is Associated with Dormancy and Bone Metastatic Tumor Formation. PLoS One **8**.

**Takahashi, Y., Rayman, J.B., and Dynlacht, B.D.** (2000). Analysis of promoter binding by the E2F and pRB families in vivo: distinct E2F proteins mediate activation and repression. Genes Dev. **14**: 804–16.

**Tamrakar, S., Rubin, E., and Ludlow, J.W.** (2000). Role of pRB dephosphorylation in cell cycle regulation. Front. Biosci. **5**: D121–37.

**Tan, Y., Sun, D., Jiang, W., Klotz-Noack, K., Vashisht, A. V, Wohlschlegel, J., Widschwendter, M., and Spruck, C.** (2014). PP2A-B55β Antagonizes Cyclin E1 Proteolysis and Promotes its Dysregulation in Cancer. Cancer Res.

**Tanaka-Matakatsu, M., Thomas, B.J., and Du, W.** (2007). Mutation of the Apc1 homologue shattered disrupts normal eye development by disrupting G1 cell cycle arrest and progression through mitosis. Dev. Biol. **309**: 222–235.

**Tedesco, D., Lukas, J., and Reed, S.I.** (2002). The pRb-related protein p130 is regulated by phosphorylation-dependent proteolysis via the protein-ubiquitin ligase SCF(Skp2). Genes Dev. **16**: 2946–57.

**The, I. et al.** (2015). Rb and FZR1/Cdh1 determine CDK4/6-cyclin D requirement in C. elegans and human cancer cells. Nat. Commun. **6**: 5906.

**Trimarchi, J.M. and Lees, J. a** (2002). Sibling rivalry in the E2F family. Nat. Rev. Mol. Cell Biol. **3**: 11–20.

**Tsue, T.T., Watling, D.L., Weisleder, P., Coltrera, M.D., and Rubel, E.W.** (1994). Identification of hair cell progenitors and intermitotic migration of their nuclei in the normal and regenerating avian inner ear. J. Neurosci. **14**: 140–52.

**Vidal, A. and Koff, A.** (2000). Cell-cycle inhibitors: three families united by a common cause. Gene **247**: 1–15.

**Virshup, D.M. and Shenolikar, S.** (2009). From promiscuity to precision: protein phosphatases get a makeover. Mol. Cell **33**: 537–45.

**Wade Harper, J. et al.** (1993). The p21 Cdk-interacting protein Cip1 is a potent inhibitor of G1 cyclin-dependent kinases. Cell **75**: 805–816.

**Wan, J. and Goldman, D.** (2016). Retina regeneration in zebrafish. Curr. Opin. Genet. Dev. **40**: 41–47.

**Wang, N., Docherty, F., Brown, H.K., Reeves, K., Fowles, A., Lawson, M., Ottewell, P.D., Holen, I., Croucher, P.I., and Eaton, C.L.** (2015). Mitotic quiescence, but not unique “stemness,” marks the phenotype of bone metastasis-initiating cells in prostate cancer. FASEB J. **29**: 3141–50.

**Wang, P., Larouche, M., Normandin, K., Kachaner, D., Mehsen, H., Emery, G., and Archambault, V.** (2016). Spatial regulation of greatwall by Cdk1 and PP2A-Tws in the cell cycle. Cell Cycle **15**: 528–39.

**Wei, W., Ayad, N.G., Wan, Y., Zhang, G.-J., Kirschner, M.W., and Kaelin, W.G.** (2004). Degradation of the SCF component Skp2 in cell-cycle phase G1 by the anaphase-promoting complex. Nature **428**: 194–8.

**Welcker, M. and Clurman, B.E.** (2008). FBW7 ubiquitin ligase: a tumour suppressor at the crossroads of cell division, growth and differentiation. Nat. Rev. Cancer **8**: 83–93.

**Willems, A.R., Schwab, M., and Tyers, M.** (2004). A hitchhiker’s guide to the cullin ubiquitin ligases: SCF and its kin. Biochim. Biophys. Acta **1695**: 133–70.

**Williams, B.C., Filter, J.J., Blake-Hodek, K.A., Wadzinski, B.E., Fuda, N.J., Shalloway, D., and Goldberg, M.L.** (2014). Greatwall-phosphorylated Endosulfine is both an inhibitor and a substrate of PP2A-B55 heterotrimers. Elife **2014**.

**Wirt, S.E., Adler, A.S., Gebala, V., Weimann, J.M., Schaffer, B.E., Saddic, L. a., Viatour, P., Vogel, H., Chang, H.Y., Meissner, A., and Sage, J.** (2010). G1 arrest

and differentiation can occur independently of Rb family function. J. Cell Biol. **191**: 809–825.

**Yao, G.** (2014). Modelling mammalian cellular quiescence. Interface Focus **4**: 20130074.

**Yao, G., Lee, T.J., Mori, S., Nevins, J.R., and You, L.** (2008). A bistable Rb-E2F switch underlies the restriction point. Nat. Cell Biol. **10**: 476–82.

**Yeh, A.C. et al.** (2015). Mechanisms of Cancer Cell Dormancy--Another Hallmark of Cancer? Cancer Res. **75**: 5014–22.

**Zambon, A.C.** (2010). Use of the Ki67 promoter to label cell cycle entry in living cells. Cytometry. A **77**: 564–70.

**Zhao, H., Chen, X., Gurian-West, M., and Roberts, J.M.** (2012). Loss of cyclin-dependent kinase 2 (CDK2) inhibitory phosphorylation in a CDK2AF knock-in mouse causes misregulation of DNA replication and centrosome duplication. Mol. Cell. Biol. **32**: 1421–32.

**Zindy, F., Cunningham, J.J., Sherr, C.J., Jogal, S., Smeyne, R.J., and Roussel, M.F.** (1999). Postnatal neuronal proliferation in mice lacking Ink4d and Kip1 inhibitors of cyclin-dependent kinases. Proc. Natl. Acad. Sci. U. S. A. **96**: 13462–13467.